SPATIOTEMPORAL DATA MODELING FOR THE ANALYSIS OF THE DYNAMIC BEHAVIOR OF URBAN HEAT ISLANDS

RUI ZHU

Ph.D

The Hong Kong Polytechnic University

2018

The Hong Kong Polytechnic University

Department of Land Surveying and Geo-Informatics

Spatiotemporal Data Modeling for the Analysis of the Dynamic Behavior of Urban Heat Islands

Rui Zhu

A thesis submitted in partial fulfilment of
the requirements for the degree of

Doctor of Philosophy

June 2017

Certificate of originality

I hereby declare that this thesis is my own work and that, to the best of my knowledge and belief, it reproduces no material previously published or written, nor material that has been accepted for the award of any other degree or diploma, except where due acknowledgement has been made in the text.

____________________________________(Signed)

_______________Rui Zhu_______________(Name of Student)

I would like to dedicate this thesis to my loving parents and wife.

Abstract

Urban Heat Island (UHI), widely acknowledged as an environmental phenomenon where temperatures in urban areas are higher than the surrounding rural areas, is a major problem in most of the metropolitan areas. Given the rapid urbanization, it is likely to be a serious problem in the growing mega cities due to the adverse effect on inhabitant health and increase of the energy consumption. To have more explicitly understanding of this phenomenon, previous research mainly focused on two aspects:

- UHI intensity estimation and super-resolution reconstruction at a fixed time instant, where thermal satellite images with very fine spatial and / or temporal resolution covering a micro-scale of urban areas can rarely be obtained; and

- causative factorial analysis by studying correlation between thermal images and the relevant factors (e.g. solar radiation, urban morphology, and anthropogenic heat).

However, these studies are not capable to track the evolutionary process of the UHIs continuously in both time and space domains. Thus, objectives of this thesis are four-fold. The first objective is to conceptualize the UHI phenomenon as an object-based behavior. The second attempts to model dynamic behaviors of UHIs in three aspects (i.e., temperatures, areal extents, and locations). The third is to track the UHI spatial behaviors over time. The last objective is to evaluate the effectiveness of the model by computing with the near-surface thermal images.

This study presents the concept of UHI and describes the previous research problems in continuously tracking dynamic behaviors of UHIs. The study also designs an

object-oriented dynamic model to reconstruct the evolutionary process of UHIs. Each *urban heat island* is modeled as a spatiotemporal field-object with its own life-cycle, and dynamic behavior of a UHI is defined by a series of *filiations*. For instance, areal extent of UHI in two consecutive time instants can expand or contract. Further, the study proposes six hierarchical graphs to track continuous changes of the three properties. Finally, several patterns can be defined and revealed from the results.

The developed model was implemented in an object-relational database and near-surface air temperature data collected from automatic weather stations on an hourly basis were applied into the model for the testing. Thematic and spatial behaviors of UHIs were analyzed, covering six months of time. Results suggest that the model can identify different behaviors and track complete life-cycles of UHIs effectively.

This study has made several contributions and impacts for GIS modeling community. Interesting phenomena and evolutionary trends of UHIs in Guangzhou across different seasons are revealed. It also develops the theory of object-oriented data modeling systematically for tracking field geographical phenomena. In addition, this study provides some new approaches for the researchers to study different types of distributed spatial phenomena. The developed models can be used in urban planning to assist in mitigating the UHI phenomenon for building a sustainable city.

Publication

Journals

1. **Rui Zhu**, Eric Guilbert, Man Sing Wong, 2016. Object-oriented tracking of spatial and thematic behaviors of urban heat islands. *International Journal of Geographical Information Science*, Submitted.

2. **Rui Zhu**, Man Sing Wong, Eric Guilbert, Pok Wai Chan, 2016. Understanding heat patterns produced by vehicular flows in urban areas. *Scientific Reports – Nature*, 7, 16309. doi:10.1038/s41598-017-15869-6

3. Jiaming Na, Xin Yang, Wen Dai, Min Li, Liyang Xiong, **Rui Zhu**, Guoan Tang, 2017. Bidirectional DEM relief shading method for extraction of gully shoulder-line in loess tableland area. *Physical Geography*, 1-19. doi: 10.1080/02723646.2017.1410974

4. **Rui Zhu**, Eric Guilbert, Man Sing Wong, 2016. Object-oriented tracking of the dynamic behavior of urban heat islands. *International Journal of Geographical Information Science*, 31(2), 405–424.

5. **Rui Zhu**, Eric Guilbert, Man Sing Wong, 2016. Tracking the spatial evolution of urban heat islands. *ISPRS Annals of the Photogrammetry, Remote Sensing and Spatial Information Sciences*, 3(2), 3–8.

6. Man Sing Wong, **Rui Zhu**, Zhizhao Liu, Lin Lu, Jingqing Peng, Zhaoqin Tang, Chung Ho Lo, Wai Ki Chan, 2016. Estimation of Hong Kong's solar energy potential using GIS and remote sensing technologies. *Renewable Energy*, 99, 325–335.

7. Fayuan Li, Guoan Tang, Chun Wang, Lingzhou Cui, **Rui Zhu**, 2015. Slope Spectrum Variation in a Simulated Loess Watershed. *Frontiers of Earth Science*, 1–12.

Proceedings

1. **Rui Zhu**, Eric Guilbert, Man Sing Wong, 2016. Understanding spatiotemporal heat patterns of vehicular flows in urban areas. *In Proceeding of the 2016 Cartographic Visualization of Big Data for Early Warning and Disaster/Crisis Management(EW&CM)- Methodology, Techniques and Applications*, 1–3. Nanjing, China, 27-29 November 2016.

2. **Rui Zhu**, Eric Guilbert, Man Sing Wong, 2016. Tracking the spatial evolution of urban heat islands, Commission II, WG II/1. *In Proceeding of the XXIII ISPRS Congress*, Prague, Czech Public, 12-19 July 2016.

3. **Rui Zhu**, Eric Guilbert, Man Sing Wong, 2015. Event-based tracking of the dynamic behavior of urban heat islands. *In Proceeding of the 2nd International Conference on Sustainable Urbanization*, 239. Hong Kong, China, 7-9 January 2015.

Acknowledgements

This study has been successfully carried out in the Department of Land Surveying and Geo-Informatics, The Hong Kong Polytechnic University with the enthusiastic support and supervision of Dr. Man Sing Wong. Collaboratively working with Dr. Wong, I always have free and effective discussion for the problems that persecute me, and I can get timely and positive response from him all the time. He gave many valuable suggestions and all-around supports for the Ph.D dissertation. I also highly appreciate the supervision of Dr. Éric Gilles Francis Guilbert from Laval University, Québec, Canada. Without his supervision from the research outline to the detailed methodology, it cannot be possible to complete my Ph.D study. Apart from teaching me the principles of research and academic writing, he has also introduced me to several new and exciting topics in the area of spatiotemporal data modeling and analysis.

My Ph.D study and the research were supported by the General Research Fund of The Hong Kong Polytechnic University under Grant Number 515513. I would also like to thank The Hong Kong Polytechnic University for the unforgettable life experience and excellent education provided.

I also sincerely appreciate the help of Prof. Zhilin Li at The Hong Kong Polytechnic University, Prof. Bo Huang at Chinese University of Hong Kong, and Prof. May Yuan at the University of Texas at Dallas. As the external examiners of the dissertation, they provided valuable comments and constructive suggestions for the built spatiotemporal data model.

I believe that motivation plays a very significant role for the education of one person. Among numerous people that encourage me, I would like to acknowledge Professor Guoan Tang and Professor Guonian Lu in the department of Geographic Information Sciences, Nanjing Normal University, China for filling a similar role during my stay–abroad at Laval University. Furthermore, I appreciate the unselfishness support from my colleagues in the Department at The Hong Kong Polytechnic University.

Last, but not least, I would like to express my gratitude to my parents, Mr. Boping Zhu and Ms. Yaolian Huang. They always encourage me even when I faced a failure so that I can achieve success ultimately. I am also sincerely thankful for the ever-lasting love and care from my wife Ms. Wenting Li. I would have not been able to complete my postgraduate study without endless support and motivation.

Contents

List of Figures

List of Tables

Chapter 1

Introduction

This chapter introduces the geographical phenomenon of an urban heat island, and the concept of such phenomenon with the descriptions of its adverse effects and causative factors. Furthermore, research objectives are introduced explicitly in four aspects followed by the introduction of dissertation structure.

1.1 What is an Urban Heat Island?

For a smart city, people tackle wicked urban-related problems (e.g., traffic jams, information communication obstruction, and environmental pollution) by integrating information and communication technologies (ICT) in an urban version (Meijer *et al.,* 2016). Solving these problems require Big Data analytics through real-time data processing to provide decision supports (Silva *et al.,* 2017). In view of the environmental pollution, Urban Heat Island (UHI) is one of the problems that arouse great attention from the public, which is an environmental phenomenon where temperatures in urban areas are higher than its surrounding rural areas (Nichol *et al.,* 2009; Unite States Environmental Protection Agency, 2017b) (Figure 1.1). It is reported that annual temperature difference between urban and rural areas is normally between 1 and 3 degrees Celsius, and it can be reached as high as 12 degrees Celsius in the evening (Unite States Environmental Protection Agency, 2017a).

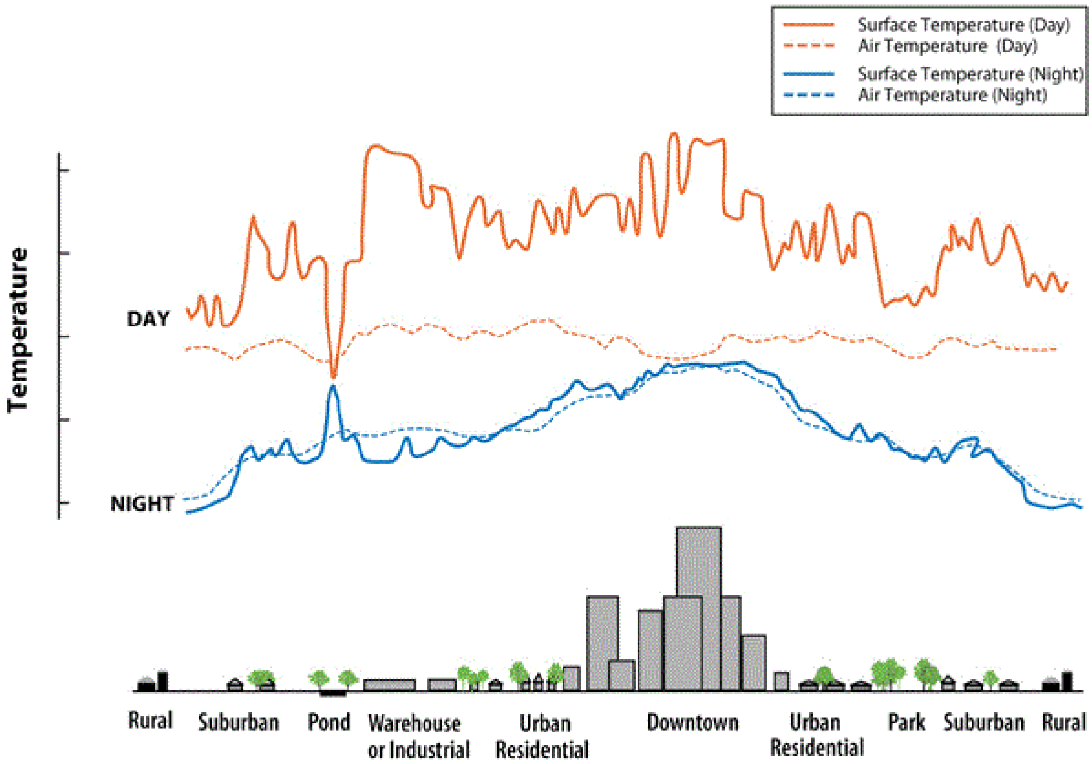

Fig. 1.1 Sketch of an urban heat island (From United States Environmental Protection Agency, 2017).

With the increasing urbanization, many rural areas have gradually become urbanized, small and middle-sized cities expand to metropolises, and spatial-contiguous city clusters merge into a mega city, which significantly affect the regional, city and micro-scale climate. The UHI effect is one of the major environmental issues caused by urbanization. Strong evidences suggest that this phenomenon can cause many adverse impacts to society in terms of health risk (Ding *et al.,* 2015; Kenney *et al.,* 2014; Morabito *et al.,* 2012), public security (Cohn & Rotton, 2000; Field, 1992; Rotton & Cohn, 2004), and energy consumption (Fung, *et al.,* 2006; Papakostas *et al.,* 2010).

In addition to estimating the magnitude of the UHI intensity, researchers have explicitly studied their formation mechanisms and a consensus is reached that this phenomenon is caused by (i) loosing of greenery area over urbanization (Chen *et al.,* 2014; Grover *et al.,* 2015; Mariani *et al.,* 2016; Susca *et al.,* 2011); (ii) buildings blocking ventilation corridors and accumulating heat (Allegrini *et al.,* 2012; Bonamente *et al.,* 2013); (iii) construction materials with low specific heat capacities which absorb solar radiations or reflect solar radiations in density built areas (Phelan *et al.,* 2015); and (iv) the increasing number of vehicles and growing electricity consumption which produce more anthropogenic heat (Chow *et al.,* 2014; Lee *et al.,* 2014; Quah & Roth, 2012).

1.2 Problem statements

The above discovered causative factors are mainly described in a coarse spatiotemporal scope or even at a static time instant. The reason is that they mainly used remote sensing images derived from satellites, which are with low temporal resolution and coarse spatial resolution. For example, resolution of MODIS thermal images is 1 kilometer, and resolutions of Landsat ETM+, ASTER, and Landsat TM are 60 meters, 90 meters, and 120 meters respectively. In addition, thermal resolution of the Landsat 8 is 100 meters. All of them are coarse for direct applications. Moreover, Landsat 8 has a revisit frequency of 16 days, which is not able to track the changes of UHI instantly. Therefore, many other studies have been devoted in the super-resolution reconstruction of thermal images. Some of them focused on multi-spectral and/or multi-resolution images for image fusion and some proposed machine learning approaches, e.g., vector support machines (Tonooka, 2005), and/or artificial neural networks (Zortea *et al.,* 2006). Instead of using satellite thermal images, an alternative approach may use temperature data sets observed from meteorological stations to represent microscope of temperature variations in urban areas. Thermal images can be derived by interpolating the station data as contiguous of thermal surfaces if each set of data can be obtained at the same time instant.

To better understand the dynamic evolutionary process of the UHI phenomenon through both time and space, many studies tend to model the behaviors of each causative factor from qualitative to quantitative description in a finer spatiotemporal resolution. It is widely acknowledged that solar radiation and anthropogenic heat (i.e., thermal emission from buildings, vehicular traffics, and latent heat from the human bodies) generate great amount of heat, and urban morphology (e.g. high rising buildings reflect the solar radiation) accumulates the heat fluxes. Following this, some studies proposed a model to simulate solar radiation fluxes on both vertical and horizontal surfaces of 3D buildings at any given time instant (Liang *et al.,* 2014; Liang *et al.,* 2015), and some studies developed a nation-wide database of hourly anthropogenic heating for different seasons (Sailor *et al.,* 2015). Even though these models can estimate heat fluxes at a series of discrete time instants, they are not able to describe the evolutionary trends of UHIs systematically over time.

In addition, there are many research questions related to the UHI effect, e.g., can there be other causative factors that we have not noticed or discovered yet? To answer this question, one problem shall be solved first: what are the evolutionary trends of UHI in both spatial and thematic domains, described in a fine temporal scale for a long-time period? The reason is that describing UHI at a static time instant may not be able to find uncovered causative factors while tracking its continuous changes can be able to. For instance, vehicles vary notably in different time and space, and heat emission from vehicular flows in an urban area can be one of the most significant contributors to the UHI phenomenon. Thus, understanding how it contributes to the UHI effect requires continuous tracking of both UHIs and vehicular flows over fine spatio-temporal resolutions. Obviously, tracking of UHI in terms of objects (i.e. causative factors) on the earth surface (e.g., moving vehicles, buildings, or land uses) needs to establish different models and each model should be customized. In contrast, tracking of UHIs themselves can provide a total solution to understand evolution of UHI explicitly. When the above question is answered appropriately, possible causative factors can be considered and determined through correlation analysis with the determined evolutionary trends.

Two more questions can also be answered benefiting from continuous tracking of UHIs: what are the UHI effects, and is urban planning effective for mitigating the UHI phenomenon? For example, a recent study tracked micro heat islands in the urban area of Hong Kong continuously, and found that these heat islands had negative effects to the public health in view of the mortality (Goggins *et al.,* 2012). In urban planning, UHIs were also determined as an indicator for urban management and planning (Santos *et al.,* 2017). No doubtfully, it requires tracking of UHIs over a long time to observe whether UHIs have mitigated when the city is re-planned. Therefore, motivation of this study is to develop a framework to instantly track the changes of UHIs and determine their evolutionary trends in different spatial and temporal scales. The framework is supposed to be used as an effective tool for researchers to have a profound understanding of UHI.

This study proposes a feasible approach to model each UHI as a field-object since it is a typical field geographical phenomenon, and changes of the UHI (e.g., temperature changes, shape variations, and locational movements) can be viewed as dynamic behaviors of the object so that their changes can be tracked continuously over time. Under this consideration, spatiotemporal data modeling can be an effective way to model all the changes of UHIs. Even though many spatiotemporal data models have been proposed, these previous models still lack the capacity to simultaneously track thematic and spatial changes of the field phenomenon, and to track these changes persistently over time.

1.3 Research objectives

Regarding the problem discussed above, this dissertation focuses on the modeling of dynamic behaviors of UHIs, which can be used as an effective tracking tool for revealing different causative factors of this phenomenon. In order to model different behaviors of UHIs from their thematic property (temperatures) to spatial properties (locations and areal extents), the study hypothesizes that each UHI is a field-object. Instead of investigating the evolutionary process of UHIs in a coarse temporal resolution (e.g., on a daily, weekly, or even monthly basis), this study aims to monitor the micro-changes of UHIs in both spatial and temporal domains, i.e., to track instant dynamic behavior of UHIs. The objectives of this study are organized as follows:

1. to conceptualize each UHI as a phenomenon such that several types of the dynamic behaviors can be modeled according to the organized information of the field property (i.e., areal extent, centroid of the extent, and UHI intensity summarized from the temperatures within the extent);

2. to conceptualize each UHI as an field-object such that it can be changed independently or interacted with each other by having dynamic behaviors at each time instant through out the whole of its life-span;

3. to propose a spatiotemporal data model to track dynamic behaviors of all the UHIs in both spatial and temporal domains simultaneously; and

4. to investigate the effectiveness of the model through an empirical test.

1.4 Dissertation structure

The rest of this dissertation is organized as follows. Chapter 2 reviews the work in related to the problems as stated above. Chapter 3 shows a new conceptual model of UHI such that UHIs can interact with each other, acting as field objects. Chapter 4 demonstrates six graphs in a hierarchical description granularity to continuously track dynamic behaviors of UHIs over time. Chapter 5 shows the evaluation of the proposed model in a case study. Finally, Chapter 6 discusses and concludes the thesis.

Chapter 2

Literature review in spatiotemporal data modeling

2.1 Introduction

Dynamic behaviors of UHIs continuously occur in space over time (Buyantuyev & Wu, 2010; Kourtidis *et al.,* 2015; Wu, *et al.,* 2012). For example, lifespan of a UHI may contain a series of snapshots, with the process of appearing, growing, shrinking, and finally disappearing. There is a need of designing an effective model to describe its dynamic behaviors and track its evolutionary trends integrating with space and time. Spatiotemporal data modeling, containing but not limited to three classes (i.e. field-based data modeling, object-based data modeling, and event-based data modeling) (Bothwell & Yuan, 2010; Goodchild *et al., 2007*; Miller & Bridwell, 2009), has been conducted in several research disciplines, which provides an enlightening approach to develop an adaptive data model for tracking the UHI phenomenon. For instance, fields were modeled as zones so that moving objects associated with a specific location can reach the boundary of the zone within a certain time period (Miller & Bridwell, 2009), and objects have several types of dynamic behaviors, which can be observed by their changes and movements (Yuan & Hornsby, 2008).

Since this study attempts to conceptualize each UHI as a field-object and model dynamic behaviors of UHIs in a fine spatial and temporal resolution, this chapter reviews the models used for monitoring of UHI related to the encountered problems as discussed in the previous chapter. Literature review firstly investigates the most original models that UHIs are viewed as static objects in Section 2.2. Hence, previous work will be introduced from field data modeling in Section 2.3; object data modeling in Section 2.4 and the necessity of combining of both modeling methods in Section 2.5. Then, Section 2.6 mainly discusses spatial changes of field-objects as several types of behaviors. More complex changes between different objects by having topological associations are further investigated in Section 2.7. Lastly, Section 2.8 presents the scientific originality and contribution of this study.

2.2 Static modeling of UHI

Most of the work in UHI consisted of correlating thermal intensity from static surface temperature images with environmental indicators such as the land covers (Dousset & Gourmelon, 2003; Lo *et al.,* 1997; Stathopoulou & Cartalis, 2007) or social indicators (Buyantuyev & Wu, 2010). There is a study to make use of data mining techniques to establish patterns between land covers and temperatures (Rajasekar & Weng, 2009a). Recently, consideration has also been given to study the dynamic evolution of UHI where UHI is defined as clusters of pixels, moving towards object-based analysis. For example, study in (Rajasekar & Weng, 2009b) estimated UHIs as Gaussian functions and research in (Keramitsoglou *et al.,* 2011) proposed an object-based image analysis to reveal thermal pattern that thermal intensities of hotspots are strongly correlated to their extents. These models attempt to determine causative factors of UHIs by correlation analysis at a static time instant. In another research direction, GIS tools were used to study and visualize UHI causative factors such as ventilation (Wong & Nichol, 2013). However conventional GIS data models and analytical tools lack the capabilities to adequately handle massive multi-dimensional data (McIntosh & Yuan, 2005), which is vital to describe the changes of UHIs in different properties such as the areal extent, and the temperatures. They also fail to provide qualitative information about the processes occurring within UHIs and trends that can take place over a long period of time. Thus, spatiotemporal data modeling shall be used to model dynamic behaviors of UHIs over time.

2.3 Field data modeling

Field-based data modeling usually models distributed phenomena such as continuous surfaces. For example, study in (Miller & Bridwell, 2009) proposed a cost field which is a function to assign measured values of movement impedance to every location so that the impedance in every location can be differentiated. Then, a velocity field is created to map velocities to all the locations in space. Hence, the minimum cost enclosed-curves are obtained through an inverse velocity field, which can be viewed as variable fields. In the field of UHI, anthropogenic heat fluxes were modeled as discrete grid cells (Allen *et al.*, 2011) and then refined to fields (i.e. enclosed polygons) (Lindberg *et al.*, 2013). However, the fields are also discrete without any internal associations between each of them in space and time. Thus, this method can model geographical phenomenon in a discrete time instant but with low capability to track the evolutionary process because it is difficult to determine the relationship of the phenomenon in a continuous time period based on field data modeling solely.

UHI can also be viewed as a typical field phenomenon that temperatures within its extent can vary differently over time. However, this conceptualization and modeling can only describe its spatial characteristics at a specific time instant and connecting a series of fields over time as different status of an individual object needs a new modeling method so that the fields can be associated logically.

2.4 Object data modeling

The GIS community has studied object-based data models to present dynamic geographical phenomena. The objective of these models is to describe the spatiotemporal behavior of objects observed in sequences of images. Geographical phenomena can be defined as field objects corresponding to geo-objects with an internal structure defined by variations of field-like properties within the boundary of the object (Goodchild *et al., 2007*). Their dynamic is driven by their activities, events and processes, and can be observed through changes and movements (Yuan & Hornsby, 2008). Such an approach works especially well with environmental phenomena such as UHI. The reason is that all the discrete spatial properties (such as UHI phenomena) can be associated with a time series relationship so that the relationship can be linked to the corresponding objects. When there are a set of the objects, all the spatial related information can be organized based on the objects.

Following this, an object shall contain information of space and it is identifiable, relevant of interest, and describable through designed characteristics as stated in (Mattos *et al.,* 1993). More specifically, an object can be described by static properties (such as object ID), structural characteristics (the object is modeled as a two-dimensional field), and behavior characteristics (a method of moving according to defined rules) (Worboys, 1994). The object-oriented data model normally requires the integration of specific disciplinary knowledge for different applications such as remote sensing theories for image classification (Aplina & Smith, 2011; Chen *et al.,* 2012; Gerçeka *et al.,* 2011; Huang *et al.,* 2012; Radoux *et al.,* 2011), computer science technologies for 3D data visualization (Shi *et al.,* 2003), and GIS methods for traveling behavior disaggregation (Frihida *et al.,* 2002). Considering the characteristics of specific geographic objects, some studies modeled the moving objects as points (Frihida *et al.,* 2002), objects as polylines (McKinney & Cai, 2002), and even track the attribute changes of objects (Khaddaj *et al.,* 2005). However, all these do not provide methods for the association and areal change between fields. Thus, a comprehensive modeling method which combines both field and object data modeling shall be considered.

2.5 Field-object data modeling

A combination of the field-based and object-based data modeling, i.e., field-object data modeling, provides a solution to the above problems. Research in (Kjenstad, 2006) conceptualized a geographic object as a UML class model *PGOModel* by integrating the extended core object-based model and the extended field-based model, which contains three core elements, i.e., (1) *PGObject* which is a class of conceptualized geographic object with m derived attributes and n degree of freedom so that attributes are varying over n dimensional domains, (2) *PGOAtom* which is a class by merging a number of attributes *ValueSet* (i.e. values of the *PGObject* class) with a number of attributes *ParameterSet* (i.e. n parameters defining the *PGObject* class), and (3) *PGOFunction* which is a relation aggregating the *PGOAtom* into a *PGObject*. The model effectively simulated a glacier which has a clear extent at a particular time and space (Kjenstad, 2006). However, tracking the field movement of the glacier in a continuous time and space is not clearly stated in the model, which is an essential functionality to track evolutionary process of the field-object. For example, a UHI can be static in the original location, and a UHI can also shift away from its origin or have an obvious displacement because of the changes of the extent.

Some advanced studies have investigated kinematic analysis to tackle this problem. Work in (Bothwell & Yuan, 2010) proposed fluid kinematic concepts to present continuous fields of temperature by adapting a Eulerian system to measure the velocity of fluid flow at each fixed time and location, and a Lagrangian system to track a fluid region over time and space. The study enabled direct tracking of velocities of fluid flows, and identified rapid moving regions of isotherms. However, this method is not able to calculate displacement vectors of isotherms with complex shapes such as multiple concavities. To tackle this problem, further research in (Bothwell & Yuan, 2012) proposed a simple displacement vector derived from grid data sets. This idea can be used for tracking locational movements of UHIs. However, as a field-object, a UHI has another vital characteristics, i.e., areal extent, since the changes of the areal extent (e.g. expansion or contraction of the extent) and the associations between different extents

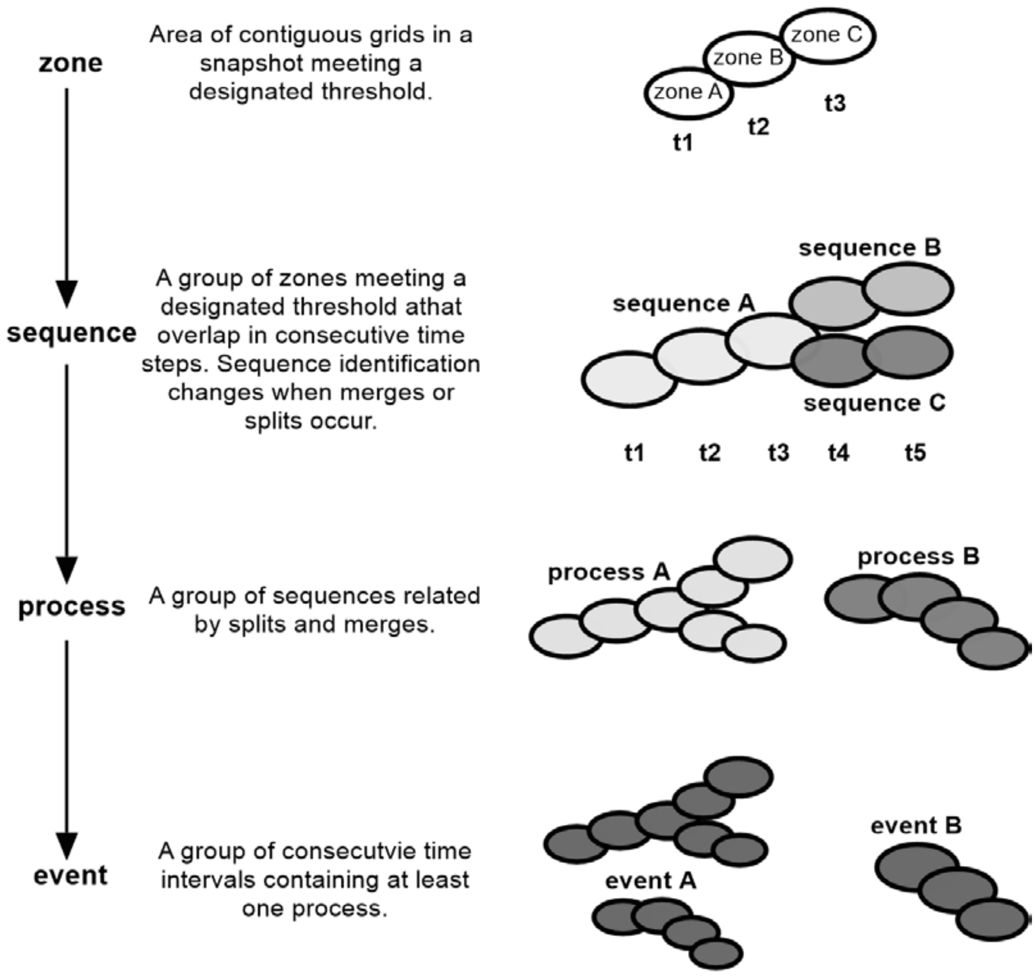

Fig. 2.1 Representational framework (From McIntosh and Yuan, 2005).

(e.g. an extent associating with two UHIs leads to a splitting of the extent) can be used as a direct indication to reflect the intensity changes and evolutionary process of UHIs. Clearly, only relying on the field-object data modeling cannot track these changes.

2.6 Event-based data modeling for field-object

Event-based method models geographical phenomena or dynamic behaviors as event properties or relationships associated with various spatiotemporal attributes (Peuquet & Duan, 1995; Worboys, 2005), which can be achieved by spatiotemporal queries (Pultar *et al.*, 2010; Zaniolo, 2009). For instance, the dynamic behavior of a moving object can be modeled as semantic *events* (e.g. *departure*, *arrival*, or *unexpected destination*) and abstracted as patterns from the event sequences (Hornsby & Cole, 2007). However, topological transition of the field-object is not discussed. By contrast, study in (Jiang & Worboys, 2009) defined basic and complex topological changes of field-objects between structured trees associated with the events classification, and hence presented topological relationships between hollow field-objects and regions.

Another study in (Yuan, 2001) created a hierarchical framework of discrete field-objects based on an event-based conceptual structure, in which a process presents a spatiotemporal sequence of the status and an event aggregates the processes. However, this work has not constructed spatiotemporal queries for knowledge discovery on processes and events. Further study in (McIntosh & Yuan, 2005) proposed a framework for moving objects which contains four definitions, i.e., *zone*, *sequence*, *process*, and *event* as drawn in Figure 2.1:

- *zone* is an area of spatial contiguous grids meeting a designated threshold in a snapshot;
- *sequence* is a set of *zone*s meeting a threshold in consecutive time steps;
- *process* is a set of *sequence*s that the geographical objects are related by splits or merges; and
- *event* is at least one type of *process* during a consecutive time intervals.

This study also created six indices to model the events (i.e. status and behavior) of objects in field characteristics and applied a nearest neighbor approach to query events for similarity assessment.

To summarize, spatiotemporal models were developed for different environmental phenomena such as precipitations (Yuan, 2001). Data were originally represented on raster layers corresponding to different times, and entities were identified on each layer, and models are event or process centred. Processes and events are spatiotemporal objects defined with time attributes (e.g. starting and ending time), thematic attributes and dynamic attributes describing movement (McIntosh & Yuan, 2005) and are linked to entities involved in the events. The data model can indeed combine both raster and vector representations as thematic and kinematic data, which are computed from grid points inside the entities (Bothwell & Yuan, 2010).

This dissertation will also propose a similar but more systematical behavior estimation model particularly for the UHIs. For example, a UHI can also be modeled as a series of zones along with a temporal domain so that a UHI can have one or several sequences that each sequence meets the same behavior for the dynamic attribute. However, this event-based approach does not involve in the topological transformation between zones neither, which is important to model a UHI having a complete life span because UHIs can either continue (e.g. a zone continues by splitting part from its origin) or destroy (e.g. a zone destroys by splitting itself as several parts) when topological transformation occurs. Thus, a further investigation in relationship between field-objects is needed.

2.7 Relationship between field-objects

Topological relationships are defined by topological transitions of two objects in two consecutive time steps. Spatiotemporal topological process involving single and several entities was defined (Claramunt & Thériault, 1995). The definition establishes three different categories to describe evolution:

- evolution of an individual object,
- functional relationships between several objects, and
- evolution of spatial structures between several objects as drawn in Figure 2.2.

In a more detailed level, evolution of a single object contains three types of processes:

- basic process for the representation of attribute variation while without spatial changes (e.g. stability means the area remains unchanged);

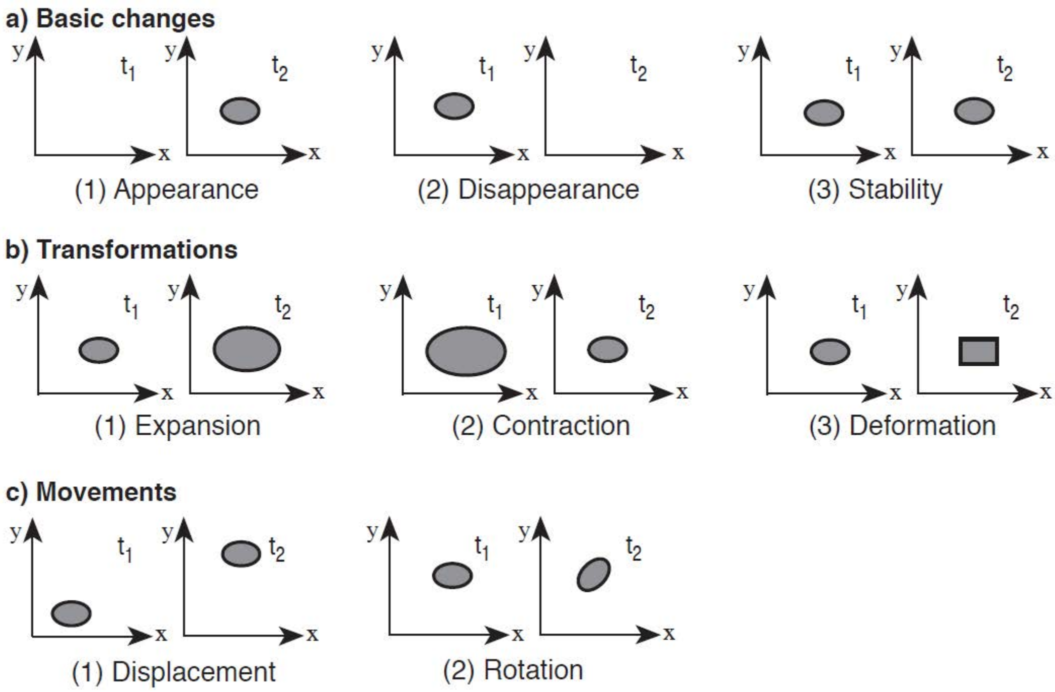

(a) Evolution of a single object.

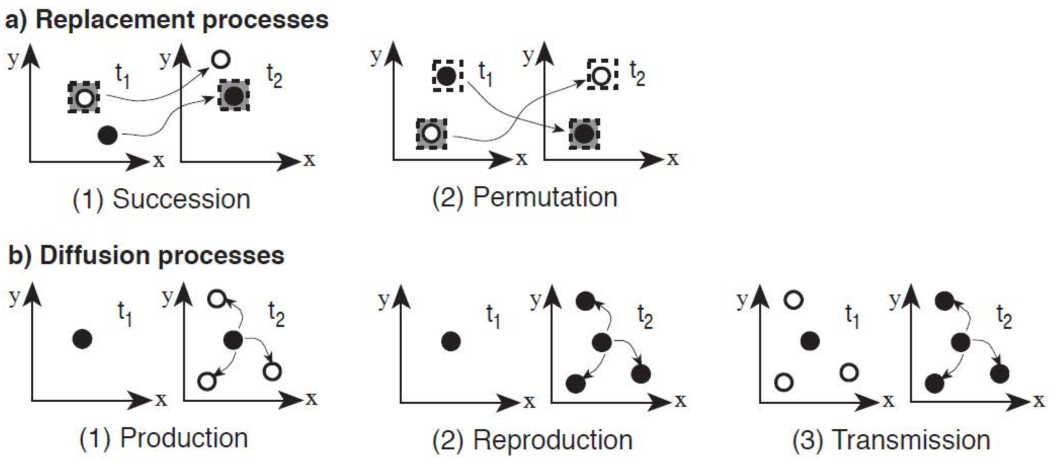

(b) Functional relationships between entities.

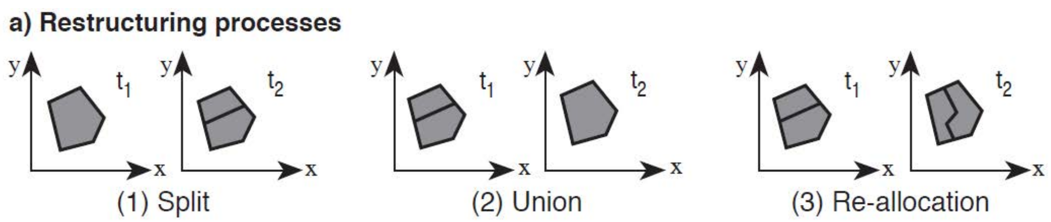

(c) Evolution of spatial structures involving several entities.

Fig. 2.2 Typology of spatiotemporal processes (From Claramunt and Thériault, 1995).

- transformation processes focusing on the changes of shape and size (e.g. expansion describes growth of the area); and

- movement processes involving locational movement (e.g. displacement indicates a polygon is moving without a change of area).

Furthermore, functional relationships involve:

- replacement processes which describe a sequence of objects that construct one process or occupy the same location in space; and

- diffusion processes which transfer characteristics between two or more objects.

The third category concerns the topological changes that link to several objects. This definition systematically describes area changes, topological transformations, and locational movements between one and several field objects. This dissertation will propose a similar but refined model for the behaviors of UHIs. For instance, stability can also be viewed as a special type of areal change so that it can fall into the same group with expansion and contraction.

A more complex taxonomy related to topological change operations (e.g. reincarnation) based on three identified states (i.e. existence, non-existence, and transition) has been provided by (Hornsby & Egenhofer, 2000), which models each entity with its own life-cycle. Similarly, study in (Renolen, 2000) introduced a behavioral modeling framework where each spatiotemporal object experiences its generic behavior as either *alive* or *dead*, and seven types of transition between two status: creation, alteration, destruction, reincarnation, annexation, deduction, and reallocation. Several studies applied this framework in different applications (Bothwell & Yuan, 2011; Guilbert & Lin, 2007; Nixon & Hornsby, 2010) where objects can merge or split leading to the creation and destruction of new objects.

Inspired by the concept of generic behavior, study in (Bothwell & Yuan, 2011) presented a kinematic analysis to tackle a problem that modeling of topological changes has not been established in (Bothwell & Yuan, 2012). The study mathematically quantified the internal changes of *divergence* (i.e. the fractional rate of area changes), *rotation* (i.e. changes in orientation because of the changes of velocities), and *deformation* (i.e. rate of the changed area) for globe water vapour transport, so as to propose six spatiotemporal transition models:

- *emergence* that objects do not exist initially but appear later;
- *dissipation* that existing objects disappear forever;
- *convergence* that objects shrink in area;
- *divergence* that objects expand in area;
- *merging* that several objects join into an object; and
- *splitting* that several objects split from multiple ones.

In particular, study in (Guilbert & Lin, 2007) proposed a snake model to keep track of the life-cycle of a cloud recorded as a polygonal boundary and presented topological operations of cloud splitting, merging, apparition, and removing. Empirical experiment suggests that the model can effectively detect topological changes of clouds; while, it highly relies on complex algorithms.

Another research in (Nixon & Hornsby, 2010) modeled splitting and merging behavior of spatiotemporal objects in two ways, i.e., splitting may result in the continuous existence of the original object or the replacement of new ones, and merging may lead to the continuous existence of one of the original objects or the replacement of a new one. However, other topological transformation operations for spatiotemporal field-object with single attribute, such appearance of a new object versus disappearance of an existing one that may be used for describing behavior of a UHI, are not systemically modeled. These transformations were explicitly described (Del Mondo *et al.*, 2013), which presents spatiotemporal relationships in a graph to continuously track changes of objects over time. Other transitions that affect the shape or thematic attribute of a field-object are not systematically modeled, which can be established by developing some new graphs. Therefore, this dissertation will further develop the topological transition models incorporating with similar generic behaviors as discussed in (Renolen, 2000), which allow temporal UHIs have status transitions between alive and dead through birth, reincarnation, and death.

Study in (Tang *et al.,* 1996) summarized the object-oriented feature-based models which not only can present topological relations among geometric elements but also incorporate non-topological (i.e. semantic) relations among features. In the study, a geographical feature is constructed by feature objects, each of which also contains a geometric object. Associations between feature objects are built by semantic relations. To describe more expressive concepts and more meanings than classical data models, five abstraction mechanisms are also presented:

- *classification* maps the objects that share the same behavior and properties into the same class;
- *generalization* generalizes a superclass that share similar types of objects, or the common properties and operations;
- *specialization* creates object classes which are inherited from that in the higher order;
- *aggregation* collects a set of objects in the subclass to form a parent object; and
- *association* groups similar object classes into a single set.

Essentially, all these abstraction mechanisms can be applied for abstracting useful information from UHIs that share a similar or the same characteristics in different granularities whenever all their behaviors can be tracked through designed groups. For example, all the UHIs which cluster together in a high density and expand significantly during a short time period can be extracted to draw a hotspot representing a serious UHI.

To solve the geo-semantic conflict among different objects, a promising study proposed a conceptual model of geographic spatiotemporal data based on the ontology theory which is a decomposition process of the recognized conceptual fields connecting the real geographical world and the computer world (Li *et al.,* 2013). The model was denoted by a tuple containing five elements, i.e., a geographic ontology model, a geographic entity object, a time set, a represented layer, and a hierarchical relationship. This study will design smart strategies to avoid the geo-semantic conflict problem since it may happen when determining specific dynamic behavior for each UHI.

This dissertation will also build topological transformations for UHIs so that UHIs can *merge* and *split* as proposed in (Bothwell & Yuan, 2012). In addition, the study will further specialize these transformations for different scenarios such as a *specialization* proposed in (Tang *et al.,* 1996) so that a *split* can be specialized as a splitting that a UHI is destroyed by splitting itself into pieces and a separation that a UHI continues by splitting one or several parts from its origin. Similar with the study in (Renolen, 2000) that objects have generic behaviors either *alive* or *dead*, a UHI will also be modeled as having different life statuses of alive or dead triggered by the expressed behaviors (e.g. appear or disappear). According to the suggestion that *emergence* leads to the appearance of objects from nonexistence (Bothwell & Yuan, 2012), a UHI will also be considered to have several exist periods connected by non-exist periods so that a UHI can be periodic, which is benefit for tracking a complete life-cycle of UHIs over a long time period. This life-cycle modeling is an original contribution in spatiotemporal data modeling.

2.8 Conclusion

Overall, traditional field-based and object-based models provide a new idea for the UHI generalization but they still face the difficulty in modeling dynamic topological transformation for fields. Kinematic analysis and event-based approach have already established some practical methodologies for topological transformation but systematic modeling particularly for UHIs is still rare and elementary.

The objective of this study is to provide a novel object-oriented model where UHIs are seen as spatiotemporal objects with their own thematic and field attributes and their relationships evolving through space and time. The purpose of this model is to extract spatiotemporal processes of UHIs in their life-cycle so as to provide a qualitative description of the UHI behavior. It can be performed by extracting the dynamics of a UHI during its whole lifetime through the analysis of a set of images automatically. Such an approach requires the inclusion of the temporal dimension and the extension of the 2D raster model to a spatiotemporal model which can also support queries to retrieve data according to dynamic phenomena of interest. This approach can also record the processes of UHI properties in a spatiotemporal database which allows the retrieval of UHI behavior through simple queries. Processes and events are stored and queried directly in the database which can allow further analysis of the relationships between UHI and the environment.

Chapter 3

Object-oriented modeling of urban heat islands

3.1 Introduction

Since previously proposed spatiotemporal data models are not able to effectively model dynamic changes of field geographical phenomena, this chapter will conceptualize UHIs as field-objects so that each UHI can have several behaviors expressed over time. UHIs are considered to have three types of behaviors in terms of the temperature changes, locational changes, and area variations. For example, a UHI can become significant because of the rising temperature difference between urban and rural areas. A UHI may grow larger continuously when its areal extent is expanding, and it may also have obvious displacement because location of the areal extent is moving away from its origin.

Section 3.2 conceptualizes each UHI as a field-object so that its spatial and thematic prosperities can change continuously over time. Five concepts related to the characteristics extracted from a series of thermal images are also proposed. Section 3.3 models thematic and locational behaviors of UHIs oriented on the extracted multiple zones of each UHI from thermal images. Furthermore, Section 3.4 considers the distribution variations of the temperatures within the zone to systematically model the behaviors.

For example, the maximum temperature of each zone is used as the representative temperature to model thematic behaviors. However, the set of the temperatures equaling to the maximum temperature within the zone may be in a dense cluster so that the areal extent of the cluster shall be too small to be representative enough. Thus, this section proposes a core-oriented model to describe the spatial behaviors. Furthermore, Section 3.5 models life-cycle of UHIs involving a long time period. Finally, Section 3.7 summarizes the findings.

3.2 UHI as a field-object

UHI can be defined as a climatological phenomenon since their temperatures are based on long-term statistics. For example, global UHI data set provided by NASA (Socioeconomic data and applications center, 2017) is a set of long-term statistical data, representing Land Surface Temperatures (LST) covering a time-span of 40 days from July to August. However, detailed investigation of this phenomenon shall depend on short-term analysis because its causative factors, as discussed in Chapter 1, are mostly dynamic such that the characteristics of UHIs can change significantly in a short time period. Thus, conceptualization of UHI will model its characteristics at a time instant, and the research will use observed data (e.g. hourly temperature data) as a proxy for both short-term analysis of UHI effects and long-term evolutionary trends.

There is a direct indication to measure the intensity of a UHI named as *sensible heat*, which is certain amount of the heat causing temperature changes in the air (Mills *et al.,* 2016). However, measuring sensible heat of air accurately over the urban area is a great challenge. The other measurable heat flux is *latent heat*, which is thermal energy released or absorbed by human bodies or a thermodynamic system (Wikipedia for latent heat, 2017). This heat flux is one of the anthropogenic heat fluxes, having a small proportion of the total amount of the anthropogenic heat (Chow *et al.,* 2014). Another method to describe the intensity of UHI is to measure ambient temperatures, which can be the land surface temperatures, near-surface air temperatures or the atmospheric boundary layer temperatures (Pal *et al.,* 2016). Thus, a UHI is widely defined as an environmental phenomenon where temperatures in urban areas are significantly higher than in surrounding rural areas (Nichol *et al.,* 2009).

Based on the above perception, a UHI can be conceptualized as a two-dimensional field where its areal extent can expand, contract, or remain stable possibly because temperatures warm up, cool down, or keep constant through continuous time and space. Therefore, a UHI can be seen as a variable field whose thematic attribute is the temperature measured in urban areas that are with certain degrees Celsius difference from a reference temperature observed in rural areas at the same time. In this stage, other factors that influence temperature variation and thermal exchanges at different elevations are not considered. Even though some studies indicated that UHI may be a localized phenomenon which does not shift from its original location and the displacement is not obvious (Hua & Wang, 2012; Jalan & Sharma, 2014), this study attempts to model its locational behavior to reveal various movement trends. In addition, UHI movements related to the areal extent are modeled. From the above conceptualization, a UHI can be integrated as a field-object with four components:

- the first spatial component defined by a polygon delineating its extent;
- the second spatial component defined by a point to describe its location and construct its moving trajectory;
- a thematic component which is the temperature intensity observed from the thermal image and defined as a field variable; and
- a temporal component allowing the description of its *life-cycle* in consecutive time instants.

On top of these, a UHI can go through spatiotemporal transformations describing a change of status or its relationships with other UHIs. For instance, a UHI may split into two UHIs or disappear when the temperature intensity decreases. This shows

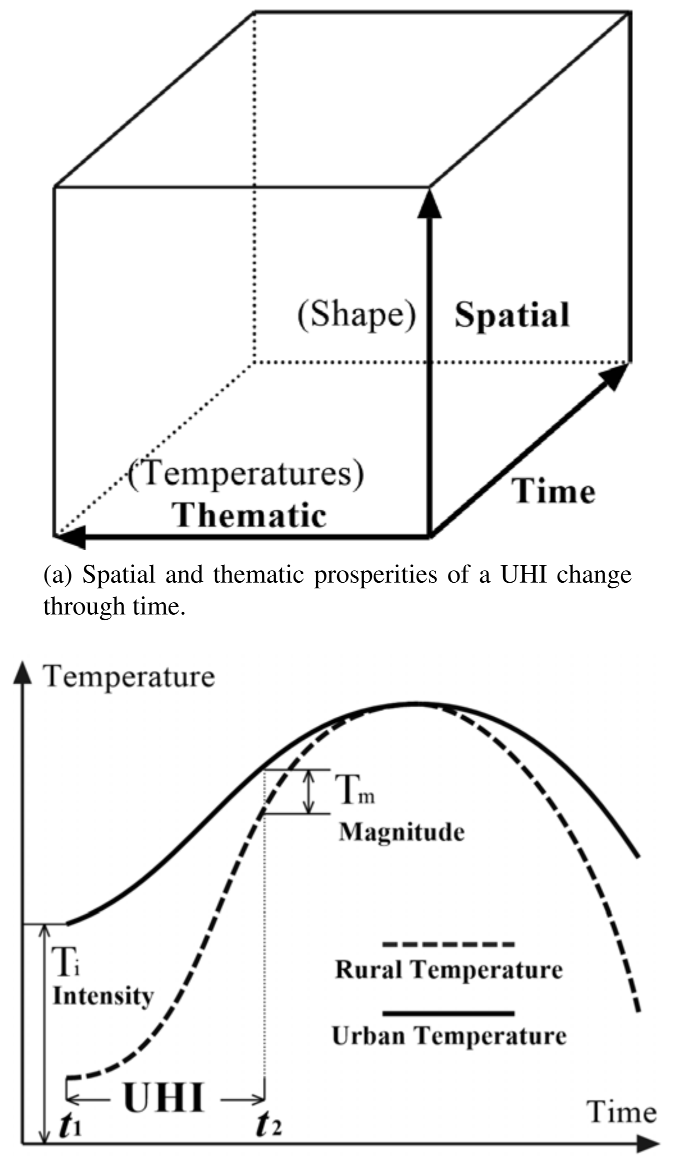

(a) Spatial and thematic prosperities of a UHI change through time.

(b) UHI is with a *magnitude* higher than the referenced rural temperature.

Fig. 3.1 Changes of the temperatures in a UHI triggers the change of its spatial extent over time.

that topological transformation determined by thematic characters can also trigger the transition of status its life-cycle.

Thematic and spatial properties of a geographical phenomenon can change simultaneously over time as shown in Figure 3.1a. For a UHI phenomenon, the changes of temperatures (i.e. the thematic property) determine the shape and location changes (i.e. the spatial property). Intensity is generally a quantity over a unit, so that temperature may be measured in area-average or per-distance and considered as UHI intensity. Recently, UHI intensity has been widely defined as the temperature difference between urban and rural areas (Martin-Vide *et al.,* 2015). This definition makes a UHI occur as long as its temperatures are higher than the reference rural temperature, and spatial extent of the UHI is deterministic. However, a UHI shall be at least with certain temperature higher than the reference rural temperature to distinguish the peaks of intensity and define several UHIs where there was only one before, which may create inclusions between UHIs. For example, one study has suggested that micro heat islands in the same urban area changed sensitively in short term, and had negative effects to the public health (Goggins *et al.,* 2012), which indicates that the study has allowed several UHIs to occur in the same urban area. In this consideration, a UHI can be viewed as an urban area where its internal temperatures are with a given temperature higher than its reference rural temperature. Thus, a UHI can be formulated.

- **An urban heat island** is a two-dimensional urban area where its internal temperatures are with a given temperature (i.e. *magnitude*) higher than its reference rural temperature.

As shown in Figure 3.1b, a UHI exists during $[t_1, t_2]$ since urban temperatures are at least with given temperatures (i.e. *magnitude*) higher than reference rural temperatures. In a wide temporal scale, a UHI can disappear and appear periodically because of the fluctuation temperatures, acting as an object in different statuses. Thereby, a UHI can be defined.

- **An urban heat island** is a field-object with four properties, i.e., *temperature* that represents the UHI intensity, *location* that depicts the geographic location so that a time series of locations can be used to represent its movement trajectory, *zone* that describes a variable extent, and *time* that provides a temporal scale for the description of the thematic and spatial evolution.

As such, a UHI can be characterized from a series of thermal images obtained at regular time interval. Following the definitions that have been introduced (McIntosh & Yuan, 2005), several definitions related to the UHI are introduced.

- A *zone* is an enclosed extent region denoting the areal extent of a UHI at a specific time instant.
- A *sequence* is a series of zones observed on consecutive images at a given location. Such a sequence corresponds to the observation over a time range of a UHI going through continuous change in shape.
- A *transformation* connects sequences together through a topological transformation such as a split or a merge. It occurs at a given time instant between two or more UHIs.
- A *transition* connects two consecutive sequences of a UHI when it continues, which possibly associates with *transformation*.
- A *chain* connects a series of zones in continuous *sequences* when *temperature* changes in a single trend over a time period, e.g., continuously increasing or decreasing.
- A *queue* connects a series of zones in continuous *sequences* when displacement develops in a single trend, e.g., constantly moving or stopping.

3.3 Zone-oriented behavior modeling

The variations of the thematic and spatial properties can be caused by the changes of ambient temperatures. Because of the air flows, thermal exchanges can lead to the variation of shapes for the region, such as expanding, contracting, or still remaining the same. Due to this reason, some air temperatures within the region may decrease continuously, which can cause that the original region divides into two parts with fuzzy boundaries, and finally splits into two independent hot-regions. In another scenario, two regions are expanding continuously and getting closer with each other because the heat in the two regions are accumulating. At certain time instant, the two regions may interact with each other and start the fusion processing with the thermal exchange immediately. This could be a complicated air-dynamic process, either the two regions merge together and become a large region or the larger region neutralizes the smaller one and remains almost the same.

Based on the above reasoning, zones of UHIs can have either area changes or topological transformations. More specifically, a UHI may contract and split into several ones when temperatures decrease, and several UHIs may also expand and merge together as a single one when temperatures increase. This section includes two categories of *areal change* and *thematic change* in terms of spatial and thematic property changes. For the ease presentation, let z_n^i be a zone index by n at time instant t_i in a spatial and temporal domain.

3.3.1 Spatial behavior of the UHI

Filiations between zones can be refined into several possible relationships. Concerning geometrical changes occurring within one UHI, filiations can be organized as:

- *continuation* when two zones z_n^{i-1} and z_n^i have a similar spatial extent;
- *expansion* from zone z_n^{i-1} to z_n^i where the geometry expands; and
- *contraction* from zone z_n^{i-1} to z_n^i where the geometry contracts.

As summarized in Figure 3.2, topological transformation can also appear associating with at least three zones at the same time. This study also adds two special transformations as the following:

- *splitting* when one zone z_n^{i-1} splits into two zones z_m^i and z_p^i;
- *merging* when two zones z_m^{i-1} and z_n^{i-1} merge into one zone z_p^i;
- *separation* when one zone z_n^{i-1} is associated to two zones z_n^i and z_m^i;
- *annexation* when two zones z_n^{i-1} and z_m^{i-1} are associated to a third zone z_n^i;

- *appearance* if a zone z_n^i is not related to any zone at t_{i-1}; and
- *disappearance* if a zone z_n^{i-1} is not related to any zone at t_i.

3.3.2 Thematic behavior of the UHI

Since the observed temperatures within the extent of a UHI can change differently, a statistical indication is needed to represent the overall trend of the UHI thematic property. Let $\{v_j\}$ be a set of thematic values within the boundary of the zone, and let s_n^i denote the thematic indication obtained from $\{v_j\}$ and named as *temperature* for UHI (denoted as u_n) at time instant t_i. s_n^i can be the maximum, mean, median or mode value of the observed data (Zhou *et al.,* 2016), i.e., $s_n^i \in \{max, mean, median, mode\}$. Each indication has its own tendency to reveal different thematic change characteristics. For instance, the maximum value reveals the most intense character of UHIs but the number of this value can be rather small and is not representative enough to describe the overall evolutionary trend. Whereas, the mode value shall fully represent the overall thematic evolution trend even it may not be the highest intensity. To maintain the unity and continuity of the thematic character, a specific thematic indication should be used constantly during the whole life span of a UHI. Hence, new relationships between zones based on the intensity can be represented as three qualitative descriptions:

- *increasing* when *temperature* s_n^{i-1} is higher than s_n^i;
- *stationary* when *temperature* s_n^{i-1} is almost the same as s_n^i;
- *decreasing* when *temperature* s_n^{i-1} is lower than s_n^i.

3.4 Core-oriented behavior modeling

In the previous section, all the filiations are determined by investigating the relations between zones in two consecutive time instants. For example, two zones that have significant overlapping in two continuous time instants can be viewed as the same UHI

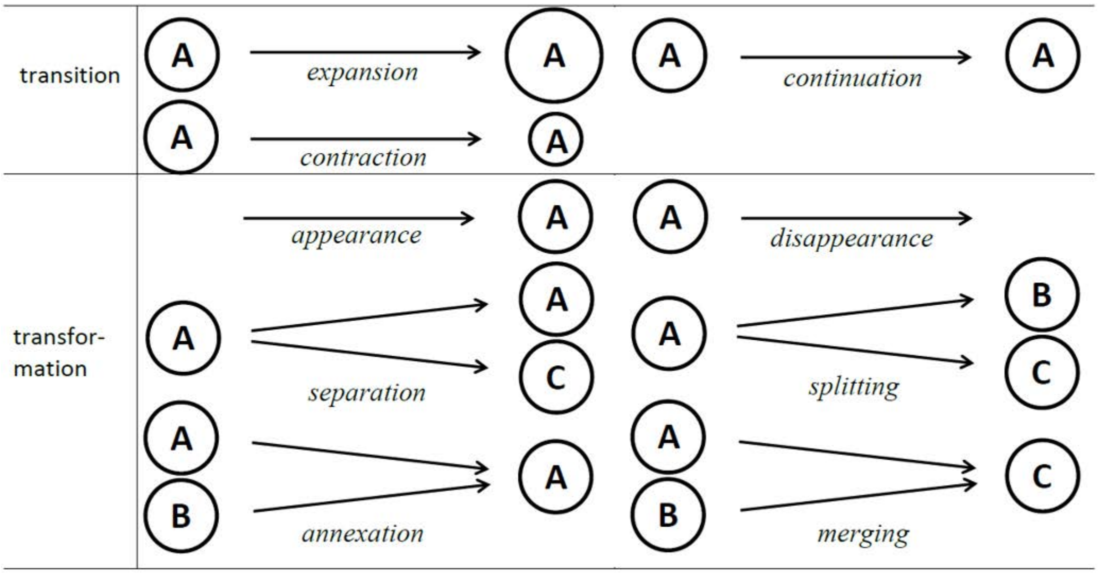

Fig. 3.2 Filiations between zones.

in two statuses. Hence, thematic behavior is determined by comparing the statistical *temperature* (i.e. *max*, *mean*, *median*, or *mode*), and spatial behavior is assigned in comparison of the two areas. However, determining the two zones as two consecutive statuses of the same object is not credible if it meets three conditions simultaneously: (i) temperatures in some areas of the zone equal to the statistical *temperature*, (ii) the areas only take small proportion of the zone, (iii) and these areas are not located in the overlapping area of the two zones. As drawn in Figure 3.3, two zones z_a^{i-1} and z_b^i have significant overlapping and the maximum temperature of the zone is used as the statistical *temperature* so that areas having the the maximum temperatures of 37 degrees Celsius at t_{i-1} and 36 degrees Celsius at t_i are separated. It is more convincing to state that the two zones are apparently touching with each other but substantially have no association with each other.

Based on the above consideration, original strategy can potentially cause misleading determination of the thematic and spatial behaviors. Thus, this section considers spatial distribution of statistical *temperature* and spatial filiations between zones to model dynamic behaviors of UHIs. Furthermore, the locational behavior of the UHI is also modeled. A study in (Guilbert & Moulin, 2017) proposed a core region to describe

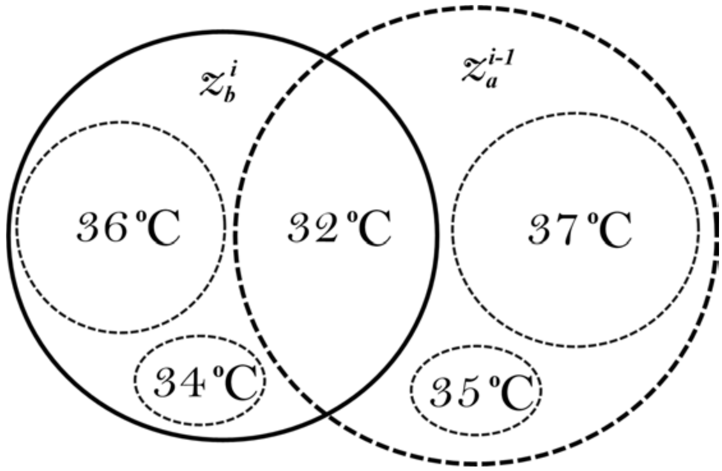

Fig. 3.3 Two zones apparently touch each other and essentially have no association since their areas equaling to the maximum temperature are not in the overlapping area.

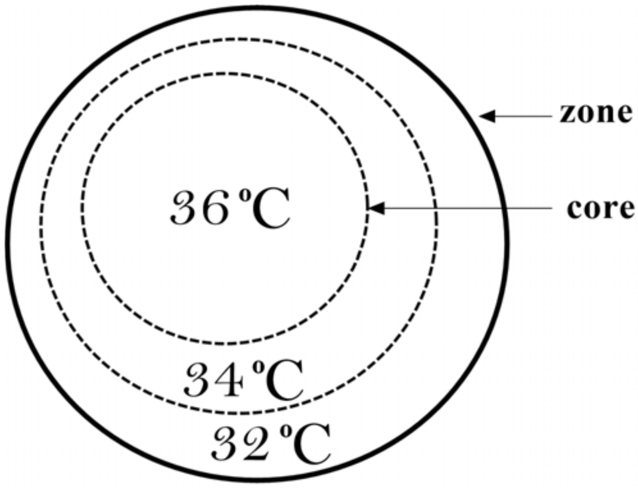

Fig. 3.4 Core is inside of the zone, which represents an extent of a set of the spatial contiguous of the statistical temperatures.

complex landform of canyons, which is one of the most representative characteristics for canyons. With the similar consideration, a zone can also have a representative core region that temperatures within the core region are equal to the statistical *temperature*. As drawn in Figure 3.4, a core is an enclosed region in the zone that temperatures within the region equal to the statistical *temperature* (i.e. the maximum temperature) of 36 degrees Celsius. For the ease of representation, a new concept of core is introduced so that the core-oriented behavior modeling can be proposed in the followings.

- A *core* is an internal area of the zone, which contains a set of the spatial contiguous of the temperatures that are equal to or higher than the statistical *temperature*.

3.4.1 Spatial behavior of the UHI

Zone filiations were determined only based on spatial relationships between zones that they have either overlapping or non-overlapping options (Zhu *et al.,* 2016). However, examining only the spatial relationships (overlapping or non-overlapping) between zones to determine their filiations can be misleading. For instance, zones of (z^{i-1}, z^i) that have significant overlapping were perceived as the same UHI, and hence specific filiation can be further identified. However, thematic cores of both zones may not locate in the overlapping region but are separated in the non-overlapping region of each zone. Then, it is reasonable to say that they are only apparently *overlapping* and they are not associated to the same UHI. For the other example, zones of (z^{i-1}, z^i) may overlap with each other insignificantly while their cores are all located in the overlapping region. In this case, it is convincing to state that these two zones belong to the same object, having locational *shifting*. Therefore, spatial relationships between zones and spatial distribution of thematic temperatures shall be considered simultaneously to model filiations between zones.

When several UHIs interact with each other in the same spatiotemporal domain (i.e. one city can have multiple UHIs simultaneously), it is crucial to firstly determine the relationship between zones at two consecutive time instants to model their dynamic behaviors, i.e., to list the sequences of zones in a temporal domain that belong to the same UHI. According to the above the perception, relationship between zones are essentially determined by topological relationships of cores between different zones. Therefore, at least one core r_n^{i-1} associating with the other one r_n^i is the pre-condition to build zone filiations. For a pair of spatially associated zones (z_n^{i-1}, z_n^i), zone filiations in view of area changes are thus organized as:

- *expansion* when r_n^{i-1} associates with r_n^i and geometry expands from z_n^{i-1} to z_n^i;

- *continuation* when r_n^{i-1} associates with r_n^i and spatial extent of geometry is similar from z_n^{i-1} to z_n^i; and

- *contraction* when r_n^{i-1} associates with r_n^i and geometry contracts from z_n^{i-1} to z_n^i.

At a time instant, UHIs alternatively have *transformation* or *areal change* (Zhu *et al.,* 2016). However, this study suggests that both can happen simultaneously in two specific scenarios, i.e., *separation* and *annexation* when the zone still exists. The reason is that deformation of the original zone z_n^{i-1} in these two affiliations is not interrupted even at a specific time instant when topological transformation occurs such that area changes still can be determined as usual. For pairs of zones $(\{z^{i-1}\}, \{z^i\})$, topological *transformations* are refined as:

- *splitting* when one zone z_n^{i-1} only spatially associates with two zones z_p^i and z_q^i;

- *separation* when r_n^{i-1} associates with r_n^i and z_n^{i-1} also has spatial association with z_n^i and z_p^i;

- *merging* when two zones z_p^{i-1} and z_q^{i-1} only spatially associate to one zone z_n^i; and

- *annexation* when r_n^{i-1} associates with r_n^i and two zones z_n^{i-1} and z_p^{i-1} are spatially associated to one zone z_n^i.

While, two special transformations may happen that either z_n^{i-1} or z_n^i cannot determine any associations, leading to the creation of a new zone or destruction of an existing zone:

- *appearance* when one zone z_n^i has no association with any other zones at t_{i-1}; and

- *disappearance* when one zone z_n^{i-1} is not related with any zones at t_i.

3.4.2 Thematic behavior of the UHI

The same as the zone-oriented approach, thematic *temperature* is needed to describe evolution of the thematic property continuously for a long time period. In addition, four statistical values can be used as the indices, i.e., the maximum, mean, median, and mode values of a complete set of the thematic property values, all of which are able to reveal the thematic characteristics in different aspects. Obviously, all the cores meet the same condition that temperatures in the cores are equal to or higher than the thematic *temperature*. When a pair of zones have been determined as the same object, thematic behaviors hence can be qualitatively described as *increasing*, *stationary*, and *decreasing* by comparing the thematic *temperatures* s_n^{i-1} and s_n^i.

Compared with the zone-oriented modeling, the core-oriented modeling describes a more constrained area (i.e. moving from a zone to one or multiple cores of the zone) for the spatial distributions of the statistical temperatures. Even there can be several cores in a single zone, their thematic statistics are homogeneous since they all meet the same statistical condition, which thus does not cause difficulties in the description of the thematic behaviors.

3.4.3 Locational behavior of the UHI

It is widely acknowledged that movement of the objects will lead to the displacement of their locations. Thus, locational behaviors can be represented by different displacements of zones. An effective method to identify different displacements is to determine topological relationships between zones. For example, a static UHI without any movement means that their zones may coincide with each other, and a UHI significantly moves far away from its origin would correspond to the disjoint of two zones at t_i and t_{t+1}. In this situation, several types of topological relationships between zones have to be refined and constructed.

Let z_n^i denote the zone of a UHI u_n $(n \in \{1, ..., m\})$ at the time instant t_i. A study proposed a Voronoi-based nine-intersection (V9I) model which includes a topological

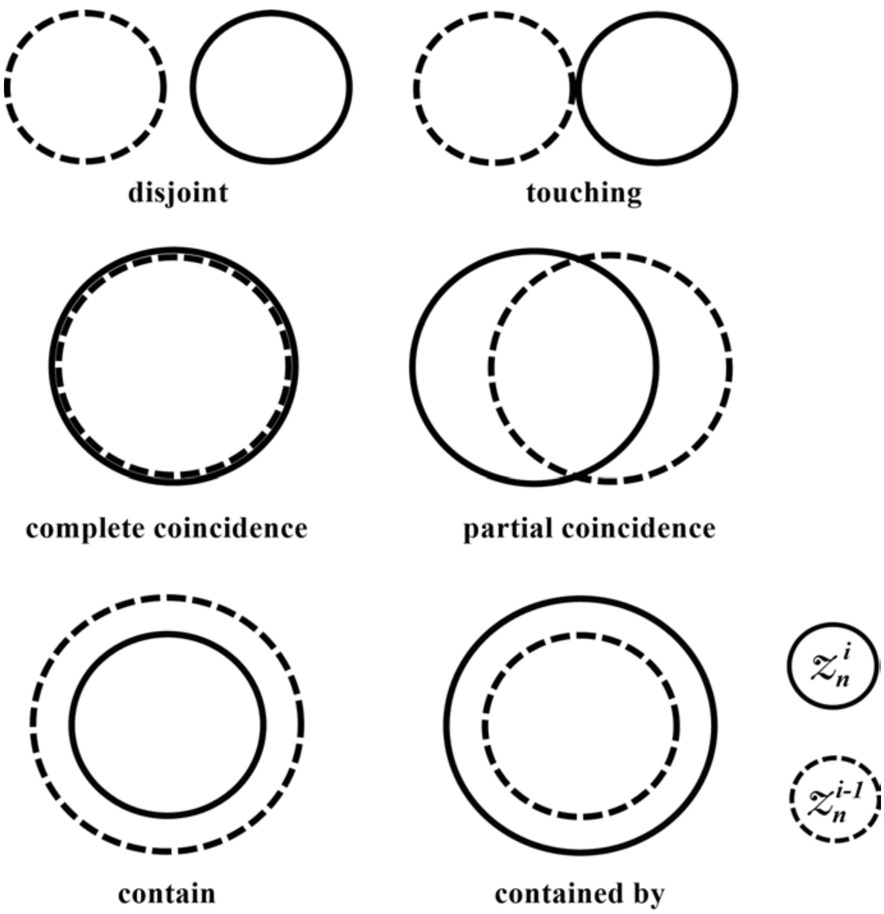

Fig. 3.5 Spatial relationship between a pair of zones (z_n^{i-1}, z_n^i).

relation between two areas with a four-intersection (area, area) matrix (Long & Li, 2013). According to the needs of this study, spatial relationships between any two zones in two time instants of the same spatial domain are summarized in Figure 3.5 and reorganized as:

- *disjoint* when z_n^{i-1} does not connect with z_n^i;
- *touching* when z_n^{i-1} just contacts with z_n^i;
- *complete coincidence* when z_n^{i-1} completely overlaps with z_n^i;
- *partial coincidence* when z_n^{i-1} partially overlaps with z_n^i;
- *containing* when z_n^{i-1} includes z_n^i; and

- *contained by* when z_n^{i-1} is inside of z_n^i.

This study considers that a pair of zones (z_n^{i-1}, z_n^i) have closer relations and have more iterative behaviors when they are spatially closer with each other. Zones which are stationary shall continuously stay at the same place without any locational displacement while extent variation, such as expansion, contraction, or stabilization, is allowed. A pair of zones can also have notable but insignificant locational displacement, allowing them to have locational changes within certain distance. The last possibility is that zones maintaining their spatial extent are moving away dramatically from their origins. Based on the above idea from Section 3.4.1 that two zones have been determined as two consecutive statuses of the same object, the two zones are thus conceptualized as:

- *stopping* when (z_n^{i-1}, z_n^i) are *containing*, *contained by*, or *complete coincidence*;
- *shifting* when (z_n^{i-1}, z_n^i) are *touching*, or *partial coincidence*; and
- *moving* when (z_n^{i-1}, z_n^i) are *disjoint*.

3.5 UHI life-cycle modeling

Establishing the periodicity would be much helpful not only to understand mechanisms of the UHI periodicity but also to reveal the thematic and spatial trends of UHIs over a longer temporal domain (i.e., monthly, seasonal, or even yearly). In a long temporal scale, a UHI can disappear and appear periodically because of the periodic declining and raising of the temperatures. For example, a UHI appears and disappears periodically at the same place for five days (Zhu *et al.,* 2016), which can be the same UHI having a periodical evolution trend. As a notable contribution to the UHI, anthropogenic heat flux also has an obvious periodical pattern in both spatial and temporal domains (Smith *et al.,* 2009).

Corresponding to this phenomenon, a UHI can have *active* and *inactive* statues in its life-cycle or it can be *dead* if it disappears for good, and the time span of each statue (either *active* or *inactive*) can be named as a *period*. As shown in Figure 3.6, a UHI

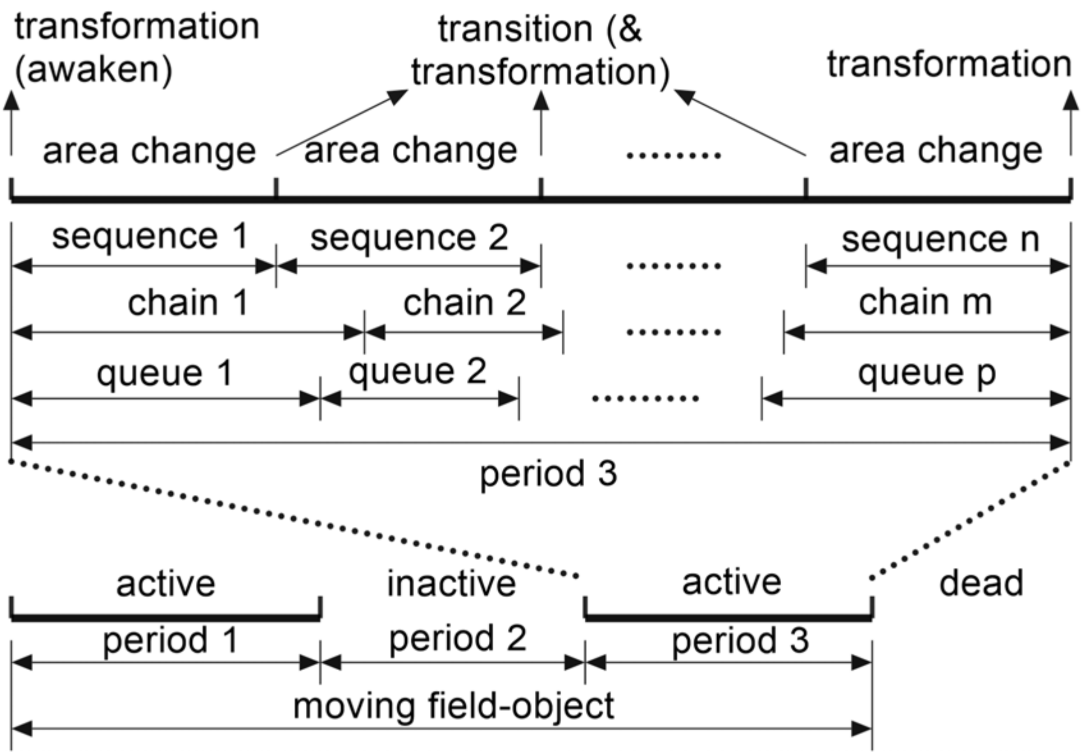

Fig. 3.6 Complete life-cycle of a UHI.

conceptualized as a field-object contains three periods, in which the inactive period has a head-to-tail ligation to two active ones, and the UHI is dead with the destruction of the second period. In this scenario, *appearance* of a UHI can indicate a special transition of *awaken* given the condition that it was *active* before. Thus, a *period* can be described by a series of behaviors continuously in a temporal domain in an either constant or inactive state. Particularly, each inactive statue corresponds to an *empty* period. Obviously, a UHI can have statue transitions between *active* and *inactive* if it has the periodicity, and it has two different time periods connecting with each other:

- the *active period* is a series of sequences that a UHI starts from creation and stops at destruction connected by transitions of area changes of the zones; and
- the *inactive period* is an empty sequence that a UHI temporally disappear, which connects two active periods in between.

An *active period* of a UHI can start from *appearance*, *splitting*, *merging*, *sepa-*

ration into zones and end by *disappearance*, *splitting*, *merging*, and *annexation* for zones that are destroyed. However, the end of the *active period* followed by an *inactive period* instead of the death of the UHI indicates that the UHI is temporally disappeared and it will appear again as an *awaken* in certain time period. This transition requires some topological constrains: the disappeared zones cannot be destroyed by the absorption (i.e. *annexation* and *merging*) since the absorption causes the zones to be destroyed for good, and the appeared zones cannot come from the dispersion (i.e. *separation* and *splitting*) because the dispersion generates totally new objects. Thus, only the consecutive *disappearance* and *appearance* can lead to an *awaken*, and difference between *formation* and *awaken* can be achieved by searching whether there is a vanished zone that can connect the existing zone by an empty sequence.

When a UHI is active, it can be described by a series of sequences where each sequence corresponds to a specific spatial behavior. These sequences are connected by transitions and transformations. A sequence is defined by a series of transitions of the same type. For two zones z and z', we note the function relation(z, z') returning the type of relation between the two zones. Given a series of n consecutive zones z^i observed between t_1 and t_n, these zones form a sequence if for two consecutive zones, we have relation$(z^i, z^{i+1}) = $ relation(z^1, z^2).

In contrast, no behavior occurs when a UHI is inactive even it still exists. In this scenario, a special sequence still can be made as an *empty* sequence during the inactive period. By this means, sequences can continue without any interruption during the statue transition process. Eventually, each UHI can be defined as an object composed by a set of sequences. A UHI also goes through changes which can be internal (continuous transitions) or external (transformations) involving topological changes. In the object-oriented model, changes can be perceived as behaviors of objects and can be specialized into continuous transitions and transformations. Continuous transitions are components of UHIs while transformations are connected to one or more UHIs with three items of associations:

- a *transformation* can generate a UHI (appearance, separation, splitting, merg-

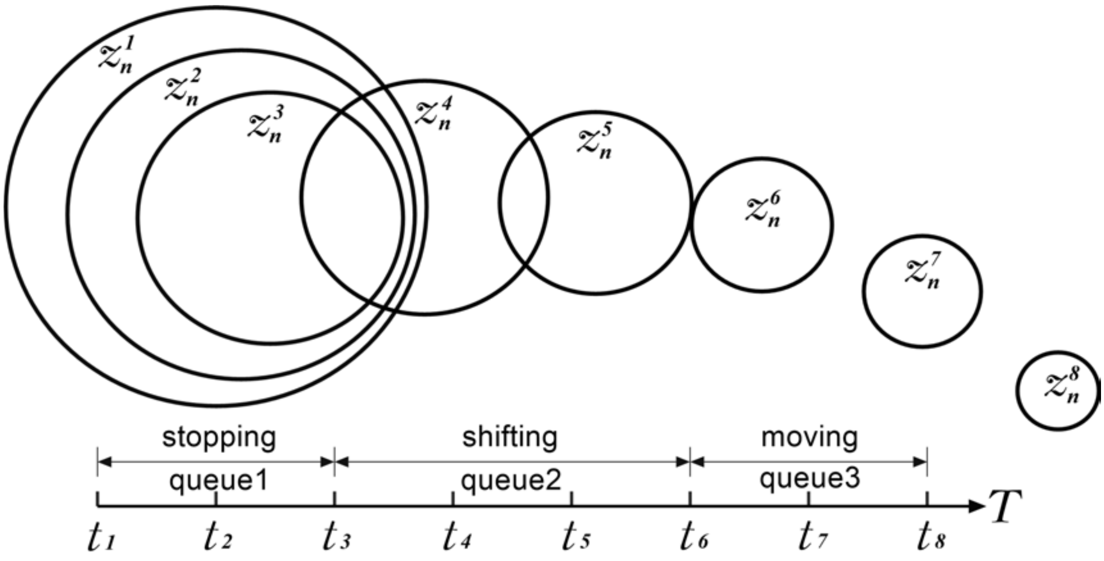

Fig. 3.7 A UHI are continuously *stopping*, *shifting*, and *moving* in three consecutive queues from t_1 to t_8.

ing);

- a *transformation* can terminate a UHI (disappearance, splitting, annexation, merging); and
- a *transformation* can modify the shape of a UHI (annexation, separation).

As proposed in Section 3.2, an uninterrupted displacement corresponds to a queue. The displacement can be either static (i.e. stopping) or dynamic (i.e. shifting or moving). With the same approach, an *empty* queue can also be designed during the inactive period so that queues will continue during the whole life span. Since a UHI does not move in a regular rule, determining its consecutive queues would explicitly describe the displacement patterns of the locations. As drawn in Figure 3.7, z_n^1 continuously contracts as z_n^2 and z_n^3, where extent of z_n^2 is covered by z_n^1 and z_n^3 is covered by z_n^2, which leads to a *stopping* queue for the locational behavior of a UHI. Hence, the UHI is *shifting* since zones partial coincide and touch with each other during $[t_3, t_6]$. Then, the UHI obtains a *moving* because their zones are disjoint. Notably, time periods for a sequence and a queue does not necessarily coincide with each other but also can be in-

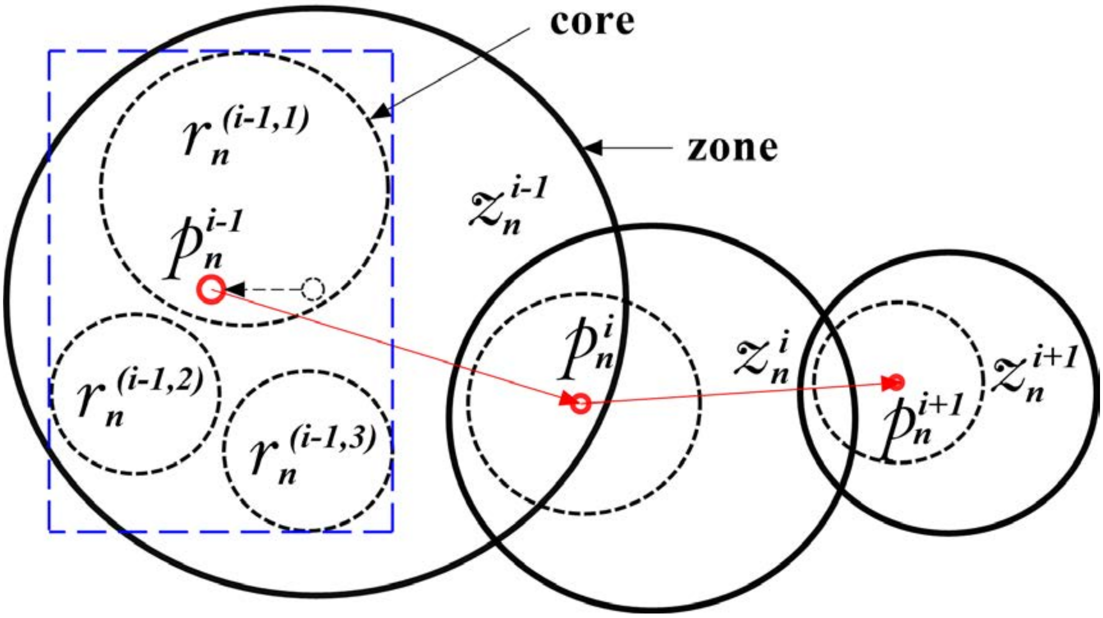

Fig. 3.8 Shift the center of mass of the zone to the centroid of the minimum enclosing rectangle of all the cores.

terlaced (Figure 3.6). For example, a UHI can have no displacement for a time period, which corresponds to a *stopping* queue. Simultaneously, areal extent of the UHI can continue and expand during the same time period, making two consecutive sequences. This interlacing shall be an interesting phenomenon to determine different causative factors.

3.6 Trajectory determination

When all the behaviors are established, an auxiliary task can be visualized areal extents and trajectory of each UHI over time. Areal extents can be visualized by simply plotting the polygon of each zone z_n^i at each time instant t_i. However, construction of trajectories shall be subjectively determined. As mentioned above, there may be several cores that values of the thematic property in these cores equal to the thematic *temperature*. Let k number of these cores in the boundary of z_n^i be denoted by $\{r_n^{(i,k)}\}$ $(k = \{1, ..., l\})$. Since cores essentially represent hotspots of the zone caused by spatial distribution of the interested temperatures, it is much more meaningful to consider that the centroid of the zone is determined by the set of cores instead of setting it at the center of the zone. Since there can be several cores that their areas are almost the same, still setting the centroid as the center of either core is not convinced. An appropriate solution is locating it at the centroid of the minimum enclosing rectangle of all the cores and noted by p_n^{i-1} as shown in Figure 3.8. This solution considers the contribution of each core to the centroid displacement. As such, routing trajectory for each UHI can be depicted by a polyline noted as $\{p_n^1, p_n^2, ..., p_n^i\}$, and it can be easily extended by adding a new point p_n^{i+1} at t_{i+1} to the trajectory.

3.7 Summary

The proposed conceptual model offers definitions that allow the complete description of the qualitative dynamic behaviors of a UHI over time for three properties of the zone, intensity, and location. A zone which continuously has areal changes can be conceptualized as *expansion*, *contraction*, or *continuation* when the area is getting larger, smaller, or almost the same, respectively. A zone can also have topological *transformation* when it has associated relationships with several zones. More specifically, it can associate with others as *separation* when part of the zone is separated from the original as one or several new ones, or as *annexation* when the zone absorbs others into its own. In contrast, a zone can also be destroyed due to *splitting* when the zone is deconstructed followed by several newly generated zones, or *merging* when the zone together with others is destroyed and aggregated as a new one. During a special transformation, a zone may *appear* or *disappear* when it is newly generated or destroyed.

For a clear description of the construction of a UHI, all the behaviors are refined into a hierarchical class diagram as shown in Figure 3.9. It shows that the life span of each UHI is composed of one or several periods transited as being active or inactive, and changes of each period in the same trend for a time period in terms of area of the

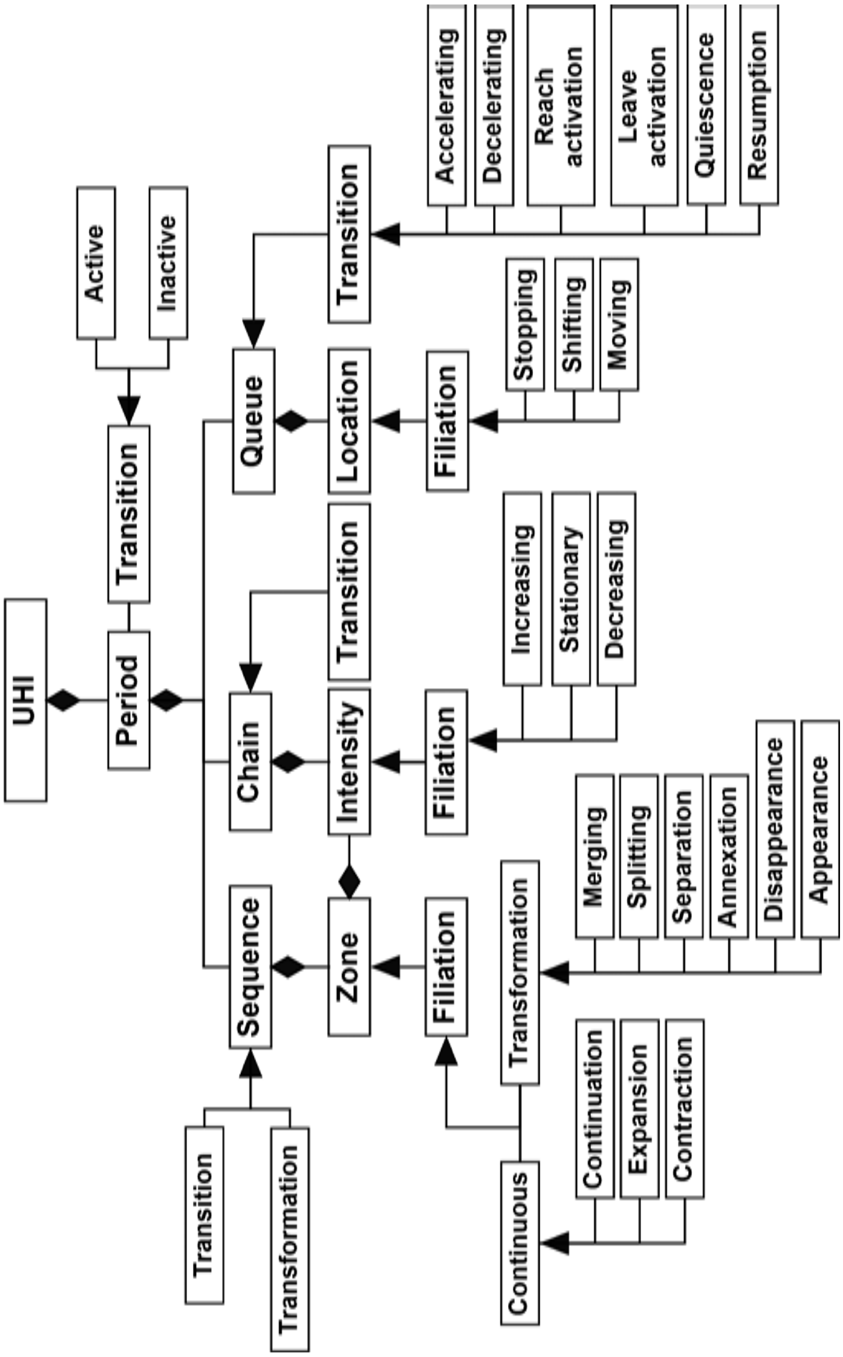

Fig. 3.9 A diagram for UHI properties and their filiations.

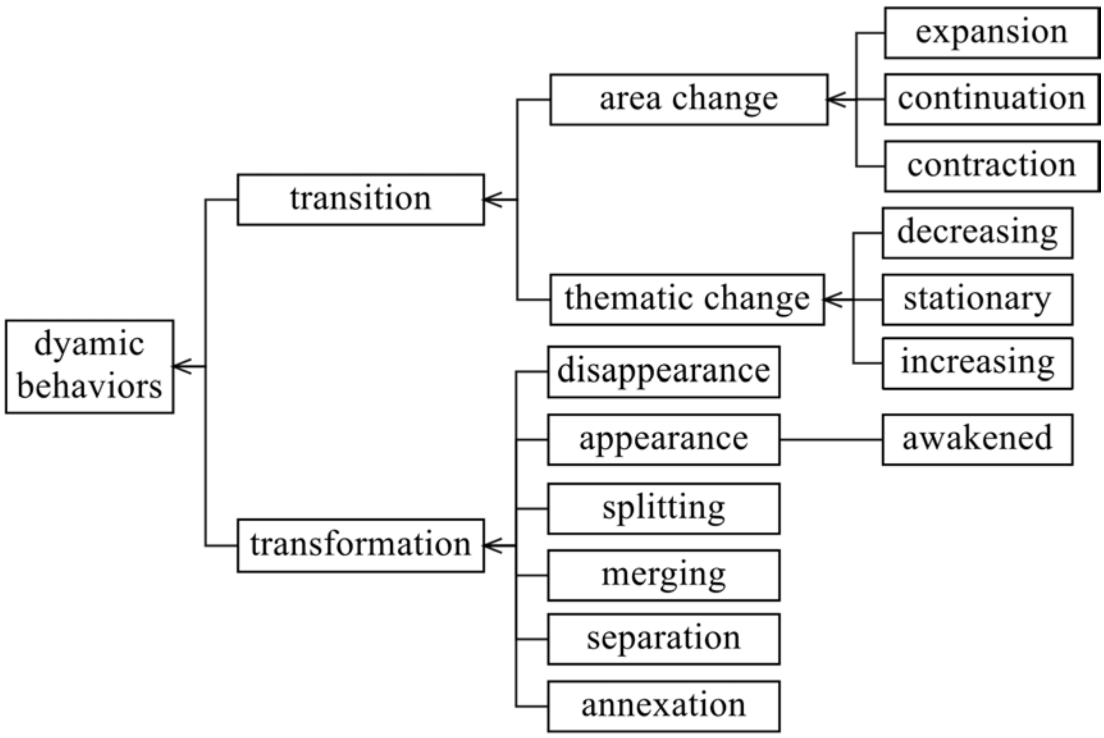

Fig. 3.10 A hierarchical set of dynamic behaviors of UHIs.

zone, intensity, and location are respectively described by a sequence, a chain, and a queue. Continuous changes of each property through time can express several typical evolutionary trends and hence are defined as several different types of transitions. With more detailed descriptions, changes of each property are expressed by behaviors that depict filiations between them. Both the intensity and location filiations are associated with the continuous filiation of the zone as long as it continuously exists. Transformation between zones may occur simultaneously with other zones that lead to the creation or deconstruction of other newly generated UHIs.

For example, UHIs are composed of sequences differentiated by zones. Zones are delineated by a polygon extracted from the thermal images such that temperatures within the polygon are higher than the reference rural temperature, and zones also have continuous or transformation filiation. UHIs are composed by their continuous transitions and are associated to their transformations. A transition is associated with two sequences while a transformation is associated with one to several sequences. Each transition and transformation class can be further specialized into subclasses corresponding to the behaviors described above. Essentially, transition and transformation describing the filiation between zones differentiates transition depicting topological transformation between sequences. Contrary to the study in (McIntosh & Yuan, 2005), processes do not include only split and merge but all topological transformation, allowing the description of a UHI life-cycle as a series of transformations.

In order to have more distinct and structured descriptions, changes of the properties can be viewed as dynamic behaviors of each UHI and are thereby conceptually summarized as a set of concepts, represented in Figure 3.10. The figure shows that *dynamic behavior* contains a *transition* continuing for a time period and *transformation* that has topological changes at a time instant associated with two or several *transitions*. Particularly, *awaken* is a special transformation undergoing exactly the same evolutionary process as *appearance* given a pre-condition that a sequence ending with a *disappearance* connects with a new sequence starting with the zone which is generated by *appearance*.

Chapter 4

Graph-based tracking of UHI behaviors

4.1 Introduction

Chapter 3 conceptualizes a UHI as a field-object and models three types of behaviors for each UHI. The modeling approach is also developed from the zone-oriented to the core-oriented modeling, considering various of spatial distributions of the thematic temperatures. Chapter 4 is one step further in the development of life-cycles of UHIs in view of automation. Compared with Chapter 3 that UHIs are continuous phenomenon over space and time, Chapter 4 discretizes the UHI phenomenon as a series of snapshots over time because the observed temperatures come from discrete data. To develop a long-term tracking, study in (Del Mondo *et al.,* 2013) proposed a graph to track the spatiotemporal relationships and their changes of over time. Inspired by this study, this chapter proposes six hierarchical graphs in different description granularities to track the UHI evolutionary process from the most original component of the zones to the most global gratuity of the UHIs.

To start with, Section 4.2 proposes a thematic graph to track the continuous changes of temperatures of zones in sequence. Different from the thematic graph which is built from the quantivative description of temperatures, the locational graph designed in

Section 4.3 is established based on the qualitative analysis of geometrical intersections between zones. Hence, the zone graph is introduced by simultaneously considering continuous relationships and transformations between zones in Section 4.4. Further, continuous tracking is moving from tracking successive sequences in Section 4.5 towards more generalized period tracking in Section 4.6. Whenever consecutive periods of each UHI can be tracked by the period graph, tracking of a set of UHIs can be obtained through the UHI graph in Section 4.7, which associates with the UHIs through transformations that lead to the creation and destruction of objects. To sum up, Section 4.8 presents a hierarchical structure of the six graphs.

4.2 Thematic-graph based tracking

Let $\mathbf{C}$ be a complete set of thematic temperatures of all the UHIs existing in the spatial and temporal domains, and $\mathbf{F}_c$ denotes a set of thematic filiations between temperatures. Let $\mathbf{F}_c = \mathbf{C}_c \cup \mathbf{T}_c$ such that $(c_n^i, c_n^j) \in \mathbf{C}_c$ occurs in the same UHI to represent the qualitative descriptions of the temperatures, and $(c_n^i, c_m^j) \in \mathbf{T}_c$ associates with several UHIs. In other words, $\mathbf{C}_c$ connects temperatures in sequences of zones that belong to the same UHI, and $\mathbf{T}_c$ describes the connection of temperatures that belong to different UHIs when they are topologically associated. Thus, a new graph for the process of thematic change can be refined as $\mathbf{G}_C = (\mathbf{C}, \mathbf{F}_c)$. Further, let a *chain* contain a series of temperatures over a time period $[t_i, t_j]$ such that all these temperatures are the thematic properties of zones which belong to the same UHI and they have only one type of the thematic filiation. Hence, a *chain* can be more formally denoted as $a_n = \{c_n^i, \ldots, c_n^j\}$ which satisfies $\forall k, i < k \leq j, (c_n^{k-1}, c_n^k) = (c_n^i, c_n^{i+1}) \in \mathbf{C}_c$.

Unlike sequences which can be interrupted by topological transformations, thematic chains continue all the time because *temperature* is a property of UHI. Apparently, $\mathbf{C}_c$ distribution along with the temporal domain can depict thematic behaviors of a UHI. Let $a_n^{i_{j-1}}$, $a_n^{i_j}$, and $a_n^{i_{j+1}}$ denote three consecutive chains of the UHI u_n, the two edges $(a_n^{i_{j-1}}, a_n^{i_j})$ and $(a_n^{i_j}, a_n^{i_{j+1}})$ can be stated as the following:

- if $a_n^{i_{j-1}}$ increases and $a_n^{i_j}$ decreases, u_n reaches the *vertex* at the transition $(a_n^{i_{j-1}}, a_n^{i_j})$;
- if $a_n^{i_{j-1}}$, $a_n^{i_j}$, and $a_n^{i_{j+1}}$ consecutively increases, stays stationary and decreases, u_n is *reaching a plateau*, *at a plateau* and *leaving a plateau* during the transitions;
- if $a_n^{i_{j-1}}$ decreases and $a_n^{i_j}$ increases, u_n reaches the *saddle* at the transition $(a_n^{i_{j-1}}, a_n^{i_j})$;
- if $a_n^{i_{j-1}}$ decreases, $a_n^{i_j}$ keeps stationary, and $a_n^{i_{j+1}}$ increases, u_n is *reaching a basin*, *at a basin* and *leaving a basin* respectively during the transitions; and
- if both $a_n^{i_{j-1}}$ and $a_n^{i_{j+1}}$ increase or decrease and $a_n^{i_j}$ is stationary, both has *upslope* in the first transition and *downgrade* in the second transition, while $a_n^{i_j}$ has a *break*.

4.3 Locational-graph based tracking

To track the displacement of UHIs and to reveal evolutionary trends of the locational movements, a new graph is thus proposed as: $\mathbf{G}_Q = (\mathbf{Q}, \mathbf{F}_q)$ where $\mathbf{Q}$ denotes a time-series of locations and $\mathbf{F}_q$ represents a set of filiations between locations, which essentially relies on the existence of the thematic graph $\mathbf{G}_C$. Note $\mathbf{F}_q = \mathbf{Q}_q \cup \mathbf{L}_q$ so that $(q_n^i, q_n^j) \in \mathbf{Q}_q$ describes each pair of consecutive queues belonging to the same UHI, which is viewed as an edge of the graph to offer qualitative descriptions of the locations, and $(q_n^i, q_m^j) \in \mathbf{L}_q$ indicates that one or several queues of different objects q_m^j associate with the same queue q_n^i of the UHI u_n. Since a *queue* contains a set of centroids for the same UHI over $[t_i, t_j]$ that ultimately constructs one particular type of the locational filiation (e.g. *stopping*, *shifting*, or *moving*), a *queue* thus can be more precisely noted as $q_n = \{l_n^i, \ldots, l_n^j\}$ which satisfies $\forall k, i < k \leq j, (l_n^{k-1}, l_n^k) = (l_n^i, l_n^{i+1}) \in \mathbf{Q}_q$.

Apart from two transitions for sequences and chains that have been proposed (Zhu *et al.,* 2016), a new transition to present trends of locations is gathered. Let $q_n^{i_{j-1}}$, $q_n^{i_j}$ and $q_n^{i_{j+1}}$ denote three consecutive queues of the same UHI u_n that transitions connect every two of them in a temporal domain. Compared with the thematic property which has quantitative records for the intensity, locational movement does not include a magnitude description domain such that the transitions have neither peaks nor troughs. Associating with the two edges $(q_n^{i_{j-1}}, q_n^{i_j})$ and $(q_n^{i_j}, q_n^{i_{j+1}})$, transitions can be redefined:

- if $q_n^{i_{j-1}}$ is stopping, $q_n^{i_j}$ is shifting, and $q_n^{i_{j+1}}$ is moving, then u_n obtains an *accelerating*;
- if $q_n^{i_{j-1}}$ has a movement, $q_n^{i_j}$ shifts, and $q_n^{i_{j+1}}$ stops, then u_n reaches a *decelerating*;
- if $q_n^{i_j}$ either moves or shifts while $q_n^{i_{j-1}}$ and $q_n^{i_{j+1}}$ are stopping, then the queue $q_n^{i_j}$ is viewed as an active phrase. u_n consequentially reaches and leaves an *activation*; and
- if $q_n^{i_j}$ stops while $q_n^{i_{j-1}}$ and $q_n^{i_{j+1}}$ either move or shift, then the queue $q_n^{i_j}$ is conceptualized as a quiescence. u_n reaches *quiescence* and *resumption* during the two transitions.

4.4 Zone-graph based tracking

A UHI is identified through time as a series of zones which can be related together through spatiotemporal relationships. We note $\mathbf{G}_Z = (\mathbf{Z}, \mathbf{F}_z)$ as a graph where $\mathbf{Z}$ is the set of all zones and $\mathbf{F}_z$ is the set of filiation relationships connecting the zones, which relies on the existence of the thematic-graph $\mathbf{G}_C$. As zones are UHI components, each zone z_n^i can be identified by a time instant t_i and the UHI u_n it belongs to and a filiation can be noted as $(z_n^i, z_m^j) \in \mathbf{F}_z$.

Among filiations for zones, *expansion*, *continuation*, and *contraction* are concerned with geometrical changes occurring within one UHI while *splitting*, *separation*, *merging*, and *annexation* imply at least three zones and a topological transformation. The set of filiations can be partitioned into two sets $\mathbf{F}_z = \mathbf{C}_z \cup \mathbf{T}_z$ defining the set of continuous relationships and the set of transformations respectively. This study also extends $\mathbf{T}_z$ by adding two specific transformations, i.e., *appearance* and *disappearance*.

4.5 Sequence-graph based tracking

Study in (Del Mondo *et al.,* 2013) suggested that sequences and processes can be defined using a spatiotemporal graph approach. A *sequence* is then defined by a series of zones over an interval $[t_i, t_j]$ such that all zones in the series are connected by the same continuous relationship. A consequence is that all zones must belong to the same UHI. Hence, a *sequence* s_n^i is a series of zones $\{z_n^i, \ldots, z_n^j\}$ such that $\forall k, i < k \leq j, (z_n^{k-1}, z_n^k) = (z_n^i, z_n^{i+1}) \in \mathbf{C}_z$.

This work models that sequences, chains, and queues those are continuous without any interruption given the condition that the UHI still exists, and transformation is depended on sequences at a time instant. Furthermore, sequences can be gathered in a third graph $\mathbf{G}_S = (\mathbf{S}, \mathbf{E}_s)$ where $\mathbf{S}$ is the set of sequences and $\mathbf{E}_s$ is the set of edges marking changes between the sequences. Each sequence can be characterized by one of the three relationships from $\mathbf{C}_z$ and edges can be characterized by the types of sequence they connect. Thus, $\mathbf{E}_s$ can be divided between a set $\mathbf{C}_s$ of continuous transitions where two consecutive sequences show an area change in the evolution of the UHI and a set $\mathbf{P}_s$ of processes where a transformation occurs. While processes have a similar meaning as transformations in $\mathbf{T}_z$, continuous transitions can further describe the behavior of a UHI. Noting $s_n^{i_{j-1}}$, $s_n^{i_j}$ and $s_n^{i_{j+1}}$ three consecutive sequences connected by continuous transitions belonging to the same UHI u_n, the study associates edges $(s_n^{i_{j-1}}, s_n^{i_j})$ and $(s_n^{i_j}, s_n^{i_{j+1}})$ with an action describing u_n's behavior:

- if $s_n^{i_{j-1}}$ is an expansion and $s_n^{i_j}$ is a contraction, u_n *peaks* during the transition $s_n^{i_{j-1}}, s_n^{i_j}$;
- if $s_n^{i_{j-1}}$ is an expansion, $s_n^{i_j}$ is a continuation and $s_n^{i_{j+1}}$ is a contraction. Sequence $s_n^{i_j}$ is qualified as a plateau. u_n *reaches a plateau* and *leaves a plateau* during the transitions;
- if $s_n^{i_{j-1}}$ is a contraction, $s_n^{i_j}$ is a continuation and $s_n^{i_{j+1}}$ is an expansion. Sequence $s_n^{i_j}$ is qualified as a floor. u_n *reaches a floor* and *leaves a floor* during the transitions;

- if $s_n^{i_{j-1}}$ is a contraction and $s_n^{i_j}$ is an expansion, u_n reaches a *low* during the transition $s_n^{i_{j-1}}, s_n^{i_j}$; and
- if $s_n^{i_{j-1}}$ and $s_n^{i_{j+1}}$ are both contractions or both expansions and $s_n^{i_j}$ is a continuation, $s_n^{i_j}$ corresponds to a pause in the evolution of the UHI. The first transition is a *stabilization* and the second is a *resumption*.

4.6 Period-graph based tracking

An *active period* contains a set of sequences listed sequentially and is denoted as $p_n^a = \{q_n^c, \ldots, q_n^d\}$. All the zones of each sequence over a temporal domain $[t_i, t_j]$ have either area changes or transformations given the condition that they belong to the same UHI, where $\forall k, i < k \leq j, (z_n^{k-1}, z_n^k) = (z_n^i, z_n^{i+1}) \in \mathbf{F}_z$. Similarly, an *inactive period* can also be denoted as p_n^b and modeled as an empty sequence connecting the *active periods* so that a *standby* connects with an empty sequence and generates another active sequence. Thereby, all the periods can be refined into a graph $\mathbf{G}_P = (\mathbf{P}, \mathbf{E}_p)$ where $\mathbf{P}$ is the set of nodes denoting periods and $\mathbf{E}_p$ is the set of edges representing the state transitions between the periods. Each *active period* can be characterized by either process of area change or constrained transformation (i.e. belonging to the same UHI), and edges can be characterized by different transformations that they associate with. Essentially, this graph describes complete life-cycle for a UHI.

In a short time period, a $\mathbf{G}_P$ can track a UHI having several periods so that some patterns caused by short-term effects may be revealed. For instance, the reason of UHIs appearing and disappearing periodically on a daily basis is that buildings release the heat during nighttime while they absorb the heat from solar radiation during the daytime. The graph can also be used to track cyclic patterns in a wider temporal scale such as in months, seasons, and even in years.

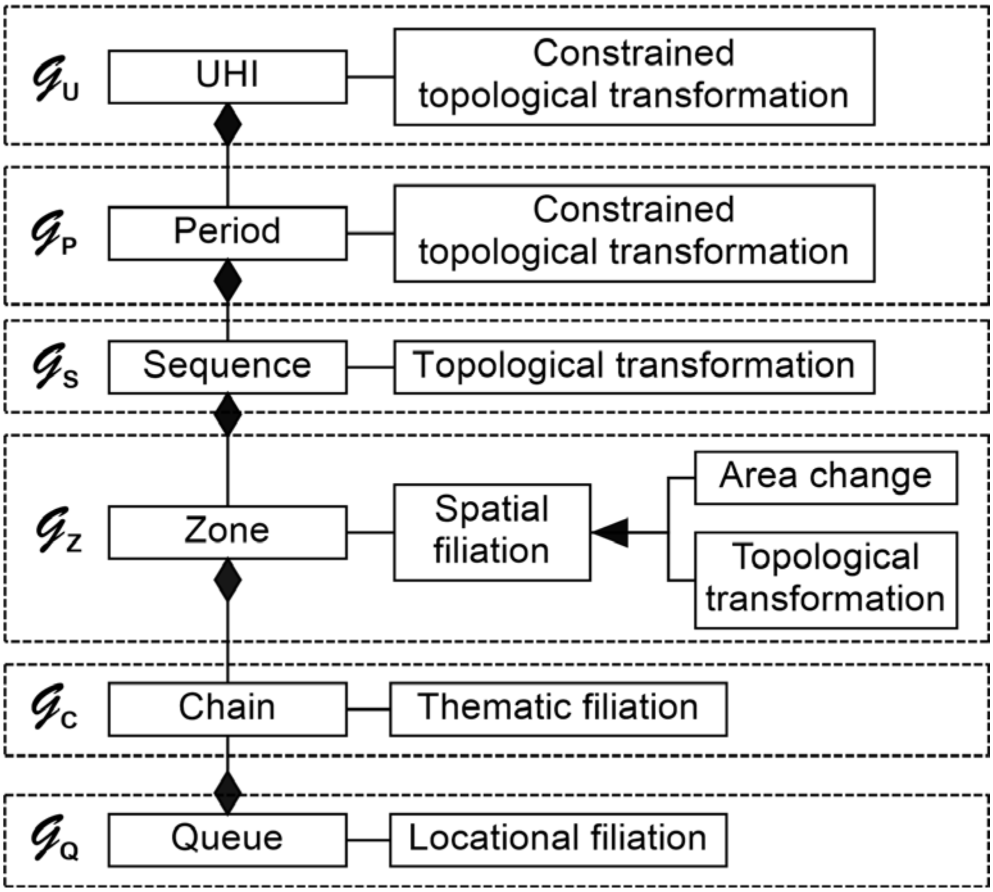

Fig. 4.1 A hierarchical structure of six graphs to track continuous evolution of UHIs.

4.7 UHI-graph based tracking

Obviously, a period-graph $\mathbf{G}_P$ can only track complete life-cycle of one UHI, which is not able to track all the UHIs at the same time when several UHIs interact with each other in the same urban area or spatial contiguous city clusters. Thus, one more graph is needed to track global evolution of all the UHIs existing in the same spatial and temporal domain. Let the UHI graph note as $\mathbf{G}_U = (\mathbf{U}, \mathbf{E}_u)$, where $\mathbf{U}$ is a set of UHIs that makes the graph nodes and $\mathbf{E}_u$ is the edges composed by topological transformations which can lead the creation and destruction of UHIs. Since UHIs can reincarnate at a time instant from the apparent death caused by *disappearance*, complete life-cycle cannot be interrupted by the consecutive disappearance and appearance that makes an *awaken* occur. Therefore, the edges of $\mathbf{E}_u$ have to exclude a pair of filiations which connect two consecutive periods of the same UHI. In other words, $\mathbf{E}_u$ shall only maintain some specific edges in $\mathbf{E}_p$ that for the first time to create a period and for the last time to destroy another period.

4.8 Discussion

The boundary of any UHI is fuzzy and undetermined, while both the object-oriented modeling and graph-based tracking of UHI rely on explicit boundaries. Therefore, fuzzy boundaries can lead to spatial uncertainty of UHIs in two aspects. First, approximation of the fuzzy boundaries can cause that UHIs boundaries are generalized or simplified. Second, because of the generalized boundaries, the proposed models cannot fully capture the complexity of UHI. Consequently, UHI behaviors can be inconclusive or differentiated. For instance, a contracting UHI is disappeared because its zone is too small and its boundary is too vague to be detected; or contracting of a zone is determined as a splitting that two zones are generated and closely located due to its fuzzy boundary. The two examples indicate that even though uncertainty behaviors can happen as special scenarios, these behaviors still present the same evolutionary trends and thus will not make significant influence on the results. In other words, evolutionary trends of UHIs detected from graph-based tracking can always be effective and reliable.

4.9 Summary

Six hierarchical graphs are shown in Figure 4.1. This conceptual model completes the qualitative description of thematic and spatial behaviors of UHIs. $\mathbf{G}_C$ is the most fundamental graph that temperatures can develop independently, which hence decides the existence and performance of the $\mathbf{G}_Z$ and $\mathbf{G}_Q$ simultaneously. Relying on $\mathbf{G}_C$, $\mathbf{G}_Z$ describes the most elementary spatial-evolution and builds the foundation of $\mathbf{G}_S$ so that spatial revolution pattern associated with topological transformations can be revealed.

Benefiting from $\mathbf{G}_S$, $\mathbf{G}_P$ records complete life-cycle of a UHI which may have several consecutive sequences associated with some particular transformations such that all of the UHIs revolution can be finally tracked in $\mathbf{G}_U$.

Chapter 5

Model evaluation and results

5.1 Introduction

The previous two chapters propose a model to track spatial and thematic behaviors of UHIs over time instantly. This chapter will test the effectiveness of the proposed model. A time series of thermal infrared images with fine spatial and temporal resolutions will be used as the input of the model. These images with high spatial resolution can also describe the temperature distribution in an urban scale for the research of the UHI phenomenon (Kourtidis *et al.*, 2015; Wang & Ouyang, 2017; Zhou *et al.*, 2016). However, spatial and temporal resolutions of the current thermal satellite images are too coarse to be used directly for this purpose (Keramitsoglou *et al.*, 2013; Nichol, 2009). To tackle this problem, many studies adopted image fusion methods to enhance the spatial resolution (Hughes & Ramsey, 2010; Hughes & Ramsey, 2013; Rodriuez-Galiano *et al.*, 2011), which yet still under research. On the contrary, machine learning methods are frequently being used for super-resolution construction in recent years.

5.1.1 Image-fusion based super-resolution modeling

Image fusion techniques normally integrate different image sources (multi-spectral and/or multi-resolution images) into a single super-resolution image with a higher temporal resolution. Based on the empirical evidence that similar materials in a similar viewing conditions and time will have similar radiance spectra, study in (Tonooka, 2005) proposed an original framework to generate super-resolved thermal infrared (TIR) images from the resolution 90 m to 15 m based on three images, i.e., the original TIR image, the visible and near-infrared (VNIR) image, and the super-resolved shortwave infrared (SWIR) image which is derived from the original VNIR and SWIR images. Performance of this framework is acceptable in visual while the study meets the challenge in testing the accuracy quantifiability. Then, significant modifications of this framework were proposed in (Hughes & Ramsey, 2010; Hughes & Ramsey, 2013). Research in (Hughes & Ramsey, 2010) utilized the ISODATA rather than k-means clustering algorithm to create and merge clusters without any prior assumption automatically, and used the Point Spread Function which transforms radiation from a point to a two-dimensional surface (Townshend *et al.,* 2000) to degrade higher resolution channels such that surfaces in different spectral regions are identical. Further improvement in (Hughes & Ramsey, 2013) simplifies the framework for adopting current ASTER configuration where SWIR bands are not available. However, both modifications depend on the solid understanding of the spectral statistical distribution of the original images for determining a number of input parameters, which obviously limits their widely applications.

Study in (Rodriuez-Galiano *et al.,* 2011) simply generated a TIR image at 30 m resolution based on Landsat 7 ETM+ image using the cokriging regression / interpolation model, which can be optimal enough for the UHI investigation. By contrast, both studies in (Aiazzi *et al.,* 2005; Merino & Núñez, 2007) obtained a higher resolution of 15 m. Study in (Merino & Núñez, 2007) modified a Variabl-Pixel Linear Reconstruction algorithm by weighting each pixel values of the input low resolution images (i.e. Landsat ETM+) based on the statistical significance, which simultaneously removes geometric distortion effects and maintains photometry. The purpose of the study in (Aiazzi *et al.,* 2005) is to create high resolution RGB images, method of which can not be adapted for generating TIR images directly. In comparison, study in (Aiazzi *et al.,* 2005) created a fused thermal infrared image from VNIR image by proposing a generalized Laplacian pyramid, i.e., a sequence of images in multi-resolution obtained from the image reduced recursively by a scale ratio, which is derived from the Gaussian pyramid to enhance the spatial resolution and maintain the spectral characteristics. Using multi-spectral (MS) and mulit-resolution images at the same time, research in (Zhan *et al.,* 2012) inversed LSTs, proxy-sharpens MS bands, and hence downscale LSTs based on a theoretical framework of thermal sharpening. To further enhance spatial resolution of thermal images for UHI analysis, a research in (Nichol, 2009) combined a higher resolution SPOT5 image (10 m resolution) with a lower resolution ASTER L1B thermal image (90 m resolution) based on an emissivity modulation (EM) equation derived from the Stephan Bolzmann Law (SBL), which simultaneously converted the image-derived brightness temperature to the true kinetic temperature at 10 m resolution. However, this study simply assumes that sub-pixel temperatures vary only based on land cover types within each large pixel, which most probably ignores the distortion that sub-pixel temperatures could be dramatically influenced by the surrounding land cover types.

In summary, studies discussed above proposed several methods for LST downscaling. However, these studies generally could not derive finer spatial resolutions which are vital for tracking and modeling the changes of the UHIs (Dousset & Gourmelon, 2003; Lo *et al.,* 1997; Nichol *et al.,* 2009; Stathopoulou & Cartalis, 2007) since evolutionary process of the UHIs obviously happen in the urban areas at a micro-scale. Investigating dynamic behaviors of UHIs requires very high temporal resolution of thermal images (i.e. an ideal resolution shall be in hour) because temperatures in the urban area could vary significantly within a short period of time.

5.1.2 Machine-learning based super-resolution modeling

More advanced approaches in machine learning, such as support vector machines (SVMs) (Zortea *et al.,* 2006) and extreme learning machines (ELMs) (Bai *et al., 2015*), were proposed to downscale the thermal infrared images. SVMs are supervised learning models associated with the designed learning method for classifications and regression analysis (Zortea *et al.,* 2006). Study in (Zhang & Huang, 2013) calibrated the spatial resolution and radiometric differences by using a nonlinear super-resolution method, i.e., support vector regression, to downscale the ETM+ data to 15 m based on the resampling of the ASTER data set. However, this method cannot derive images with very high temporal resolution since the same or similar time phrase for the ETM+ and ASTER data sets are required in the method. To improve the coarse spatial and temporal resolutions, one study in sequential upscaled the component data set to the same coarse resolution of the LST image, used a set of machine learning machines to correspondingly downscale LTS images, and combined the derived of downscaled LST images based on gradient boosting (Keramitsoglou *et al.,* 2013). The result is promising for the downscaling from 3 km to 1 km since a much stronger regression model was established. However, 1 km resolution is still too coarse for investigating UHIs in micro-scale. This study in (Keramitsoglou *et al.,* 2013) is empirical-based and may not be applicable to other studies. To define the optimal internal parameters of SVMs for LST estimation automatically, study in (Moser & Serpico, 2009) adapted Powell's algorithm with span-bound functional to establish a configuration of quasi-optimal parameter to minimize regression errors. Although the initial input parameter would impact the computational time considerably, the process time is still significantly shorter than the one without this function, which would be interesting to extend the method to the SVMs.

Though not widely used, many artificial neural network (ANN) methods have been proposed in the super-resolution reconstruction for thermal infrared images (Huang *et al.,* 2004; Huang *et al.,* 2012; Yao & Han, 2010). For example, research in (Yang *et al.,* 2011) firstly obtained land use classification at 30 m resolution using a SVM with four remote sensing indices as input parameters, then trained the relationship between MODIS LST (990 m), area ratios and endmember indices (990 m) using an artificial neural network which essentially is a self-organized genetic algorithm, and finally estimated the sub-pixel (at 90 m resolution) temperature of MODIS LST based on the trained network model. However, the applicability of this method depends on particular application requirements since the estimation errors (i.e. RMSE and MAE) are higher than that of images in 990 m resolution. This problem is probably due to the scale dependence that information derived from one image could be significantly different from internal information in the other image, if the spatial resolution of the two images have a significant difference. Motivated by this problem when predicting LST, a study in (Ghosh & Joshi, 2014) firstly trained the relationship between reflectance and LST in four spatial resolutions with support vector machine (SVM), gradient boosting machine (GBM), and partial least square (PLS). Then images at coarse resolution were imported into the three trained model to predict the LST images at finer resolutions. The proposed method suggests that GBM and SVM models have better performance in a relatively homogeneous land use area.

Overall, previously proposed machine learning methods of downscaling LST images still face challenges for UHI analysis such as downscaled spatial resolution of LST images is still coarse, some methods rely on images derived from multiple satellite sensors, and accumulated errors may be high. Moreover, fused images also limit their practical use because source images fulfilling the same time or criteria of overpass time are not frequently available. Instead of using satellite thermal infrared images, a new strategy is to collect near-surface air temperatures from a sufficient number of automatic weather stations and generating contiguous measurements by interpolation.

5.1.3 Chapter structure

Section 5.2 selects an appropriate study area for the empirical test. Section 5.3 uses an interpolation method to obtain a series of thermal images with fine spatial and temporal resolutions that cover the study area. Section 5.4 develops two methods (i.e. zone-oriented and core-oriented methods) to extract behaviors of zones since the data sets are essentially discrete. When the zones have been extracted, Section 5.5 determines the behaviors based on two computational methods. Specifically, Section 5.6 discusses some vital constraints for determining the behaviors. Hence, Section 5.7 implements the proposed computational methods in a spatial database such that results can be finally presented in Section 5.8.

5.2 Study area

Guangzhou in China is selected to evaluate the effectiveness of the model, which is the core area of an urbanized city-clusters in the southern China with 13 million population in total and more than 1700 inhabitants per square kilometer (Guangzhou, 2017). The urban heat island phenomenon in this city is evident sine the annual temperature difference can reach up to 14.5 degree Celsius in the subtropical monsoon climate (Guangzhou, 2017).

5.3 Preprocessing

Near-surface (approximately 1.5 meter above the land surface) air temperatures were collected at hourly for six weeks (i.e., July 31 – August 6, July 28 – September 3, September 25 – October 1, October 23 – October 29, November 20 – November 26, and December 18 – December 24) in year 2015, so that it covers a continual of six months. Specifically, 216 automatic weather stations are mainly located in the urban areas as shown in Figure 5.1. Thereby, a series of near-surface thermal images are generated by interpolating hourly data, and are used as the input data of the model. Ordinary Kriging was used since it models the surface by assuming that an overriding trend exists in the data sets, which is beneficial for highlighting the hotspot character of UHIs (Chai *et al.*, 2011; Hofstra *et al.*, 2008; Irmak *et al.*, 2010; Stahl *et al.*, 2006).

Rural temperatures observed at the triangle (Figure 5.1) were used as the reference temperature to extract zones of UHIs because this site is in the Dajinfeng Eco-scenic, which is not only located in the rural area (i.e. land cover is forest) but also next to the urban areas of Guangzhou. Thus, extracting zones of UHIs using this reference temperature is confidential since rural and urban temperatures can be unambiguously differentiated. Previous study proposed a feature extraction method to extract zones of UHIs automatically (Keramitsoglou *et al.,* 2011). In the method, temperature pixels are clustered as a group (i.e. a *zone*) if each pixel in the group has at least one neighborhood pixel when searching with k-pixels distance in all directions. Thereby, the method can possibly merge smaller groups into a bigger one. In comparison, this study also developed an automatic extraction method in the system implementation to extract a time series of zones automatically. However, the k-group method (Keramitsoglou *et al.,* 2011) was not used for extraction since spatial behaviors between zones proposed by this study have already addressed this issue (e.g. *merging*: two or several zones merge together as a single one).

Collecting air temperatures for six weeks with three-weeks time interval still costs time even though a batch processing was used to edit the original data set to generate a homogeneous format, and shapefile points, interpolate the points into contiguous images, and import them into the database (Figure 5.2).

5.4 Extraction of UHI changes

As a simplified consideration, zone filiations are built only based on topological relationship between zones. A refined method constructs the filiations based on the relationship between zones and cores. Therefore, extraction for UHI changes are either zone-oriented or core-oriented.

5.4.1 Zone-oriented extraction

Hourly updated rural temperatures observed at the triangles in Figure 5.1 were used as the reference threshold temperature to extract zones of UHIs. UHI zones are defined by urban areas where the temperature is defined as the difference between the reference temperature and observed temperatures. Areal variations were computed at each time instant. If there is no overlapping area between two consecutive UHI polygons or if the proportion of the overlapping area to either of the two polygons is small, it is

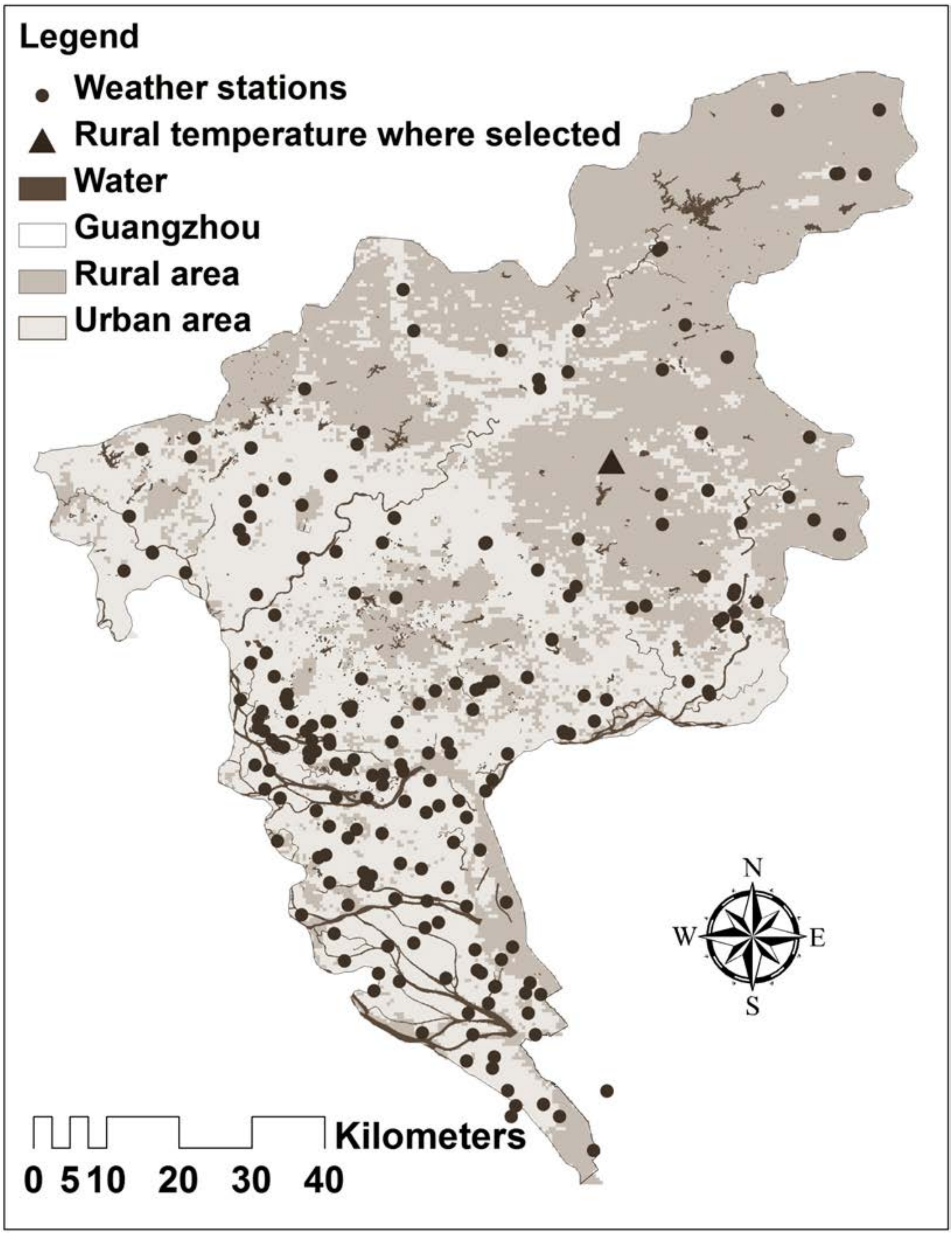

Fig. 5.1 Automatic weather stations are located in Guangzhou city, China.

reasonable to define that they have no relationship and belong to different UHIs. In opposite, they can be regarded as belonging to the same object if they overlap on a significant area.

Let z_n^i denote a zone indexed as n at time t_i. As shown in Figure 5.3, significant

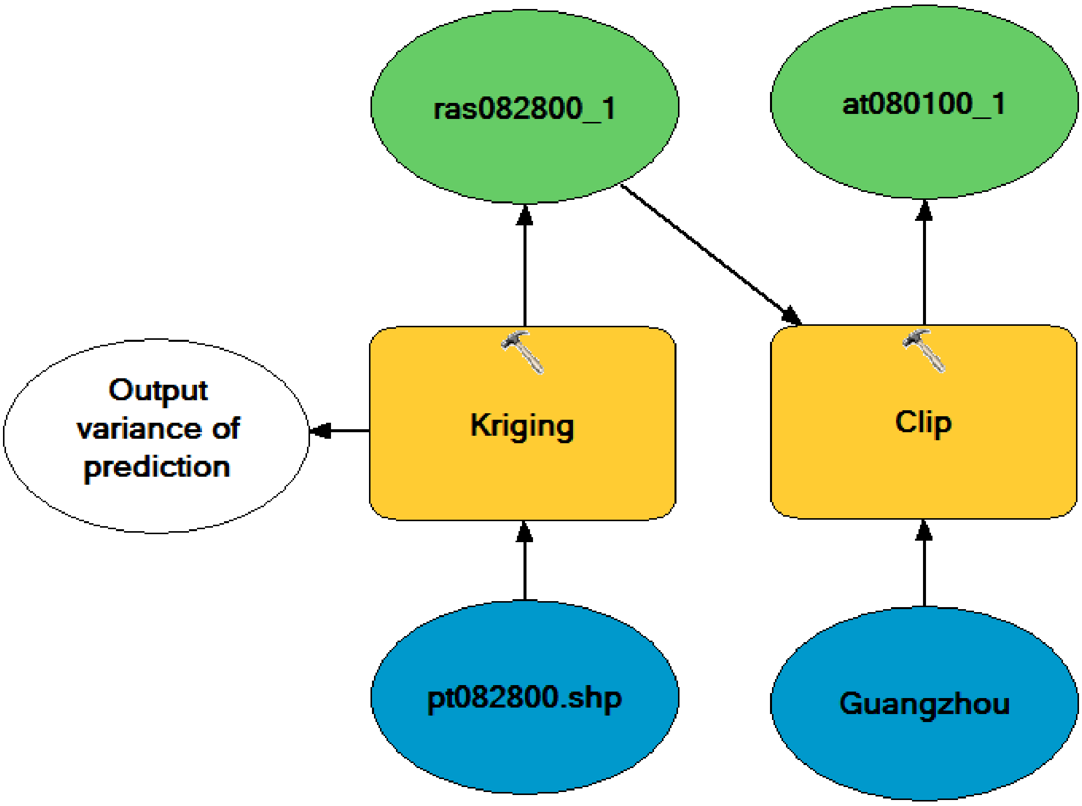

Fig. 5.2 Batch processing to obtain contiguous of thermal images from points in the shapefile format in ArcMap.

overlapping between z_n^{i-1} and z_n^i corresponds to two statuses of a single UHI in two consecutive time instants, and areal change occurs when comparing the areas of the two zones. Similarly, insignificant overlapping between the two leads to a disappearance and appearance. More complicated scenarios can happen if z_n^{i-1} associates two ones at t_i or two zones at t_i relate with the same zone z_n^i. Hence, changes at time t_i are more specifically defined as follows.

- *appearance*: the zone at time t_i has insignificant overlapping area or does not overlap with any zones at time t_{i-1}.
- *disappearance*: the zone at time t_{i-1} has no significant overlapping area or does not overlap with any zone at time t_i.
- *expansion*: the UHI polygon significantly overlaps with a UHI at time t_{i-1} and

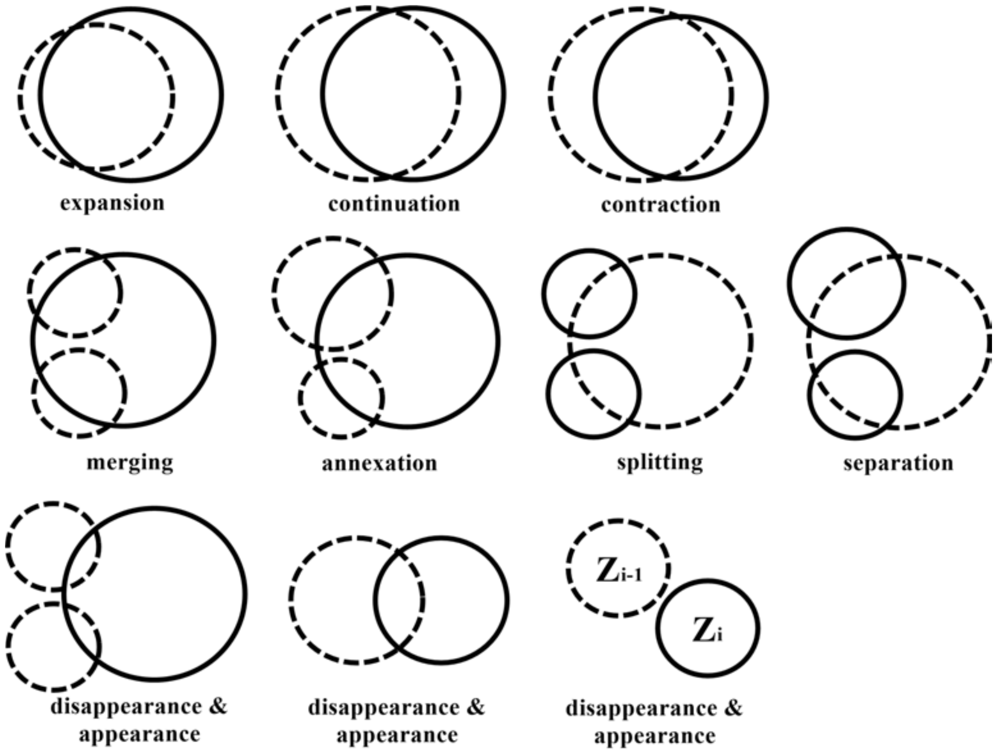

Fig. 5.3 Overlapping instance of UHI zones in two consecutive times instants.

its area is bigger.

- *contraction*: the UHI polygon considerably overlaps with a UHI at time t_{i-1} and its area is smaller.

- *continuation*: the UHI significantly overlaps with a UHI at time t_{i-1} and their areas are equivalent.

- *merge*: one UHI polygon at t_i overlaps with several UHIs at t_{i-1}. If one UHI at t_{i-1} is much larger than the others and its area is close to that at t_i, the UHI is supposed to be in the continuity of the big UHI and an *annexation* can be determined. If the new UHI cannot be associated to one specific UHI, it is considered as a new UHI and a *merging* is derived.

- *split*: several UHI polygons at t_i overlap with one polygon at t_{i-1}. If the shape at t_i is similar to one specific polygon at t_{i-1}, it is a *separation* otherwise it is a *splitting*.

5.4.2 Core-oriented extraction

Section 3.4 considers that cores are more representative for the description of spatial distribution of thematic intensities, and association of cores in two continuous time instants which is the most fundamental determinant to identify affiliation between zones (i.e. zones that belong to the same object) so that areal changes can be investigated. Further, any other zones that have spatial association with the current zone are viewed as affiliated zones to have topological transformations. For the convenience of representation, different relationships between cores of (r_n^{i-1}, r_n^i) are proposed as:

- *thematic relation* if at least one core r_n^{i-1} locates in the extent of z_n^i;
- *close relation* if most of the area of the cores $area(\{r_n^{(i-1,k)}\})$ locates in the extent of z_n^i; and
- *untight relation* if a small proportion of the area of the cores $area(\{r_n^{(i-1,k)}\})$ locates in the extent of z_n^i.

In organizing of the spatial relationships between zones, if z_n^i overlaps with z_n^{i-1} and the pair of the zones have *thematic relation*, then they are confidentially viewed as continuous status of the same object. Specifically, when z_n^i coincidentally overlaps with z_n^{i-1}, this pair of zones have the strongest thematic and spatial association since the overlapping is exclusive that any other spatial relationships relating with any other zones cannot occur. Obviously, this pair of the zones go through areal changes as:

- *expansion* when z_n^{i-1} and z_n^i are closely related with each other, and $area(z_n^i)$ is larger;
- *continuation* when z_n^{i-1} and z_n^i are in close relation, and $area(z_n^i)$ and $area(z_n^{i-1})$ are equivalent; and
- *contraction* when z_n^{i-1} and z_n^i have close relation, and $area(z_n^i)$ is smaller.

A zone z_n^i at t_i can also thematically relate with two zones at t_{i-1}, leading to a merge (i.e. *merging* or *annexation*) as shown in of Figure 5.4. While, they may only apparently touch with each other without topological association even though z_n^i overlaps with the two ones simultaneously if they are not in thematic relation (i.e. cores in the two zones are not associated). A similar but different scenario is that two zones z_n^i and z_p^i at t_i have thematic relation with a single one at t_{i-1}, which triggers a split (i.e. *splitting* or *separation*). In summary, topological transformations can be determined as:

- *merging* when both z_n^{i-1} and z_p^{i-1} relate with z_q^i not closely;
- *annexation* when z_n^{i-1} and z_p^{i-1} respectively have close and untight relation with z_n^i;
- *splitting* when z_n^{i-1} has loose relation with z_p^i and z_q^i; and
- *separation* when z_n^{i-1} has close and untight relation with z_n^i and z_p^i respectively.

A zone z_n^i may contain one or several zones noted by $\{z_m^{i-1}\}$ ($m = \{n,...,p\}$), which indicates that $area(z_n^i)$ is larger than any individual zone in $\{area(z_m^{i-1})\}$. Sequentially, z_n^i also contains cores of $\{r_m^{(i-1,k)}\}$ such that all the cores at t_{i-1} are located in the extent of z_n^i. Thus, z_n^{i-1} expands as z_n^i if there is only one zone at t_{i-1}, or z_n^{i-1} annexes other zones and expands as z_n^i. In the opposite, one or several zones $\{z_m^i\}$ ($m = \{n,...,p\}$) can also be *inside* of z_n^{i-1}. Even though it may not satisfy the above proposed thematic relation, thematic and spatial associations are still strong since zones at t_{i-1} completed fall in the extent of the zone at t_i. Therefore, z_n^{i-1} expands as z_n^i when only z_n^{i-1} existed at t_{i-1}, or alternatively z_n^{i-1} separates and contracts as z_n^i by simultaneously associating with other zones at t_i.

When UHIs have obvious displacements (i.e. z_n^i touches or disjoints z_n^{i-1}), thematic cores of both zones do not have any relation because they are separated in two disjoint zones. Since each UHI can travel for a certain distance at its maximum capability during a given time period, pair of zones are considered to have the closet relationship and can be associated into a sequence of zones in a temporal domain if they have the shortest distance in between and the distance is uniquely within a distance threshold. Hence,

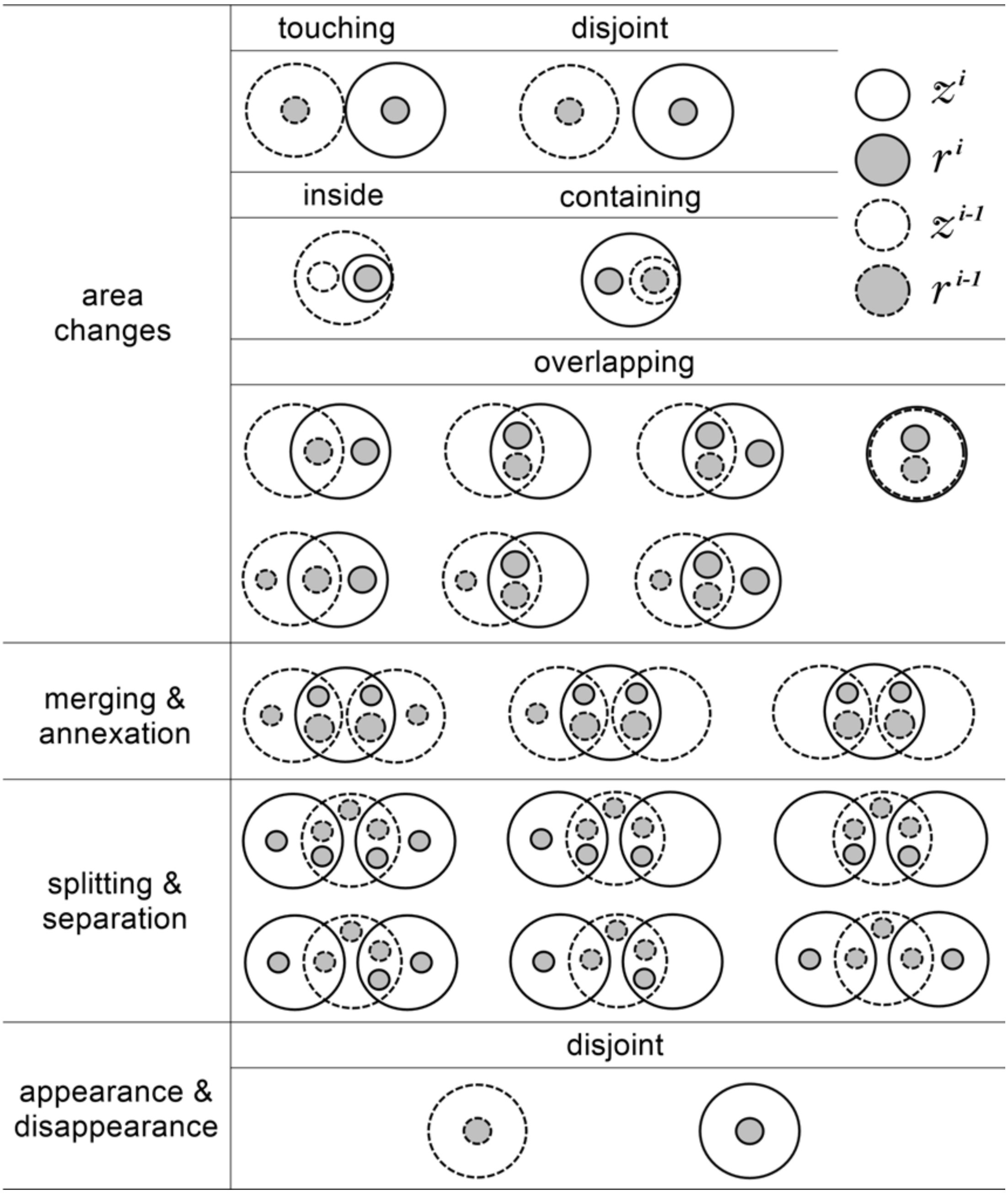

Fig. 5.4 Spatial relationships between zones and cores in two continuous time instants.

the two zones (z_n^{i-1}, z_n^i) are also conceptualized as two continuous statues of the same object with areal changes. Based on the above discussion, creation and deconstruction of an object o_n are accordingly determined as:

- *appearance* when $(\{z_m^{i-1}\}, z_n^i)$ has no thematic relation and each pair of the zones are in a remote distance; and

- *disappearance* when $(z_n^{i-1}, \{z_m^i\})$ has no thematic relation and each pair of the zones are in a remote distance.

5.5 Computation

This dissertation proposes two computational methods (i.e. unidirectional and bidirectinal zone-overlapping) to determine spatial filiations between zones. Unidirectional zone-overlapping determines *unidirectional* relationships of zones at t_{i-1} to zones at t_i to compute spatial behaviors of UHIs. However, this method may cause a problem that z_n^{i-1} is still associated to z_n^i even though z_n^i insignificantly overlaps z_n^{i-1} but significantly overlaps with z_m^{i-1}. In this case, determining z_n^{i-1} and z_n^i as the components of the same UHI is not confident enough. A better method is considering *bidirectional* overlapping scenarios that z_n^{i-1} overlaps z^i and z^i overlaps z^{i-1} to determine the spatial filiations between zones.

5.5.1 Unidirectional zone-overlapping

Several threshold parameters were defined to recognize different types of continuous and transformation filiations. First, in order to be related together, zones identified at two consecutive time instants need to overlap significantly. This is done by checking if the overlapping of two zones is significant compared to the zone at t_{i-1}. Thus, a magnitude threshold $\varepsilon_{related}$ is defined for this (equation 5.1).

$$\frac{area(z^i \cap z^{i-1})}{area(z^{i-1})} \geqslant \varepsilon_{related} \tag{5.1}$$

Then, the type of filiation that the UHI undergoing depends on the associated relationship that has been determined above and the number that a zone associates with other zones. If a zone is associated with one single zone, no transformation occurs and the UHI is changing. If no association can be determined with only one single overlapping or no overlapping, the UHI is appearing or disappearing. If several associations are made, a merge is taking place. Finally, a split occurs if there is several overlapping but with no association.

Two UHI zones are considered to be of the same size if their relative area difference is smaller than a threshold ε_{area} (equation 5.2). A UHI is considered to expand if its area has increased by ε_{area} between two consecutive time instants. Similarly, if the UHI area decreases by ε_{area}, the UHI is contracting.

$$\frac{\mid area(z^i) - area(z^{i-1}) \mid}{area(z^{i-1})} \leqslant \varepsilon_{area} \tag{5.2}$$

A merge occurs when z_k^i is associated with several zones $\{z_j^{i-1}\}$ $(j = 1, \ldots, l)$. More distinctly, an *annexation* occurs if one of the zones at t_{i-1} significantly merges into the z_k^i. Hence, a UHI will undergo an *annexation* if it has the maximum overlapping area which also occupies significant area of z_k^i (Equation 5.3). Otherwise, all the older zones corresponding to the new zone have a *merging*.

$$\frac{max(\{area(z_k^i \cap z_j^{i-1})\})}{area(z_k^i)} \geqslant \varepsilon_{merge} \; (j = 1, \ldots, l) \tag{5.3}$$

In contrast, a split occurs when z_j^{i-1} overlaps but is not associated with several zones of $\{z_k^i\}$ $(k = 1, \ldots, l)$. A *separation* occurs if area of one of the zones z_k^i still notably splits from its origin. Thus, a UHI will experience a *separation* if it has the maximum overlapping area which also takes considerable area of the preceding zone (Equation 5.4). Otherwise, *splitting* will be derived for all the UHIs.

$$\varepsilon_{split} \leqslant \frac{max(\{area(z_k^i \cap z_j^{i-1})\})}{area(z_j^{i-1})} < \varepsilon_{related} \; (k = 1, \ldots, l) \tag{5.4}$$

5.5.2 Bidirectional zone-overlapping

Obviously, the type of spatial behavior that a UHI could been determined by (i) the number of zones it associates with and (ii) the associated filiations it has with other zones. The UHI has areal change if it associates with only one zone and without any topological transformations. If no overlapping or no association occurs, this UHI will appear or disappear. Otherwise, it can have transformations when overlapping and associating with several other zones.

Thus, spatial behaviors can be stated based on the number of zones in two consecutive time instants denoted as $num = (num(\{z^{i-1}\}) : num(\{z^i\}))$, where the relation for each zone at t_{i-1} to each zone at t_i is denoted as $r(z^{i-1} \to z^i)$, and the reversal relation is $r(z^i \to z^{i-1})$. z^{i-1} has close relation to z^i if the overlapping area has significant proportion to the area of z^{i-1} (Equation 5.5). Inversely, z^i has close relation to z^{i-1} if it satisfies Equation 5.6. Hence, the two zones are determined as the same object if they have significant overlapping with each other by satisfying both conditions. To have more structured statement, let T (stands for *true*) denote the scenario when z^{i-1} relates to z^i and let F (stands for *false*) denote the case when z^{i-1} does not. Thus, relation of each pair of $(r(z^{i-1} \to z^i) : r(z^{t_i} \to z^{i-1}))$ has four possible scenarios, i.e., $relate = \{(F : F), (F : T), (T : F), (T : T)\}$.

$$\frac{area(z^{i-1} \cap z^i)}{area(z^{i-1})} \in [\varepsilon_{spaRelated}, 1] \tag{5.5}$$

$$\frac{area(z^{i-1} \cap z^i)}{area(z^i)} \in [\varepsilon_{spaRelated}, 1] \tag{5.6}$$

A UHI continues from z^{i-1} to z^i if $num = (1 : 1)$ and $relate = (T : T)$. This UHI remains at *continuation* when its areal variation is relatively limited as shown in Equation 5.7. While, the UHI can also expand or contract if it falls above the upper limit of $(1 + \varepsilon_{spatStable})$ or below the lower limit of $(1 - \varepsilon_{spatStable})$.

$$\frac{area(z^i)}{area(z^{i-1})} \in [1 - \varepsilon_{spaStable}, 1 + \varepsilon_{spaStable}] \tag{5.7}$$

A merge occurs when several zones $\{z^{i-1}\}$ relate to the same zone z^i, satisfying num=$(m : 1)$ $(m \geqslant 2)$ and $relate$=$(T : T/F)$. Moreover, an *annexation* can be determined if the maximum overlapping area is also significant to $area(z_k^i)$ (Equation 5.8), which means the zone z_k^{i-1} continues as the zone z_k^i by absorbing others. Otherwise, all the zones are merging together as a new zone.

$$\frac{max(\{area(z_j^{i-1} \cap z_k^i)\})}{area(z_k^i)} \in [\varepsilon_{annex}, 1)\ (j = 1, ..., l) \tag{5.8}$$

One the opposite, a split happens when several zones $\{z^i\}$ overlap and relate to the same zone z^{i-1}, which satisfies num=$(1:m)$ $(m \geqslant 2)$ and $relate$=$(F:T)$. More specifically, a *separation* occurs if the maximum overlapping area to the $area(z_j^{i-1})$ is still considerable though it does not satisfy the significant condition, which can be computed in Equation 5.9. Alternatively, a split is obtained if all the overlapping areas to the $area(z_j^{i-1})$ are negligible.

$$\frac{max(\{area(z_j^{i-1} \cap z_k^i)\})}{area(z_j^{i-1})} \in [\varepsilon_{separ}, \varepsilon_{spaRelated})\ (k = 1, ..., l) \tag{5.9}$$

Whenever spatial filiation of each pair of zones (z_n^{i-1}, z_n^i) has been determined, UHI constructed by sequences of zones $\{z_n^i\}$ $(i = 1, ..., l)$ can be tracked instantly such that thematic changes can be investigated in time series. If thematic *temperature* c_n^i is almost the same as c_n^{i-1} and difference between the two temperatures is negligible, it is reasonable to consider that thematic filiation of z_n^i is *stationary* computed as in Equation 5.10. However, it can be depicted as *increasing* or *decreasing* if the relative change exceeds the upper limit or the lower limit.

$$\frac{c_n^i}{c_n^{i-1}} \in [1 - \varepsilon_{theStable}, 1 + \varepsilon_{theStable}] \tag{5.10}$$

5.6 Constraint determining for spatial filiations

Since each UHI can only involve in one *transition* and/or *transformation* at each time instant, the model has to ensure that spatial filiation of each zone is neither omitted nor determined duplicately. As seen in Figure 5.5a, z_b^i overlaps on z_a^{i-1} and z_c^{i-1} significantly, and z_a^{i-1} and z_c^{i-1} also have a significant overlapping with z_b^i. Therefore, both z_a^{i-1} and z_c^{i-1} shall associate with the same z_b^i based on the bidirectional zone-overlapping method. Further, z_a^{i-1} shall become z_b^i by absorbing z_c^{i-1} because the overlapping area between z_a^{i-1} and z_b^{i-1} is larger. Since the transformation of z_a^{i-1} has been determined, it is impossible for z_a^{i-1} to contract as z_d^i simultaneously. This scenario can be automatically excluded when z_a^{i-1} can only have one significant overlapping area satisfying Equation 5.5, which requires $\varepsilon_{spaRelated}$ is larger than 0.5. Because of the same reason, z_c^{i-1} cannot be determined as the same object as z_b^i. This can be achieved when the overlapping area $area(z_a^{i-1} \cap z_b^i)$ occupies more than half of the $area(z_b^i)$ such that $area(z_b^i)$ and $area(z_c^{i-1})$ will never satisfy in Equation 5.8 when ε_{annex} is larger than 0.5.

However, the proposed method may still come across a conflict in determining spatial filiations. For example, z_b^{i-1} and z_c^{i-1} have merged together and a new zone z_d^i has generated as shown in Figure 5.5b, which means sum of the overlapping area $area(z_b^{i-1} \cup z_c^{i-1})$ takes rather small proportion of $area(z_d^i)$. This consequently causes one possibility that the overlapping area $area(z_a^{i-1} \cap z_d^i)$ is significant, and hence z_d^i can split from z_a^{i-1}. To solve this conflicting problem, the model gives z_d^i the first priority to have the merging behavior.

5.7 System implementation

5.7.1 System architecture

The object-relational database management system (DBMS) PostgreSQL 9.3.4 was to manage the data sets, and pgAdmin III 1.18.1 was utilized as an administrative and management tool for the database development. Experiments for evaluating performance of the system have been conducted in Windows 8 64-bit with Intel(R) Core(TM) i7-4770 CPU (4 cores, 8 processors, 3.4GHz, and 16.0 GB RAM).

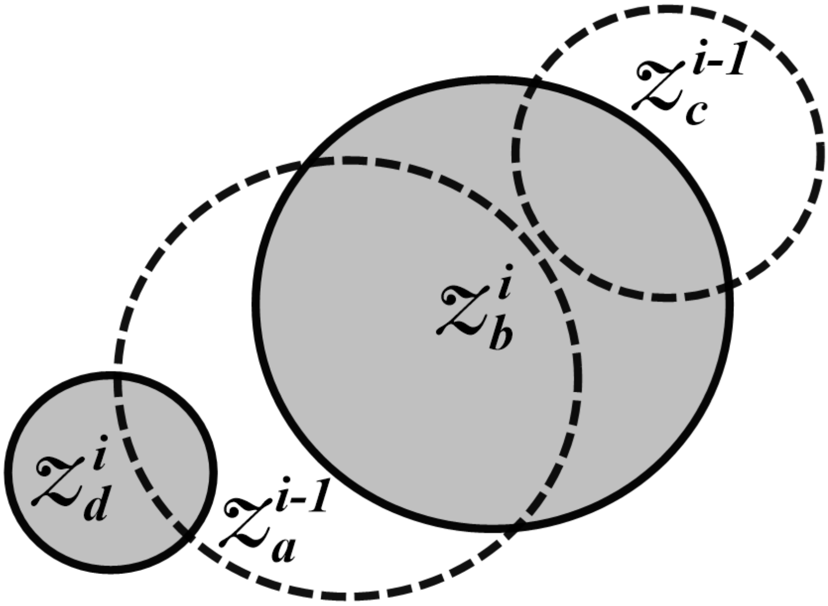

(a) z_a^{i-1} absorbs z_c^{i-1} and becomes z_b^i (annexation).

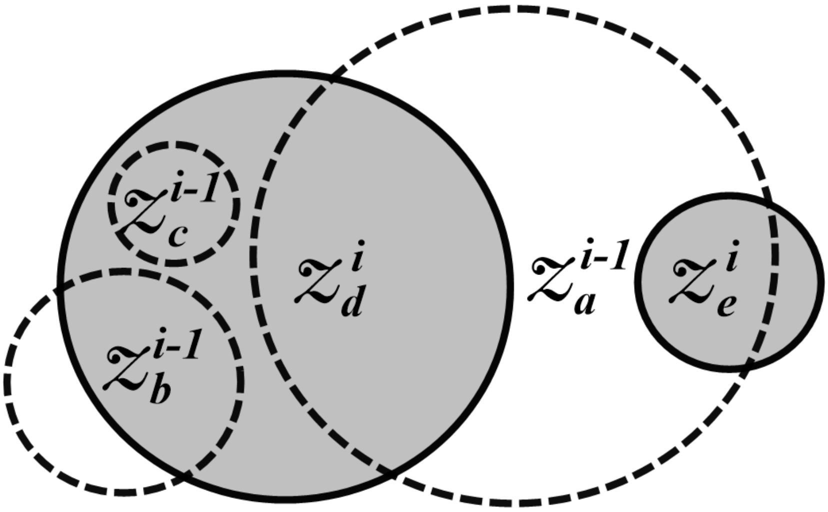

(b) z_b^{i-1} and z_c^{i-1} merges together and becomes z_d^i (merging).

Fig. 5.5 Constraint analysis to avoid duplicate clustering of spatial filiations between zones.

5.7.2 Database model

A database model for summarizing all the classes and their associations is presented in Figure 5.6. First, a time series of thermal images interpolated from the air temperatures are imported into the `image` tables. To reduce the computational cost, each set of zones that have been extracted from each image is firstly stored as a union zone (i.e. a set

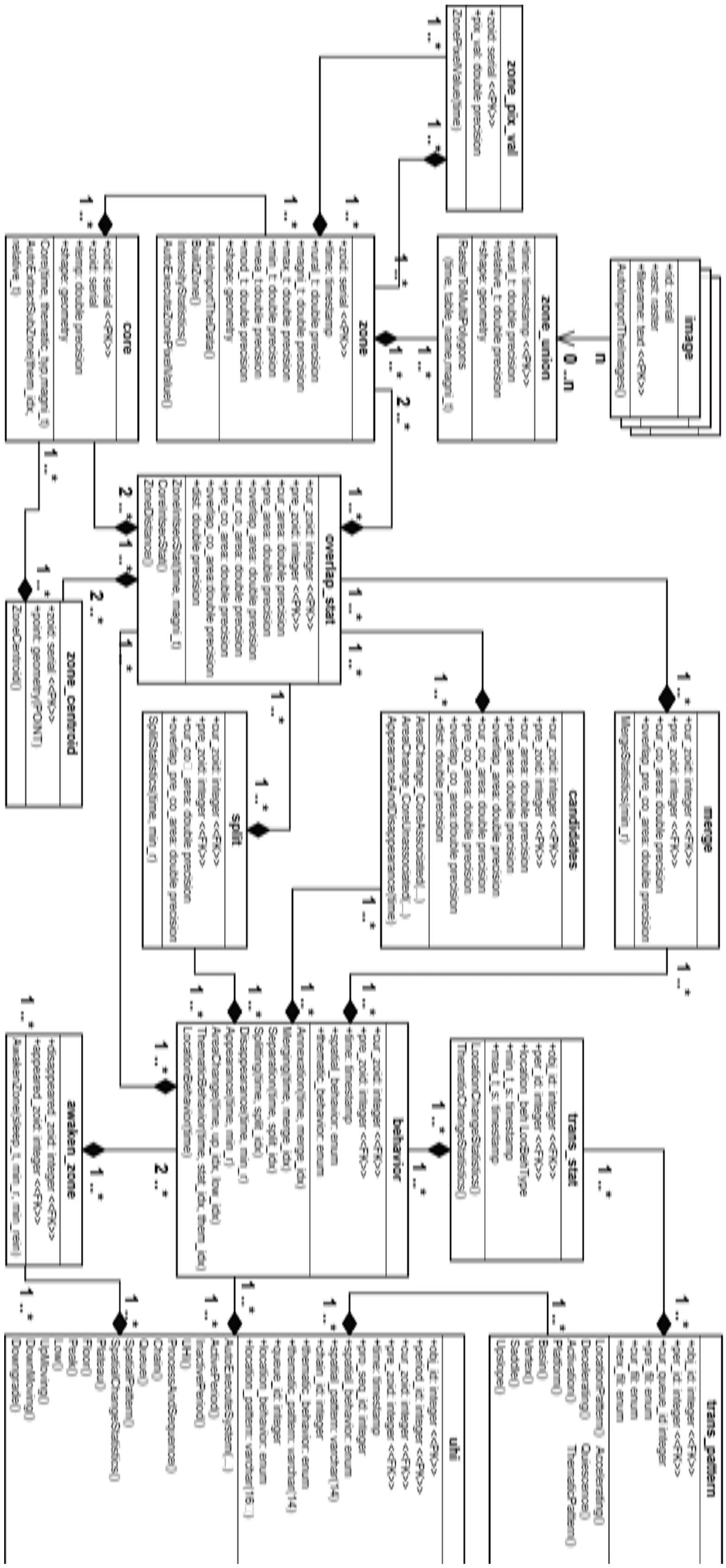

Fig. 5.6 Database tables, functions, and their associations for tracking behaviors of UHIs over time.

of zones that are unionized as a single zone) in the `zone_union` table. Then, each union zone is discretized as a set of single polygons and stored in a geometry column named as `shape` in the `zone` table so that temperatures within each zone are with a given temperature (i.e. `m_t`) higher than the rural temperature (i.e. `rural_t`). Pixel values of each zone are summarized and recorded in the table of `zone_pix_val` so that an appropriate temperature value can be specified for constructing cores of each zone in the table of `core`. For each time instant, overlapping statistics between the zones are recorded in the `overlap_stat` table so that whether the overlapping area is significant to both $area(z_n^{i-1})$ and $area(z_n^i)$ which can be checked for zone filiation determination. More specifically, overlapping area (i.e. `overlap_area`) of each pair of zones ⟨`pre_zid, cur_zid`⟩ respectively at t_{i-1} and t_i are calculated. Simultaneously, additional information such as the distance between each and every two zones in the two time instants is recorded as the `dist` in the `overlap_stat` table, which is derived from the records of their centroids in the `zone_centroid` table.

Three types of filiations (i.e. spatial, locational, and thematic filiations) between zones at each time instant can be determined at this stage. To avoid duplicated determination of behaviors of zones, zones which are merged, split, or still continued are respectively listed in the `merge`, `split`, and `candidates` tables. Hence, a new table named as `behavior` can be added storing the filiations computed for each zone in order to build up *sequences* and *transformations*. This table includes not only the continuous but also topological transformations of Figure 3.2. Each type of the filiation instance is composed of two attributes which are the current zones (i.e. `cur_zid`) and preceding zones (i.e. `pre_zid`). Particularly, the three functions associated in the `candidates` class are one-click solution that can determine zones which will continue (i.e. *expansion*, *continuation*, and *contraction*), appear and disappear, and can insert them into the `behavior` table. When the system has reconstructed all the filiations at each time, pairs of zones which have disappeared for certain time period and appeared again at t_i can be determined and listed in the `awaken_zone` table. Based on this table, active periods and inactive periods hence can be constructed by the `ActivePeriod()`

and InactivePeriod() functions, which are uniquely recorded as the period_id attribute in the uhi table. Consequentially, complete life-cycle for each UHI is built from the periods and listed as the obj_id.

Finally, zones belonging to the same sequence and zones relating topological transformations are recorded in the pro_seq_id through the ProcessAndSequence() function. According to the obtained process-and-sequence IDs, spatial behaviors can be easily determined (i.e. spatial_behavior) and hence their patterns are discovered (i.e. spatial_pattern) in the uhi table. Similarly, zones which have been continuing for certain time period can have transitions for both locational and thematic properties. The statistics for two transitions are carried out respectively in the trans_stat table such that the designed patterns are discovered and listed in the trans_pattern table, which are ultimately organized in the uhi table.

5.7.3 Populating the tables

All the filiations and evolution occurring in whole of the life-cycle of each UHI are retrieved through SQL queries. Algorithm 1 computes all the zones that to be merged at each time instant. Firstly, the number of zones ⟨cnt, c_oid⟩ which are related with ones at previous time instant are listed based on simple aggregations (Lines 2-4). Thus, all the pairs of zones ⟨p_oid, c_oid⟩ that each c_oid has more than one association are determined (Lines 1-6), suggesting which will be merged. Then, Algorithm 2 determines zones (named as p_oid) which are absorbed by zones (named as c_oid). Line 3 firstly lists the largest intersection area for each zone ⟨max_i_a, c_oid⟩ so that zones ⟨p_oid, c_oid⟩ that have the largest intersection area are obtained (Lines 2-5). Inversely, the algorithm computes pairs of zones which only have the topological transformation when p_oid has no the largest intersection area (Line 6). Algorithm 3 calculates zones which only have areal changes (i.e. *expansion* more specifically). Based on the zones {c_oid} that are related with {p_oid} derived from one simple aggregation (Lines 2-3), the function further selects the only instance for c_oid (Line 4) that ⟨p_oid, c_oid⟩ are related (Lines 5-6) and area of c_oid is larger than p_oid

SQL 1 FUNCTION PreMergeStat(min_r)

```
SELECT ints_st.c_oid, ints_st.p_oid, ints_st.c_a, ints_st.i_a
FROM  (SELECT count(c_oid) AS cnt, c_oid
       FROM  (SELECT ints_st.c_oid
              FROM   ints_st
              WHERE ints_st.i_a / ints_st.p_a >= min_r
              AND p_a > 0) AS cur_g GROUP BY c_oid) AS cnt_cur_g, ints_st
WHERE  cnt_cur_g.cnt > 1 AND cnt_cur_g.c_oid = ints_st.c_oid
AND    ints_st.p_a > 0 AND ints_st.i_a / ints_st.p_a >= min_r;
```

SQL 2 FUNCTION AnnexationDiffObj(time, merge_idx)

```
SELECT time, merge.c_oid, merge.p_oid, annex_diff_obj
FROM  (SELECT merge.c_oid, merge.p_oid
       FROM  (SELECT c_oid, max(i_a) AS max_i_a
              FROM   merge GROUP BY c_oid) AS p_key, merge
       WHERE  merge.c_oid = p_key.c_oid AND merge.i_a = p_key.max_i_a
       AND    merge.c_a > 0
       AND    merge.i_a / merge.c_a >= inh_merge) AS inh_mer_obj, merge
WHERE  inh_mer_obj.c_oid = merge.c_oid AND inh_mer_obj.p_oid <> merge.p_oid;
```

SQL 3 FUNCTION Expansion(time, min_r, up_idx)

```
SELECT time, ints_st.c_oid, ints_st.p_oid, expansion
FROM   ints_st, (SELECT count(c_oid) AS cnt, c_oid
                 FROM ints_st WHERE p_a > 0
                 AND i_a / p_a >= min_r GROUP BY c_oid) AS maintain_obj
WHERE  maintain_obj.cnt = 1
AND    ints_st.c_oid = maintain_obj.c_oid
AND    ints_st.i_a / ints_st.p_a >= min_r
AND    ints_st.p_a > 0 AND ints_st.c_a / ints_st.p_a >= up_idx;
```

SQL 4 FUNCTION Appearance(time, min_r)

```
SELECT time, potential_oid.c_oid, appearance
FROM  (SELECT c_oid FROM ints_st
       WHERE  c_a > 0 GROUP BY c_oid) AS potential_oid
LEFT JOIN (SELECT c_oid FROM ints_st WHERE p_a > 0
           AND i_a / p_a >= min_r GROUP BY c_oid) AS ints_oid
ON         potential_oid.c_oid = ints_oid.c_oid
LEFT JOIN (SELECT c_oid FROM merge GROUP BY c_oid) AS merged_oid
ON         potential_oid.c_oid = merged_oid.c_oid
LEFT JOIN (SELECT c_oid FROM split GROUP BY c_oid) AS split_oid
ON         potential_oid.c_oid = split_oid.c_oid
WHERE ints_oid.c_oid IS NULL
AND   merged_oid.c_oid IS NULL AND split_oid.c_oid IS NULL;
```

SQL 5 FUNCTION ActivePeriod()

```
1 INSERT INTO period(per_id, t_s, c_oid, p_oid, spat_beh, them_beh)
2 SELECT max(path) AS path, per.t_s, per.cur_zoid,
         per.pre_zoid, per.spat_beh, per.them_beh
3 FROM  (WITH RECURSIVE per_u(path, t_s, cur_zoid, pre_zoid, spat_beh, them_beh)
4        AS  (SELECT row_number() OVER (ORDER BY t_s) AS path, root.t_s,
5                    root.cur_zoid, root.pre_zoid, root.spat_beh, root.them_beh
6             FROM   behavior AS root UNION
7             SELECT leaf.path, root.t_s, root.cur_zoid, root.pre_zoid,
                     root.spat_beh, root.them_beh
8             FROM   behavior AS root, per_u AS leaf
9             WHERE  root.cur_zoid = leaf.pre_zoid
10            AND    leaf.pre_zoid > 0 AND leaf.spat_beh <> 'separa_d_obj'
11            AND    root.spat_beh <> 'annexa_d_obj'
12            AND    root.spat_beh <> 'merging' AND root.spat_beh <> 'splitting')
13       SELECT * FROM per_u ORDER BY path, t_s) AS per
14 GROUP BY per.t_s, per.cur_zoid, per.pre_zoid, per.spat_beh, per.them_beh;
```

(Line 7). Algorithm 4 computes appeared zones with a simple excluding method. First, line 2 lists zones that possibly are appeared ones in the current time instant. Second, the function queries all the zones of {`c_oid`} which have areal changes (Lines 3-5), merges (Lines 6-7) and splits (Lines 8-9). Third, zones having *appearance* can be selected by excluding the above scenarios from derived {`potential_oid`} (Line 10).

It is necessary to identify topological relations associated with zones that can create and destroy an active period (Algorithm 5), and it is also vital to connect the active periods that belong to the same UHI by determining the awaken zones that trigger the new periods (Algorithm 6). In Algorithm 5, lines 4-6 generate serial numbers as the candidates of period IDs, which are viewed as the roots of periods. Lines 7-12 extend sequences of zones starting with which are newly generated. More specifically, line 9 connects the leaves on the root. Line 10 avoids the computational dead circle by ensuring that the appearance and disappearance behaviors are included in the period, and generates the period when zones are separated as different objects. Hence, lines 11-12 terminate the extension of sequences when zones are destroyed. Lastly, lines 3-13 execute the recursive calculation and lines 2-14 select the maximum value of path used as the final period ID. In the Algorithm 6, lines 5-6 and 7-8 respectively list zones having *appearance* as the head and *disappearance* as the tail, where time interval

SQL 6 FUNCTION AwakenZone(sleep_t, min_r, min_rein)

```
1 CREATE TABLE awaken_cand AS
2 SELECT tail_seq.zoid AS disap_zo, head_seq.zoid AS reapp_zo,
3       (head_seq.t_s - tail_seq.t_s) AS dth_t,
4        ST_Area(ST_Intersection(head_seq.geom, tail_seq.geom)) AS i_a
5 FROM  (SELECT zone.* FROM zone, period
6        WHERE spat_beh = 'appearance'
         AND zone.zoid = period.cur_zoid) AS head_seq,
7       (SELECT zone.* FROM zone, period
8        WHERE spat_beh = 'disappearance'
         AND zone.zoid = period.pre_zoid) AS tail_seq
9 WHERE  head_seq.t_s - tail_seq.t_s <= sleep_t * 3600 * '1 second'::INTERVAL
10 AND   head_seq.t_s - tail_seq.t_s >= 2 * 3600 * '1 second'::INTERVAL
11 AND   ST_Area(ST_Intersection(head_seq.geom, tail_seq.geom))
         /ST_Area(head_seq.geom) >= min_r
12 AND   ST_Area(ST_Intersection(head_seq.geom, tail_seq.geom))
         /ST_Area(tail_seq.geom) >= min_r
13 AND   ST_Area(ST_Intersection(head_seq.geom, tail_seq.geom))
         /ST_Area(head_seq.geom) >= min_rein;

14 INSERT INTO awaken_zone(disappeared_zone, reappeared_zone)
15 SELECT awaken_cand.disap_zo, awaken_cand.reapp_zo
16 FROM   awaken_cand,
17       (SELECT awaken_cand.reapp_zo, min(awaken_cand.dth_t) AS min_dth_t
18        FROM   awaken_cand,
19              (SELECT min(dth_t) AS min_dth_t, disap_zo
20               FROM awaken_cand GROUP BY disap_zo) AS dth_cand,
21              (SELECT max(i_a) AS max_i_a, dth_t, disap_zo
22               FROM awaken_cand GROUP BY disap_zo, dth_t) AS ints_cand
23        WHERE dth_cand.min_dth_t = awaken_cand.dth_t
          AND   dth_cand.disap_zo = awaken_cand.disap_zo
24        AND   ints_cand.max_i_a = awaken_cand.i_a
          AND   ints_cand.disap_zo = awaken_cand.disap_zo
25        AND   dth_cand.disap_zo = ints_cand.disap_zo
          GROUP BY awaken_cand.reapp_zo) AS uhi_cand
26 WHERE  awaken_cand.reapp_zo = uhi_cand.reapp_zo
27 AND    awaken_cand.dth_t = uhi_cand.min_dth_t ORDER BY awaken_cand.reapp_zo;
```

between them is more than two hours but not longer than the maximum sleeping time (lines 9-10). Thus, pairs of the heads and tails that satisfy the awaken condition (lines 11-13) are selected as the awaken candidates (lines 2-3). However, several disappeared zones can map to the same appeared zone in the awaken candidates. On the basis of the candidates which have the minimum sleeping time (lines 19-20), zones having the maximum overlapping area are selected (lines 21-22) from the records of awaken candidates (lines 23-25). Finally, zones satisfying all the conditions are imported into

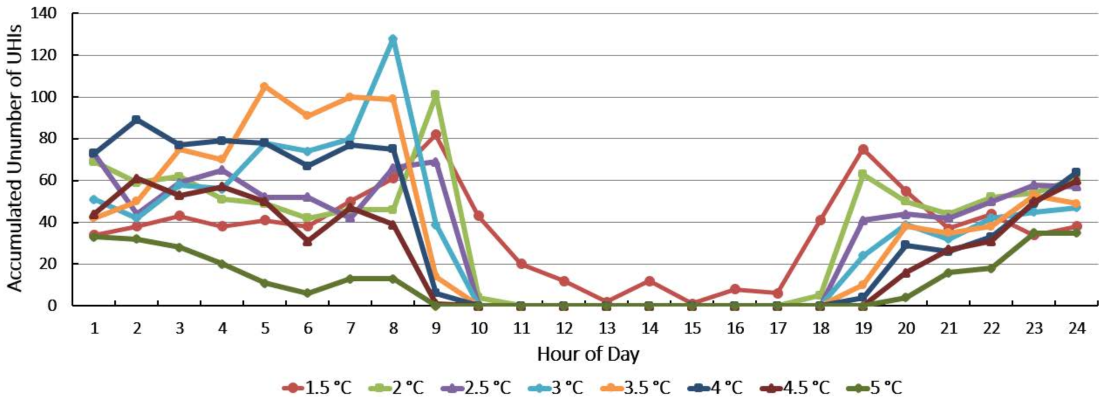

Fig. 5.7 Accumulated number of UHIs with different magnitudes summarized by hour-of-day for seven days.

the awaken table (lines 14-17).

5.8 Results

The spatial and thematic filiations between zones to track the whole life-cycles of UHIs. Section 5.8.1 mainly focuses on the spatial filiations between zones, which is computed using the *unidirectional zone-overlapping* method as proposed in 5.5.1. Each active period is viewed as a complete life-cycle for a UHI since cycles are not constructed in this section. By contrast, Section 5.8.2 represents the results for both spatial and thematic filiations, using the *bidirectional zone-overlapping* computing method according to 5.5.2. Active and inactive periods construct a complete life-cycle in this case because UHIs are viewed as objects that can have reincarnation process. Lastly, Section 5.8.4 instantly tracks the changes of all the designed behaviors, and some interesting patterns are also revealed.

5.8.1 Spatial filiations between zones

Temperature which is with a given threshold temperature (i.e. magnitude) above the referenced rural temperature was used as the threshold to extract zones from images. Based on the magnitudes that are between 1.5 and 5 degree Celsius, accumulated num-

Table 5.1 An active period for an urban heat island

time	curZID	preZID	objID	s/pID	spaBeh	spaPat
15-07-31 21:00	67	51	251	152	annex_s_obj	annex_s_obj
15-07-31 22:00	70	67	251	152	annex_s_obj	annex_s_obj
15-07-31 23:00	74	70	251	174	continuation	plateau
15-08-01 00:00	2765	74	251	174	continuation	plateau
15-08-01 01:00	2694	2765	251	174	continuation	plateau
15-08-01 02:00	2626	2694	251	191	contraction	leave_plateau
15-08-01 03:00	2630	2626	251	196	annex_s_obj	annex_s_obj
15-08-01 04:00	2771	2630	251	199	continuation	null
15-08-01 05:00	2775	2771	251	205	annex_s_obj	annex_s_obj
15-08-01 06:00	167	2775	251	205	annex_s_obj	annex_s_obj
15-08-01 07:00	174	167	251	222	contraction	null
15-08-01 08:00	2776	174	251	229	splitting	splitting

ber of UHIs summarized in unit of hour-of-day for seven days is drawn in Figure 5.7. The figure shows that the numbers of UHIs with eight different magnitudes decrease dramatically from 8 am when the sun is rising, while there is no UHI during 11 am and 5 pm apart from the case of 1.5 degrees intensity. After 5 pm, all the lines grow significantly in a whole trend with some variation between 7 pm and 9 pm. In general, this figure shows that the UHI phenomenon is much obvious during the night as this has been widely acknowledged.

To reveal the evolutionary trend of UHIs in the whole study area, a low magnitude (1.5 degree Celsius) was selected to simulate all the *events* and track all the life-cycles given the input parameters of $\varepsilon_{related}$, ε_{area}, ε_{merge}, and ε_{split} equaling to 0.53, 0.1, 0.65, and 0.5001, respectively. This set of parameters is determined based on several empirical tests, all of which satisfy the constraint conditions in Section 5.6. Table 5.1 lists a complete *life-cycle* of a UHI directly plotted from the `uhi` table. In the table, a UHI is identified by the ID (`objID`), which contains a pair of zones in the current and previous time instants (`curZID` and `preZID`) at every time instant (`time`), and its behavior (`spaBeh`) and transition (`spaPat`) are recorded for each sequence or transformation (s/pID). The table shows that this UHI exists from 9 pm to 8 am on the next day with several continuous processes of *annexation* and sequences of *continuation*. Changes

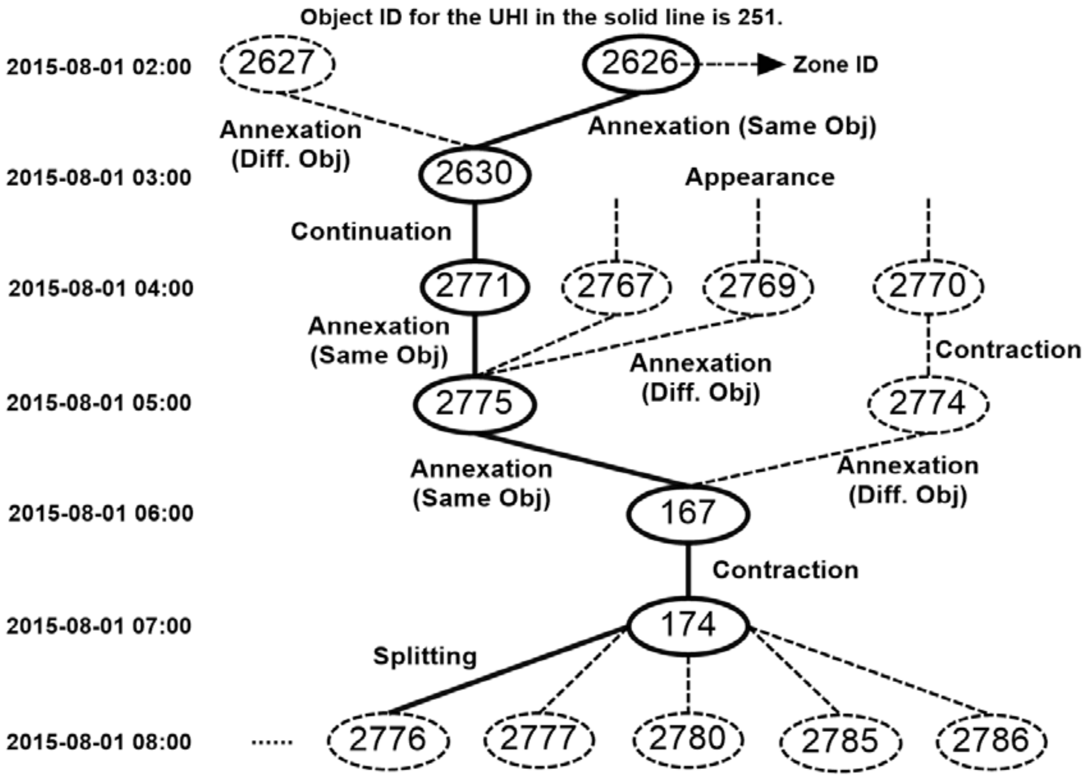

Fig. 5.8 Evolutionary trajectory of a UHI drawn from part of its life-cycle.

between sequences are also listed having the *plateau* and *leave a plateau* behaviors. To have an in-depth investigation of this UHI, Figure 5.8 draws part of its evolution interacting with other UHIs, which can be viewed as a graph $\mathbf{G}_S$ containing the vertices of zones connecting with the edges of several *events*. Obviously, zone of 2626 absorbs zone of 2627 and becomes 2630 at 3 am. Then, this UHI is stabilized as zone of 2771 in a given range of area variation, and three new UHIs appear simultaneously. In the next hour, the zone 2771 merges the other two into its own body, and the newly appeared zone 2770 becomes 2774 contracting its areal extent in the meanwhile. Subsequently, the zone 2775 absorbs 2774 and becomes 167 at 6 am. Finally, the zone 167 contracts as 174 and splits as several new UHIs.

Figure 5.9 shows the spatial distribution of the above UHIs in six consecutive hours, which clearly presents that the UHI phenomenon is obvious and stable at night. More specifically, the large UHI covers the most urbanized urban areas throughout the night with variations of appearing and disappearing of some small UHIs in the northwest.

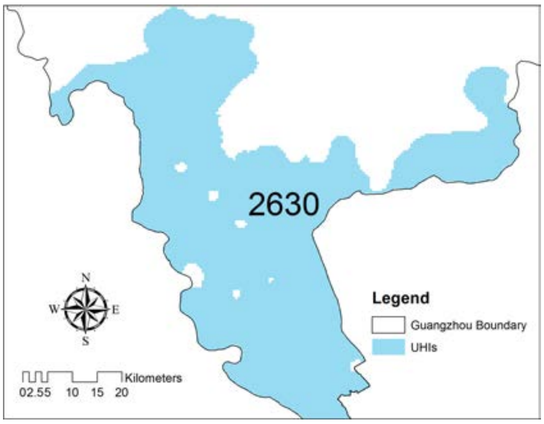

(a) Two zones merge together as a single zone 2630 at 3 am.

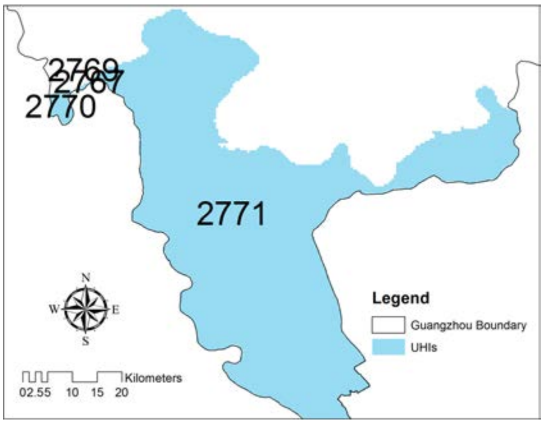

(b) Zone 2630 continues as 2771 and three new ones appear at 4 am.

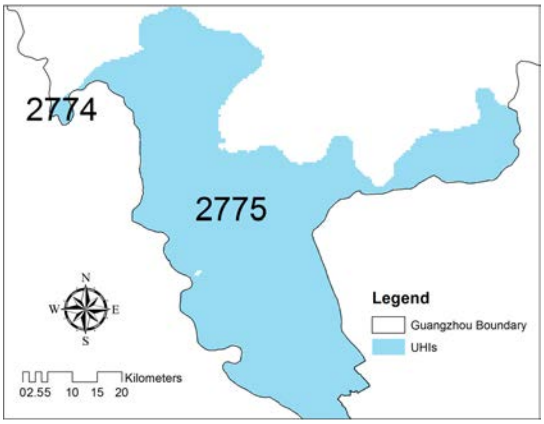

(c) Zone 2771 merges two others as 2775, and zone 2774 contracts at 5 am.

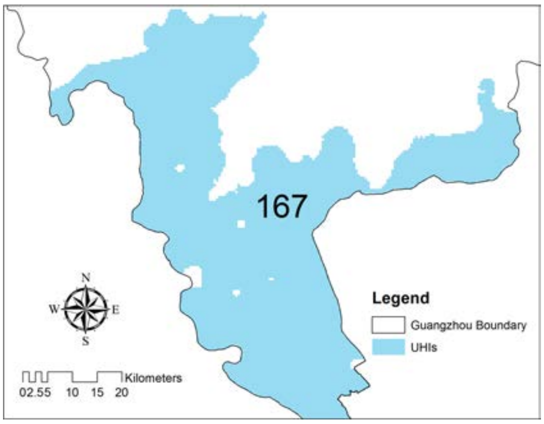

(d) Zone 2775 grows and merges the other one as 167 at 6 am.

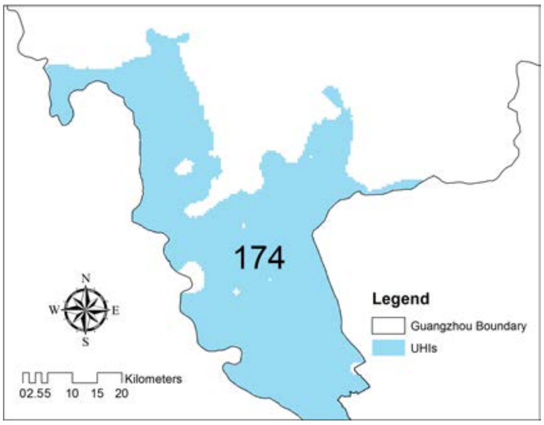

(e) Zone 167 contracts as 174 at 7 am.

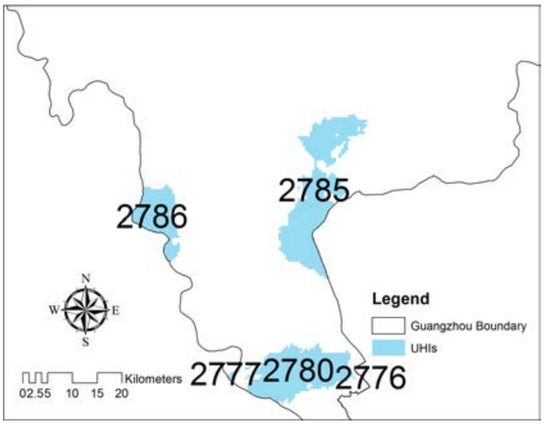

(f) Zone 174 contracts and splits as five pieces at 8 am.

Fig. 5.9 Areal changes of UHIs at six consecutive time instants.

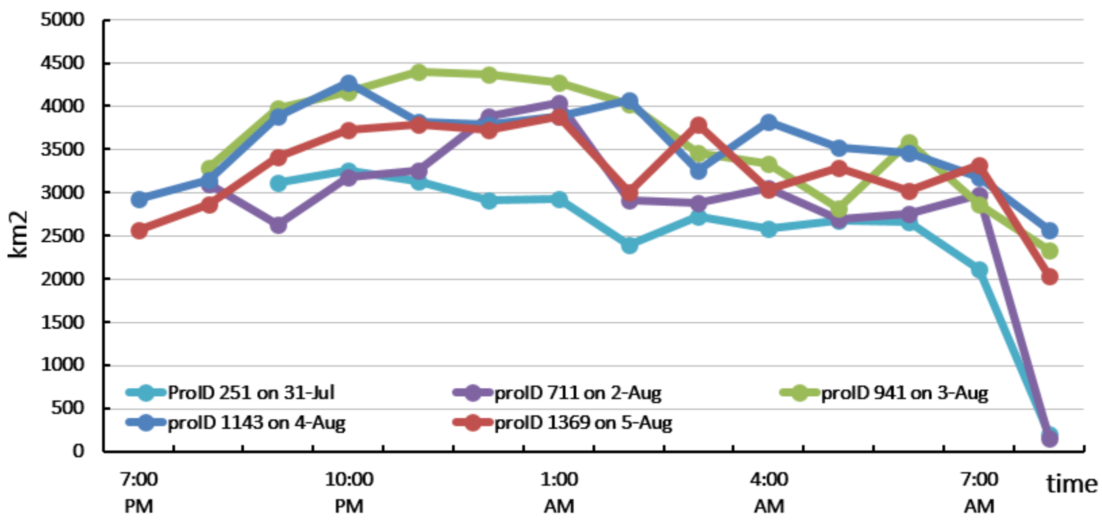

Fig. 5.10 Area tracking of five UHIs in five different days.

This is probably because of the thermal emission of the urban areas absorbed from the solar radiation and anthropologic heat flux during the day time. Area of the UHI then decreases significantly in the early morning and continuously dissipates and splits into several pieces at 8 am, which corresponds to sunrise and a rising reference temperature. A similar phenomenon revealed by (Kourtidis *et al.,* 2015) would also support the effectiveness of this model. Areal change tracking of this UHI (i.e. `objID 251`) together with the other four in five different days is also drawn in Figure 5.10, which shows that all of them share the very similar trend of areal change, starting from stable increase followed by notable variation, and ending with dramatic decrease. More interestingly, all of these UHIs appear at around 8 pm benefiting from *annexation* and disappear at 8 am caused by *splitting* or *disappearance*, which indicates an obvious periodical trend for them. Thus, this example explicitly suggests that the system can effectively track the dynamic behaviors of the UHIs in areal changes and transformations.

Based on the results as illustrated above, temporal evolution trend of UHIs can be revealed by accumulating the number of different *events* in unit of hour-of-day as shown in Figure 5.11. Obviously, the *appearance* and *merging* events mostly occur from 7 pm, which indicates the UHIs increasingly expand and merge together after the sunset. In contrast, the *splitting* and *disappearance* events dominantly happen at 9

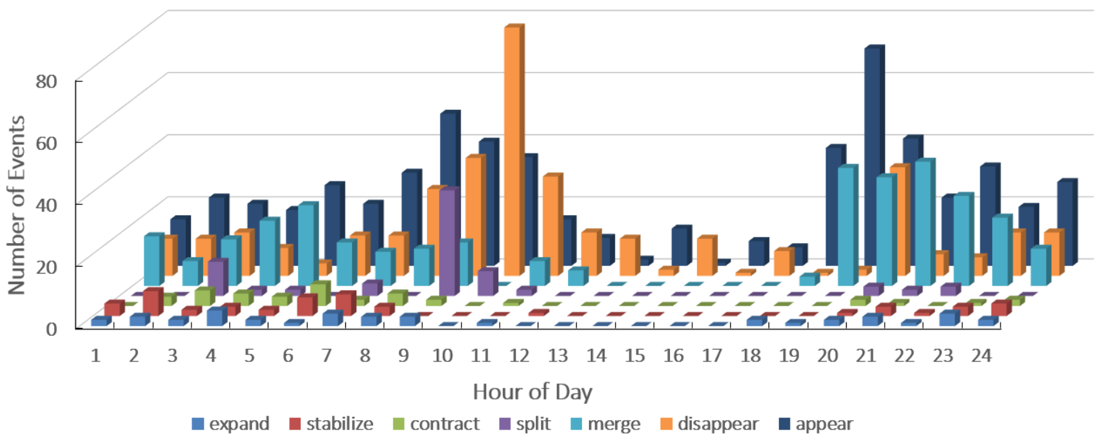

Fig. 5.11 Number of different events accumulated by hour-of-day for seven days.

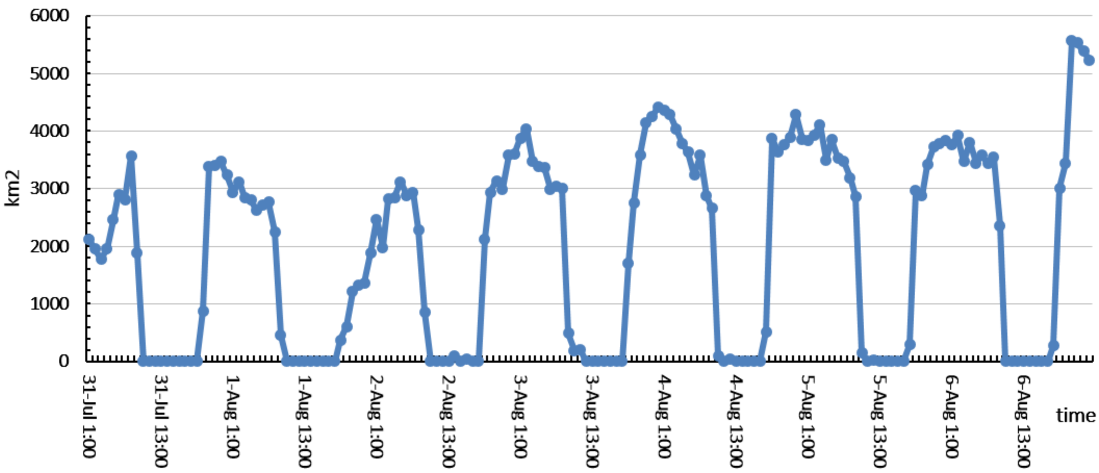

Fig. 5.12 The total area of UHIs during seven days in the whole study area.

am and 10 am respectively, suggesting the fact that UHIs are splitted and disappeared rapidly most probably caused by the increase of referenced rural temperature after the dawn. While, other three events are not observed frequently during the whole night. This indicates that only a few UHIs have independent evolution, while most UHIs interact with each other frequently due to the significant variation of air temperatures perpetually.

Figure 5.12 shows that the total area of UHIs in the study area has an apparent periodical trend, which expands significantly at around 8 pm, reaches to the largest extents at around 1 pm, and contracts dramatically around 8 pm every day. To discover periodical trend of UHIs, zones of UHIs when disappeared and appeared are extracted

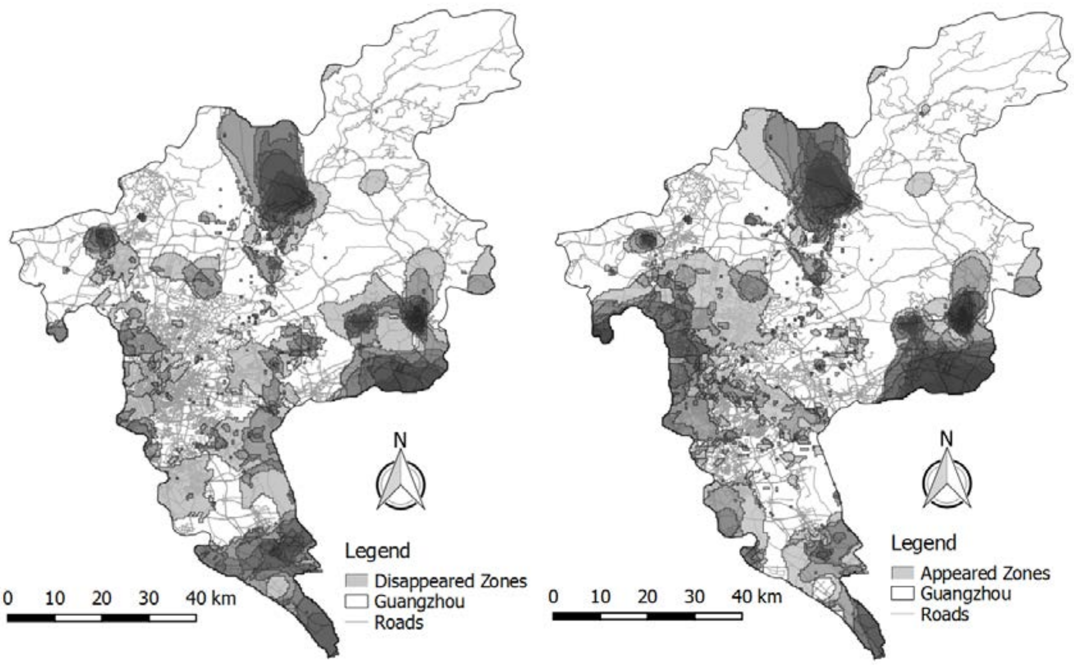

(a) Disappeared zones of UHIs (b) Appeared zones of UHIs

Fig. 5.13 Roads are overlapped with disappeared and appeared zones of UHIs.

from *transformations* overlapping with the road networks (Figure 5.13). Obviously, occurrence of the disappeared and appeared zones of UHIs has almost the same spatial distribution indicating that they are most probably the same UHIs with periodical *life-cycle* trend. It also represents that the most frequently disappeared and appeared zones are located in the less dense urban areas (i.e. north and east regions of the study area). Interestingly, several small and discrete areas in the urbanized core areas with high density of road networks in the middle region of the study area also have the most frequent occurrence. This suggests that human activities (e.g. transportation) may have considerable periodical influence to the UHI phenomenon as discussed in the literature (Alonso *et al.,* 2003; Srivanit & Hokao, 2012). The southern part also has high frequent occurrence where a great number of factories are located although the density of road network is not high.

Table 5.2 Spatial and thematic filiations of a UHI in its active period.

objID	perID	time	curZID	preZID	s/pID	spaBah	spaPat	chaID	theBeh	thePat
15	315	15-07-31 21:00	2277	2262	188	annex	annex	150	dec	reaBas
15	315	15-07-31 22:00	135	2277	188	annex	annex	150	dec	reaBas
15	315	15-07-31 23:00	144	135	188	annex	annex	150	dec	reaBas
15	315	15-08-01 00:00	2872	144	188	annex	annex	150	dec	reaBas
15	315	15-08-01 01:00	182	2872	244	expan	reaPek	203	sta	basin
15	315	15-08-01 02:00	188	182	251	cntra	leaPek	203	sta	basin
15	315	15-08-01 03:00	1473	188	263	annex	annex	203	sta	basin
15	315	15-08-01 04:00	2876	1473	266	cntra	null	203	sta	basin
15	315	15-08-01 05:00	2881	2876	273	annex	annex	203	sta	basin
15	315	15-08-01 06:00	195	2881	273	annex	annex	203	sta	basin
15	315	15-08-01 07:00	2889	195	273	annex	annex	230	inc	leaBas
15	315	15-08-01 08:00	2890	2889	296	cntra	null	230	inc	leaBas
15	315	15-08-01 09:00	0	2890	300	disap	disap	236	null	null
15	316	15-08-01 10:00				null	null		null	null
15	316	15-08-01 22:00				null	null		null	null
15	409	15-08-01 23:00	2891	0	357	appea	appea	280	null	null
15	409	15-08-02 00:00	3532	2891	358	expan	null	282	dec	reaBas
15	409	15-08-02 01:00	3546	3532	358	expan	null	282	dec	reaBas
15	409	15-08-02 02:00	357	3546	400	merge	merge	323	sta	basin

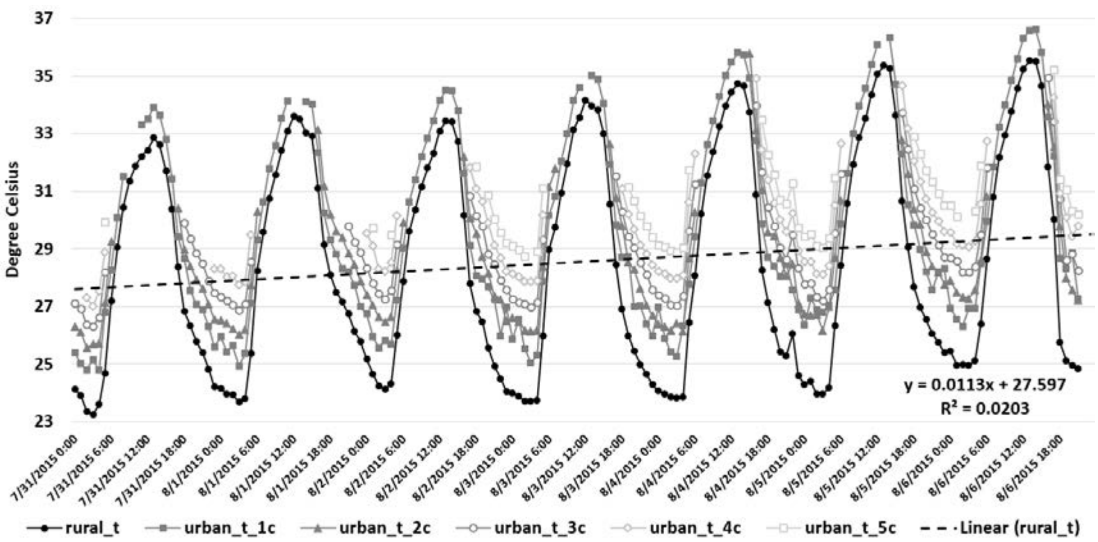

Fig. 5.14 Temperature variations of the UHIs in five different thematic intensities for consecutive seven days calculated based on the observed rural temperatures.

5.8.2 Spatial and thematic filiations between zones

Temperatures with at least one to five degree Celsius (which is also viewed as five UHI magnitudes) higher than the observed rural temperatures were identified and used to extract zones of UHIs. Figure 5.14 represents seven consecutive days of the averaged rural temperatures (*rural_t*) and UHI temperatures in five different intensities (*urban_t_1c* to *urban_t_5c*). The figure shows that both rural and UHI temperatures have very obvious periodical trends each day, growing from the lowest value in the middle of the night to the highest at noon. Nevertheless, both temperatures have slightly growth every day during the whole temporal span, which suggests that the significance of the UHI is gradually increasing. On each day, the most significant UHI phenomenon occurs in the middle of the night, which is also notable at noon for UHIs in the low intensity (*urban_t_1c*). It also reveals that UHI with lower intensities has longer temporal span than that with higher intensities, which, however, has less significant phenomenon because temperature difference with the rural temperature is smaller.

Let the UHI magnitude be 2 and the thematic temperature of each UHI be the mean value of temperatures within the UHI zone such that all the UHI behaviors can be simulated. Table 5.2 shows a complete life-cycle of a UHI (`objID`) with an inactive period (`perID`=316) connecting with two active periods, and spatial and thematic filiations (`spaBeh` and `theBeh`) of each pair of zones (`curZID` and `preZID`) are listed at each time instant (`time`). This indicates that all the information of the proposed five graphs can be easily queried from the built model. Particularly, the UHI areas expand during the first four hours followed by the expansion and contractions. Hence, the UHI continuously embraced others and then contracted and disappeared temporally during the sun rising, following an awaken in the middle of night of the same day. Notably, the UHI also had a very obvious thematic evolutionary pattern from *reaching a basin* (`reaBas`), *at a basin* (`basin`), *leaving a basin* (`leaBas`) during the first period.

To investigate spatial variation of the UHI, zones in the first period of the above mentioned UHI (`obj_id` equals to 15) are plotted in light gray color, which are overlapped by other UHI zones having higher magnitudes (Figure 5.15). The figure shows an overall trend that most of the zones expand gradually with a mild shrinking in between, shrink dramatically, and finally disappear. Zones with higher intensities have more discrete and smaller areas located within the zones having lower intensities, and their life spans are much shorter. In addition, some urban heat sinks (UHSs) appear as holes in the zones of UHIs, areas and locations of which are very stable with insignificant change for a time period. Further investigation suggests that locations of these UHSs are associated with the green lands, water body, and open areas in the delta region. However, detailed process of the dramatic contraction of the UHIs starting from 7 am cannot be tracked without more thermal images.

Observation samples by different spatial and thematic behaviors were also summarized that Chi-square test could be used to investigate correlation relations between them since they are qualitative indicators (i.e. non-numeric data). Considering that behaviors can be influenced notably when zones are extracted in different magnitudes, a series of intensities are used to calculate the P-values. For example, if two zones merge together as one, then other zones with higher magnitudes located within the two zones

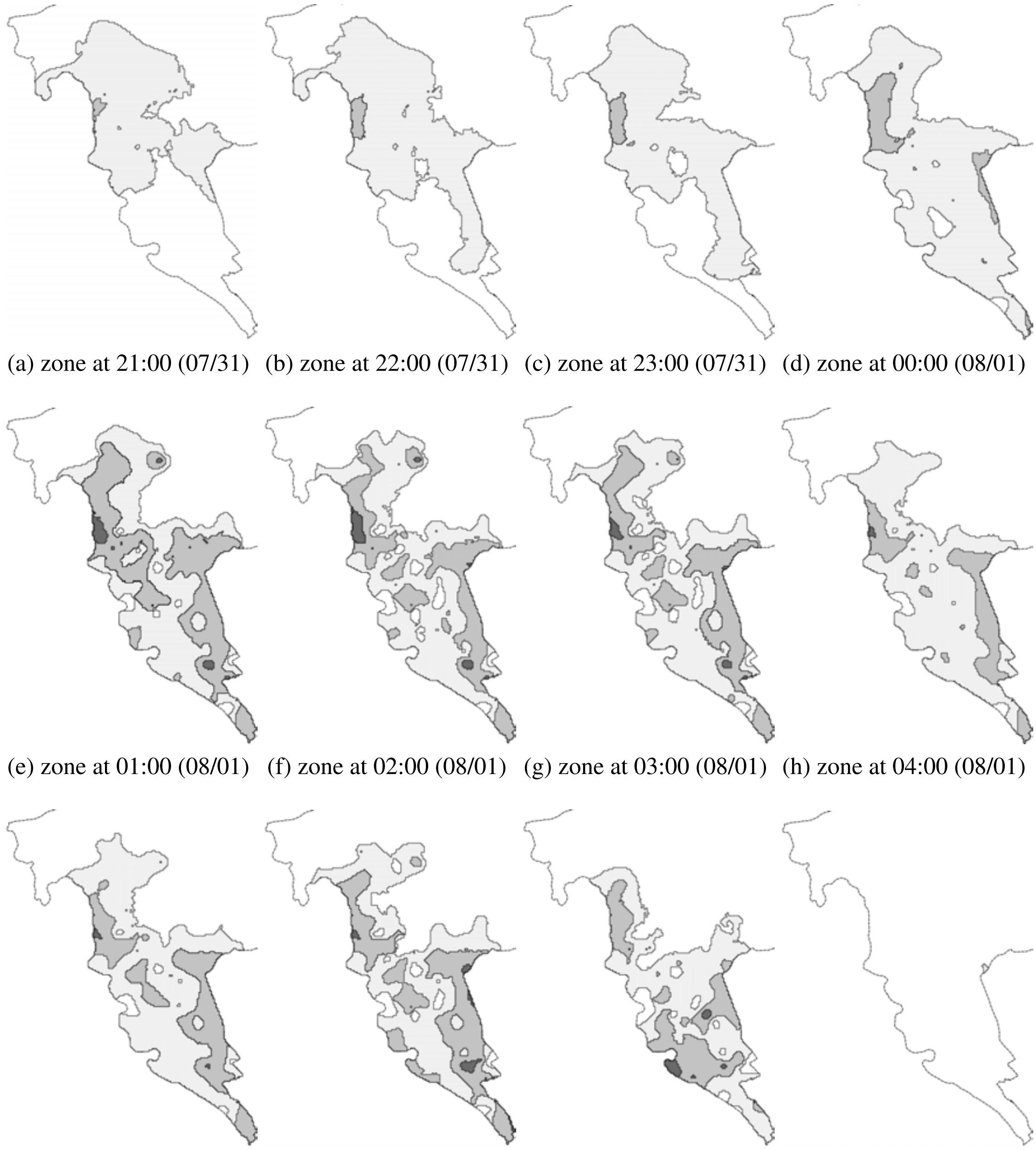

(a) zone at 21:00 (07/31) (b) zone at 22:00 (07/31) (c) zone at 23:00 (07/31) (d) zone at 00:00 (08/01)

(e) zone at 01:00 (08/01) (f) zone at 02:00 (08/01) (g) zone at 03:00 (08/01) (h) zone at 04:00 (08/01)

(i) zone at 05:00 (08/01) (j) zone at 06:00 (08/01) (k) zone at 07:00 (08/01) (l) zone at 08:00 (08/01)

Fig. 5.15 Overlapped zones of UHIs in sixteen consecutive time instants, where zones in the light gray, gray, and dark gray are respectively with three magnitudes of 2, 3, and 4 degree Celsius. (a)-(l) Continuous of areal changes for zones of UHIs from 2015-07-31 21:00 to 2015-08-01 08:00.

may have either areal change or merging behaviors but definitely not disappearing. Thus, P-values are calculated and drawn in Figure 5.16 based on a set of magnitudes.

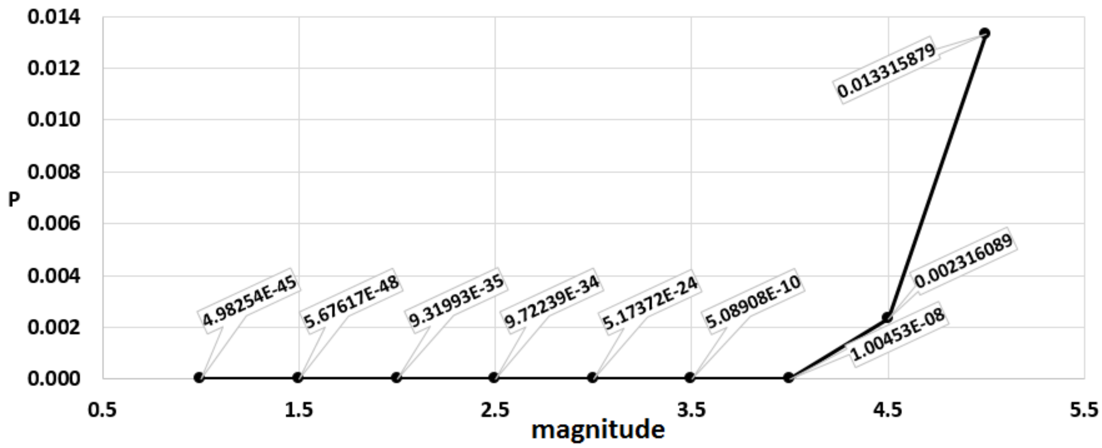

Fig. 5.16 Chi-square test to investigate the correlation relation between the spatial and thematic behaviors.

Interestingly, all the P-values are extremely small even though they grow increasingly with the increase of the magnitudes, which means the spatial and thematic behaviors have very strong correlations with highly accepted significance when the significance level is 0.001.

Table 5.3 The number of observations group by spatial and thematic behaviors when magnitudes equal to 1 and 5.

magnitude	behaviors	increasing	stationary	decreasing	sum
	expansion	45	20	20	85
	continuation	0	1	5	6
	contraction	28	26	31	85
1	annexation	113	49	53	215
	merging	117	42	178	337
	separation	1	0	0	1
	splitting	317	33	42	392
	sum	621	171	329	1121
	expansion	2	13	31	46
	continuation	0	1	1	2
	contraction	6	26	24	56
5	annexation	1	1	3	5
	merging	0	15	51	30
	separation	0	0	0	0
	splitting	0	9	32	41
	sum	9	65	106	180

Table 5.3 summarizes the number of both spatial and thematic behaviors using the Chi-square test when magnitudes equal to 1 and 5. When it equals to 1, UHIs have large extents but low intensities, and the increase of the temperatures brings more expansions and annexations, which probably happens during the day time because of the solar radiation. Increasing temperatures also generates a great number of splits, and UHIs having these splits can appear during the night time due to the latent heat from the surface with dense artificial buildings and disappear during the sun rise. Nevertheless, contraction and merging have notable numbers of increasing and decreasing, both of which also can be determined by the above two reasons simultaneously. By contrast, UHIs with higher magnitude (equals to 5) have much smaller extents but higher intensities. More expansions, annexations, and mergers are associated with the decreasing, which represents a growing trend for the dense hotspots during the night time. More UHIs tend to have splits when decreasing, suggesting that existence of these UHIs heavily relies on the heat resources contributed during the day time such as the anthropogenic heats and solar radiations. Moreover, no separation indicates a fact that all these zones in the high intensity shrink so fast that none of them is significantly larger or still exists in the next hour.

5.8.3 Life-cycle of UHIs

To investigate the evolutionary process of UHIs with several temporal periods, the vital input parameters should be defined. First, the magnitude is set at 3 degree Celsius to extract zones of UHIs to obtain a balance between getting larger extent of zones and more diversity of filiations. Second, the maximum distance that a UHI can move for each time instant is 11.1 km, which equals to the length of 0.1 latitude in Guangzhou.

Table 5.4 lists the complete life-cycles of three UHIs that interact with each other. More specifically, a UHI (`objID`) has one or more periods (`perID`), and for each pair of zones (`preZID` and `curZID`) at a time instant (`time`) have three types of filiations (`spaBeh`, `theBeh`, and `locBeh`). In addition, sequences (`s/pID`), chains (`chaID`), and queues (`queID`) are listed corresponding with their transitions (`spaPat`, `thePat`, and `locPat`). To start with, a UHI (object ID is `21`) contains three active periods (period IDs are `212`, `262`, and `740`) connected by two inactive periods (period IDs are `213` and `263`). The first inactive period has extended only for one hour from 5 to 6 am, while the second one covers three days from 1 August to 4 August. During the same time period as shown in Figure 5.17 which is directly plotted from the `uhi` table, the other one (object ID is `10278`) develops independently from 2 to 8 am. The last UHI appears at 5 am, which is then destroyed by merging with the UHI `21` at 6 am.

Table 5.4 indicates that the model is very sensitive to detect and track the changes of UHIs even they are inactive for a short time (i.e. inactive period `213` for the UHI `21` is one hour). Specifically, the UHI (object ID is `10278`) has two spatial behaviors of *continuation* and *annexation* at 6 am. This is different from the original proposed conceptualization that a UHI can only have one spatial behavior of either areal change or topological transformation at a time instant. The reason is that some transformations do not mean that a UHI will be destroyed but can still extend its life span by separating apart from its origin (i.e. *separation*) or absorbing one or several ones into its own (i.e. *annexation*). Therefore, the UHI can simultaneously have areal changes at the time when particular transformations occur. In contrast, destruction of a UHI caused by *splitting* and *merging* excludes areal change scenarios.

By investigating at the UHI `10278`, its spatial extent shrinks at 4 am, and then continuously approaches to, stays at, and leaves the plateau. Interestingly, its thematic transition is opposite to the spatial transition, i.e., it reaches, stays at, and leaves the basin. This observation indicates a very interesting phenomenon that a UHI existing during the nighttime can grow larger even though its thematic intensity decreases. Spatial behaviors of the UHI (ID is`10278`) is relatively simple without topological transformations. By investigating the locational behavior, this UHI only shifts away from its original location insignificantly at a time instant and it stops most of time, which suggests that UHI can be locationally fixed and the displacement is not obvious, which is also proved by other studies (Hua & Wang, 2012; Jalan & Sharma, 2014). Regarding Figure 5.18, the area covered by this UHI is the concrete seaport, which tends to dis-

Table 5.4 Spatial, locational and thematic filiations of three UHIs in their complete life-cycles.

objID	perID	time	curZID	preZID	s/pID	spaBah	spaPat	chaID	theBeh	thePat	queID	locBeh	locPat
21	212	15-08-01 01:00	4936	4769	150	expans	null	128	weaken	reaBas	118	shif	begQui
21	212	15-08-01 02:00	4942	4936	170	contra	reaFlo	137	steady	basin	137	stop	quiesc
21	212	15-08-01 03:00	4962	4942	197	cntiue	floor	137	steady	basin	137	stop	quiesc
21	212	15-08-01 04:00	0	4962	211	disapp	disapp	163	null	null	146	null	null
21	213	15-08-01 05:00											
21	213	15-08-01 05:00											
21	262	15-08-01 06:00	5029	0	250	appear	appear	187	null	null	169	null	null
21	262	15-08-01 07:00	0	0	256	disapp	disapp	187	null	null	169	null	null
21	263	15-08-01 08:00											
21	263	15-08-04 03:00											
21	740	15-08-04 04:00	1912	0	674	appear	appear	526	null	null	459	null	null
21	740	15-08-04 05:00	1249	1912	682	expans	null	533	steady	null	464	stop	null
21	740	15-08-04 06:00	1268	1249	703	merge	merge	538	streng	null	474	null	null
10278	278	15-08-01 02:00	4940	4925	173	cntiue	null	136	steady	null	135	stop	begAct
10278	278	15-08-01 03:00	4960	4940	173	cntiue	null	136	steady	null	135	stop	begAct
10278	278	15-08-01 04:00	4975	4960	209	contra	null	162	weaken	reaBas	135	stop	begAct
10278	278	15-08-01 05:00	5001	4975	221	expans	reaPla	180	steady	basin	165	shif	activa
10278	278	15-08-01 06:00	5028	5001	252	cntiue	platea	182	streng	leaBas	175	stop	resump
10278	278	15-08-01 06:00	5028	5001	252	annexa	platea	182	streng	leaBas	175	stop	resump
10278	278	15-08-01 07:00	5040	5028	262	contra	leaPla	182	streng	leaBas	175	stop	resump
10278	278	15-08-01 08:00	0	5040	282	disapp	disapp	212	null	null	196	null	null
10725	725	15-08-04 05:00	1257	0	689	appear	appea	530	null	null	467	null	null
10725	725	15-08-04 06:00	1268	1257	707	merge	merge	544	streng	null	467	null	null

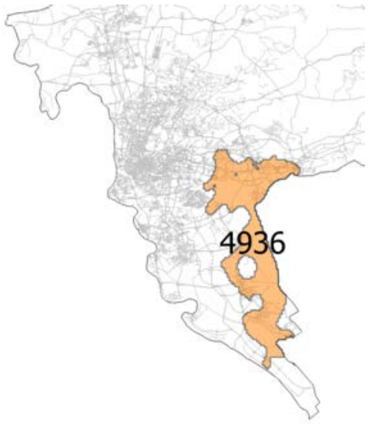

(a) Zone at 1:00 of 08/01/2015

(b) Zone at 2:00 of 08/01/2015

(c) Zone at 3:00 of 08/01/2015

(d) Zone at 4:00 of 08/01/2015

(e) Zone at 5:00 of 08/01/2015

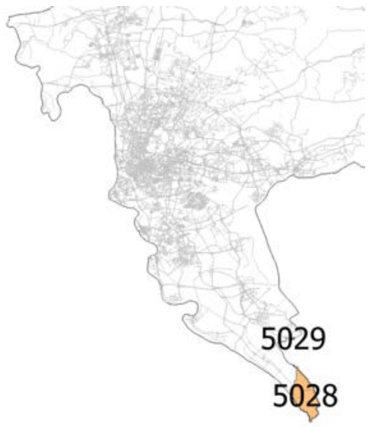

(f) Zone at 6:00 of 08/01/2015

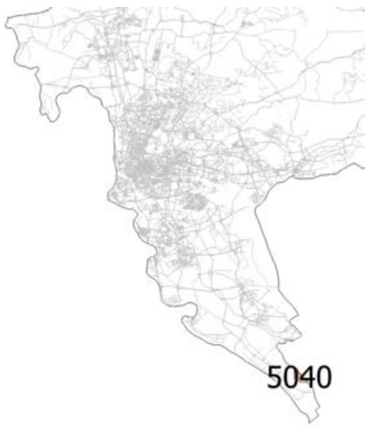

(g) Zone at 7:00 of 08/01/2015

(h) Zone at 4:00 of 08/04/2015

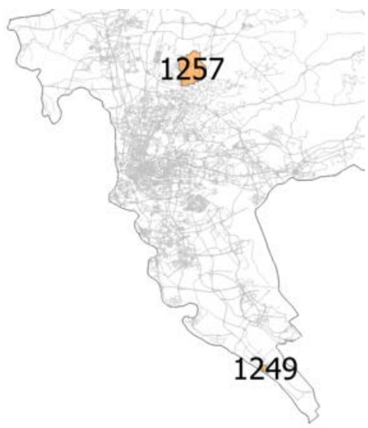

(i) Zone at 5:00 of 08/04/2015

Fig. 5.17 Complete life-cycle for three UHIs.

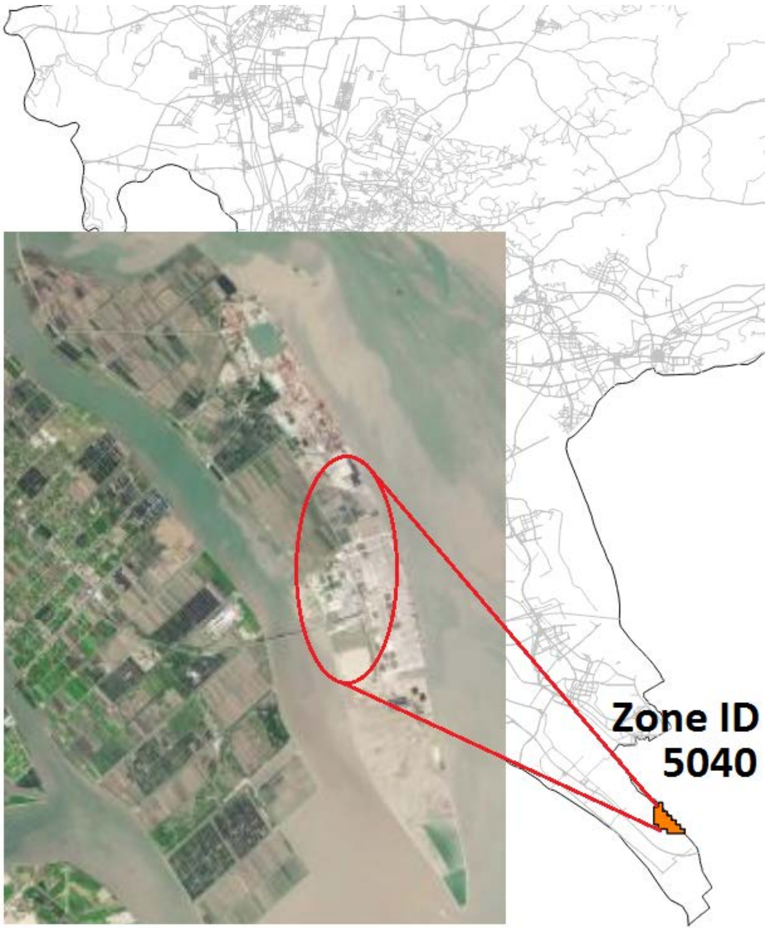

Fig. 5.18 The zone (`curZID` is `5040`) of a UHI (`objID` is `10725`) mainly covers the concrete floor of a seaport.

perse the heat during the nighttime absorbed from solar radiations during the daytime. Still, this seaport is surrounded by the sea and the farmland that no other UHIs can be generated so that this UHI only develops independently throughout its life-cycle.

Table 5.4 also shows that both UHIs of `21` and `10725` merge together as a new one ID `1268` as drawn in Figure 5.19a. It shows that the two small UHIs destroying at 5 am are followed by a large one at 6 am, which contains several holes within the zone because of the heat emission from the land surface that heat dispersion shall decrease gradually over time. Instead, it is most probably caused by sunrise that the land accumulates great volume of the heat and air temperatures in urban areas in a faster rate than that in rural areas. Most of the holes in the zone `1268` are in the green

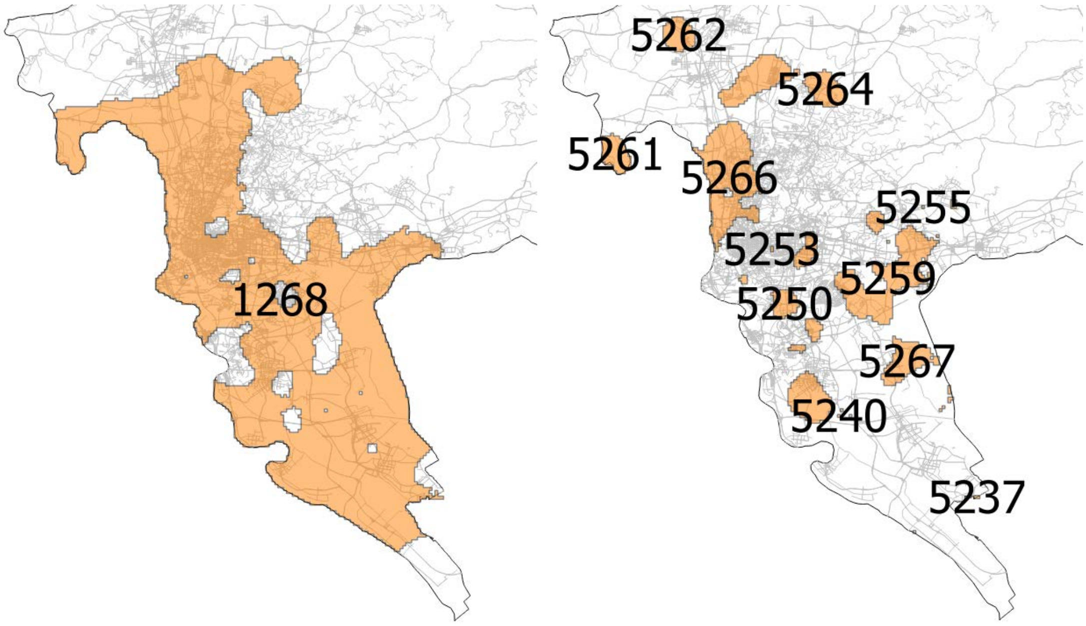

(a) Zone at 6:00 of 08/04/2015

(b) Zone at 7:00 of 08/04/2015

Fig. 5.19 A UHI generated from *merging* at 6 am is splitted at 7 am, leading to the deconstruction of itself and generation of 32 new UHIs.

areas or high-rising buildings that provide shades. Lastly, this large UHI is destroyed by splitting itself into 32 new ones at 7 am (Figure 5.19b). Causative factors for these UHIs existing during the daytime shall be different from that in the nighttime, which shall be investigated further.

Notably, some heat sinks are within the extent of the UHI (Figure 5.19a) because temperatures of the sinks do not satisfy the condition to form the UHI, i.e., temperatures of the sinks are lower than the minimum temperature of the UHI. Preliminary results suggest that most of these sinks have a correlated but opposite evolutionary trend with the UHI. While others have static extents or insignificant areal variations. Since the sink is also enclosed with certain area, it hence can be conceptualized as a field object and named as the urban heat sink (UHS).

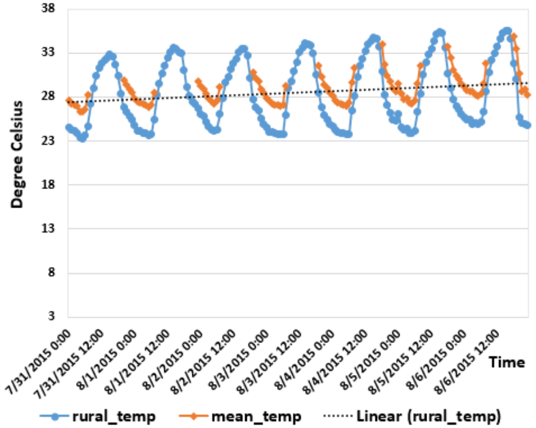

(a) Temperatures from 31/07/2015 to 06/08/2015.

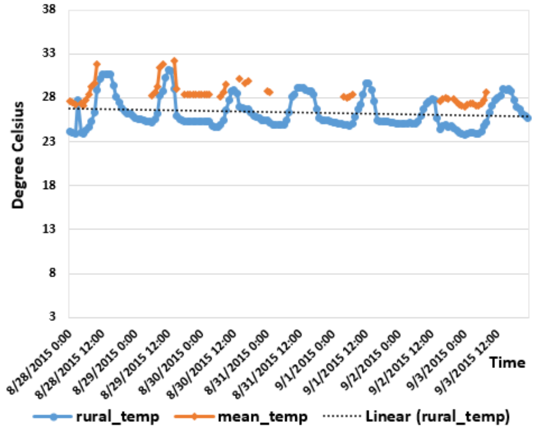

(b) Temperatures from 28/08/2015 to 03/09/2015.

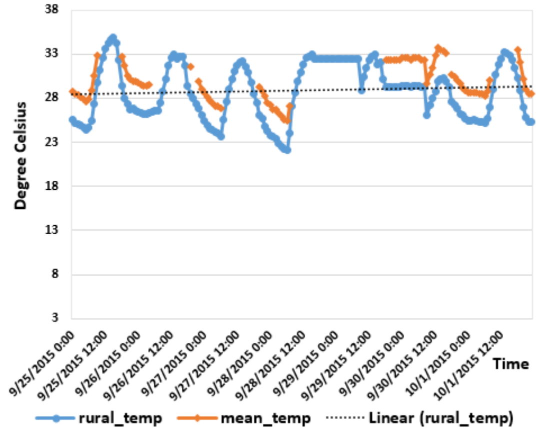

(c) Temperatures from 25/09/2015 to 01/10/2015.

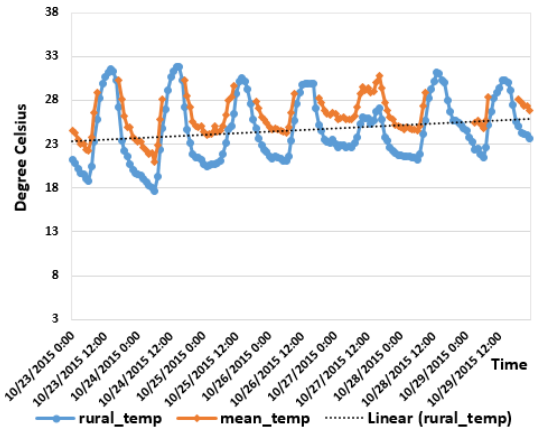

(d) Temperatures from 23/10/2015 to 29/10/2015.

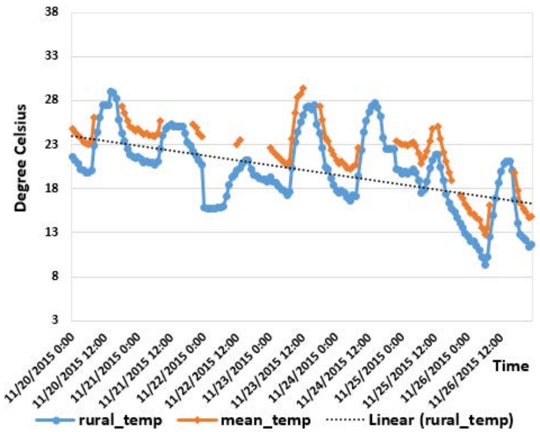

(e) Temperatures from 20/11/2015 to 26/11/2015.

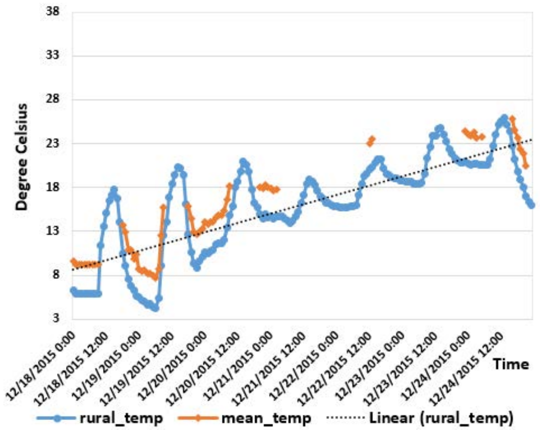

(f) Temperatures from 18/12/2015 to 24/24/2015.

Fig. 5.20 Rural temperatures and urban heat island intensities over six continuous months.

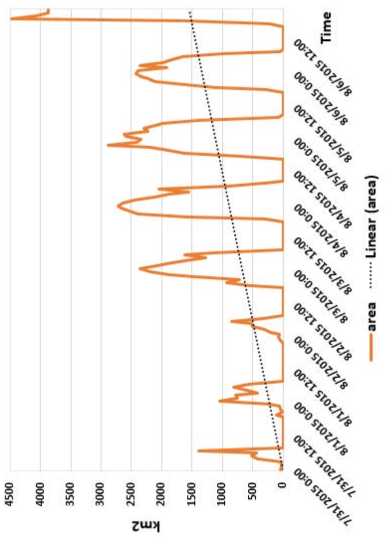

(a) Total areas from 31/07/2015 to 06/08/2015.

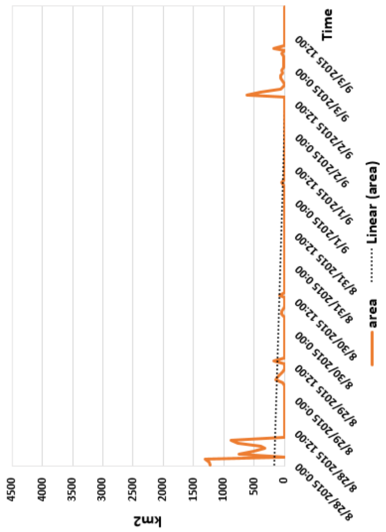

(b) Total areas from 28/08/2015 to 03/09/2015.

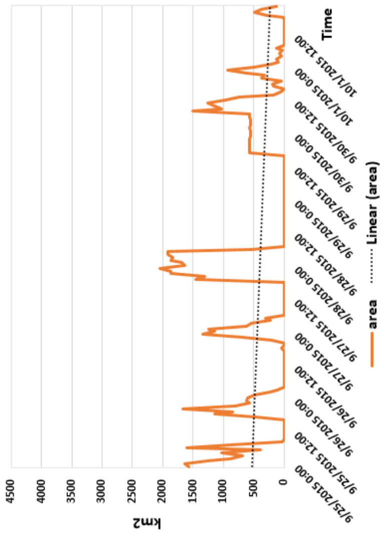

(c) Total areas from 25/09/2015 to 01/10/2015.

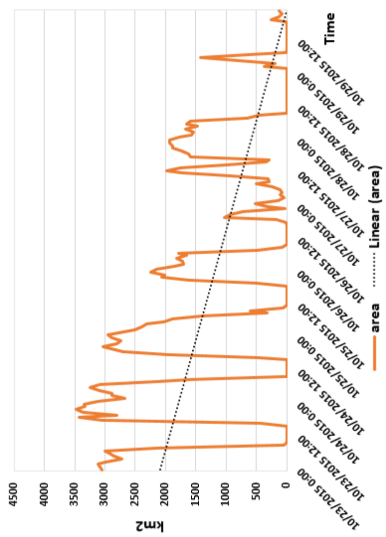

(d) Total areas from 23/10/2015 to 29/10/2015.

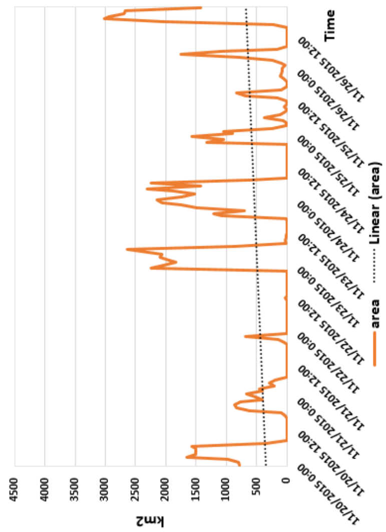

(e) Total areas from 20/11/2015 to 26/11/2015.

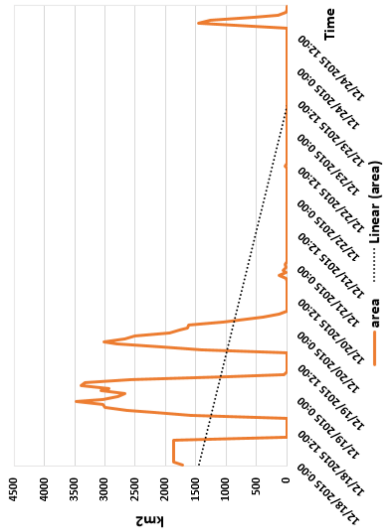

(f) Total areas from 18/12/2015 to 24/24/2015.

Fig. 5.21 Total areas of UHIs over six weeks.

5.8.4 Revolutionary trends of UHIs

To find the evolutionary trends of UHIs over a long time period, the study investigates the changes of UHIs in six weeks covering a continual of six months from July to December in 2015. The magnitude is defined as 3 degree Celsius to cover a large urban area, and the core-oriented behavior modeling is used for this investigation. Figure 5.20 draws the curves of the referenced rural temperatures and the mean of UHI intensities are calculated for each of the three weeks. Between July 31 and August 6, the rural temperatures and UHI intensities are increasing gradually, which has been discussed in the above section (Figure 5.20a). An interesting phenomenon occurs between August 28 and September 3 that the rural temperatures have a slight decrease and UHIs are insignificant through the whole week (Figure 5.20b). This abnormal phenomenon was caused by rainstorms in the whole week that the heat is dispersed obviously. UHI intensities between September 25 and October 1 has an unconspicuous decrease and increase (Figure 5.20c). In comparison, difference between the maximum and the minimum rural temperatures are decreasing between October 23 and October 29 (e.g. variation between the maximum and the minimum temperature shrinks from 13 °C on Oct 23 to 7 °C on Oct 29) while both the absolute rural temperatures and UHI intensities have a growth trend (Figure 5.20d). Obviously, rural temperatures and UHI intensities have obvious decrease, and occurrence of the UHIs is shortening between November 20 and November 26 (Figure 5.20e). By contrast, a significant increase occurs from a low temperature (i.e. around 8 degree Celsius) for both rural temperatures and UHI intensities during December 18 and December 24, and UHIs occur more rarely (Figure 5.20f).

Overall, intensities of UHIs are changing around 28 degree Celsius in August and September, and it gradually decreases to 23 and 17 degrees during October and November. It supposed that the intensities continuously decrease to 8 degrees in the late of December, following by a growth that reaches to 23 degree Celsius. The figure shows that UHIs mostly happen and are the most significant during the night. However, an entire opposite phenomenon also occurs in some specific days that UHIs are the most significant at noon on September 30 (Figure 5.20c), October 27 (Figure 5.20d), and November 25 (Figure 5.20e). This abnormal phenomenon always accompanies with a prodigious decrease of the temperatures that it was sunny in the previous day while it rains in the current day. It can be explained that the heat accumulated in the previous daytime cannot disperse immediately during the night because of the thermal insulation contributed by the urban canopy (i.e. rain-clouds). Thus, the heat accumulated in the previous day gradually releases in the next day, and the UHI is getting more obvious with the anthropogenic heat fluxes generated in the current day. This explanation is also suggested by some other studies (Holderness *et al.,* 2013; Zhong *et al.,* 2015).

Figure 5.21 draws the curves of the total area of UHIs as the same time period as that draws in Figure 5.20. It shows a positive relationship that the total areas grow with the increase of the UHI intensities during the summer (Figure 5.21a), and the areas are small all through the existence of UHIs because of the continuous rains (Figure 5.21b). However, the areas are with slight decrease in the late of September, which is with an opposite trend as the changes of the UHI intensities (Figure 5.21c). The areas are continue shrinking even though the UHI intensities are increasing, and this trend is getting much more significant in October (Figure 5.21d) and December (Figure 5.21f) when UHI intensities become lower. This negative relationship also occurs on December 25 and 26 (Figure 5.21e), i.e., decrease of the UHI intensities is with the increase of the areas. Moreover, daily occurrence of UHIs is shortening gradually from October to December. This special phenomenon can be caused by that the urban temperatures raise up or drop down slower than that of the rural temperatures during the winter time, so that areas of UHIs are contracting since magnitudes (i.e. temperature difference between the rural temperature and the urban temperature) are decreasing with the increase of the rural temperatures, and areas of UHIs are expanding because magnitudes are increasing with the decrease of the rural temperatures. One explanation is that urban areas absorb less solar radiation which is one of the most majority heat resources of UHIs (Giridharan *et al.,* 2007) and release more accumulated heat during the winter because of the seasonal winds (Wang, 2006) so that it is more difficult to form UHIs and areas of UHIs more tend to contract even though rural temperatures increase in winter.

SQL 7 FUNCTION SummativeStatistics()

```
1  SELECT period.obj_id, COUNT(*) AS hours,
2         ST_MakeLine(ST_Centroid(zone.geom)) AS geom
3  FROM   period
4  LEFT JOIN zone ON period.c_oid = zone.oid
5  WHERE  period.c_oid > 0
6  GROUP BY obj_id ORDER BY obj_id;
7  SELECT period.obj_id, period.c_oid, period.t_s,
8         EXTRACT(HOUR FROM period.t_s) AS time,
9         ST_Area(zone.geom) AS area, ST_Centroid(zone.geom) AS geom
10 FROM   period
11 LEFT JOIN zone ON period.c_oid = zone.oid
12 WHERE  period.c_oid > 0
13 ORDER BY period.obj_id, period.t_s;
```

5.8.5 Exploratory discovery

This section explores spatio-temporal variabilities of trajectories through summative statistics. The proposed model is interactive and allows SQL query (Lines 1-6 in SQL 7) to construct trajectories of UHIs and summarize their active hours. Figure 5.22 draws all the trajectories of UHIs over six independent weeks. The figure shows that UHIs associate in the core urban area of Guangzhou and shift back and forth to urban areas of the surrounding districts periodically when the *magnitude* is intermediate ($m = 3$). Accordingly, a series of zones of each UHI categorized by area are plotted along with the trajectories (Figure 5.23), derived from the second simple query (Lines 7-13 in SQL 7). It obviously shows that larger zones are clustering in the core urban area while smaller zones are discretized in different districts, apart from raining days (Figure 5.23b). The two figures also reveal that: (i) the UHI phenomenon becomes inconspicuous from summer to winter since trajectories are getting sparse; (ii) UHIs having the same *magnitude* maintain their travels between cores and suburbs disregarding with the change of seasons; and (iii) their extents contract moving from cores to suburbs while the extents expand when turning round.

The above findings motivate us to further investigate trajectories when UHIs are in

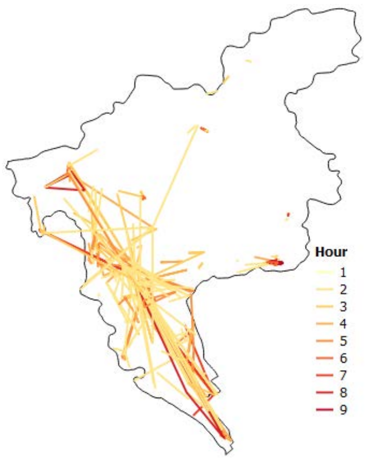

(a) Traj. in 07/31-08/06

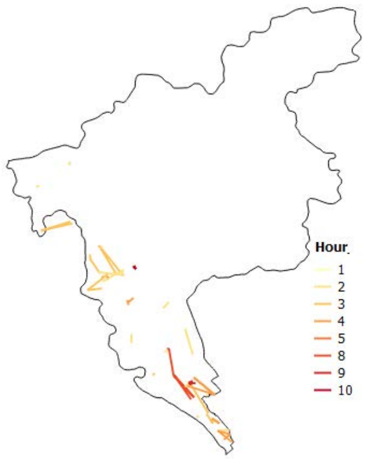

(b) Traj. in 07/31-08/06

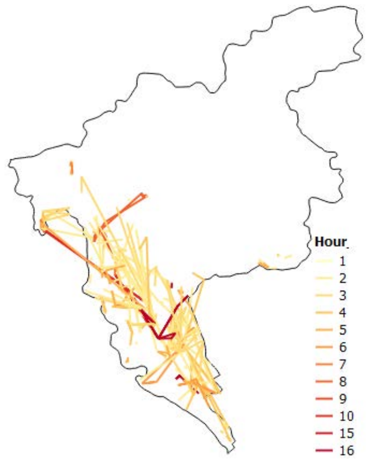

(c) Traj. in 09/25-10/01

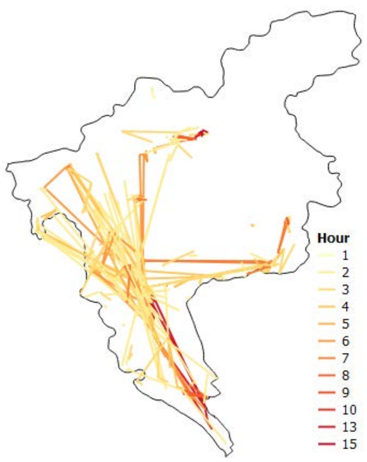

(d) Traj. in 10/23-10/29

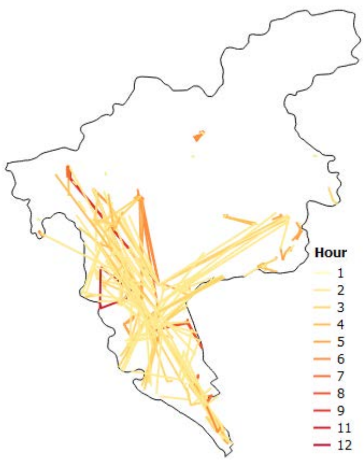

(e) Traj. in 11/20-11/26

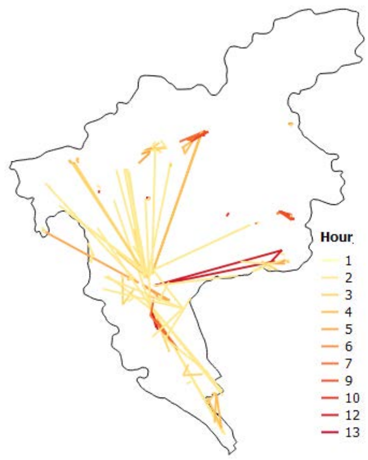

(f) Traj. in 12/18-12/24

Fig. 5.22 Trajectories of UHIs ($m = 3$) for six weeks. Longer life-span of a UHI is presented in darker color.

higher *magnitudes*. Focusing on a single week between July 31 and August 6, areal information of zones and their occurrence time along with the trajectories are drawn in Figure 5.24 and Figure 5.25 respectively, both of which are derived from SQL 7 as well. It is found that trajectories are getting sparser and shorter, and gradually centralized in the core urban area with the increase of magnitudes. This means that UHIs with higher intensities would have smaller extents and tend to associate in more density urban areas. Figure 5.25 also visualizes temporal occurrence of UHIs. It presents that UHIs with low magnitude ($m = 3$) can exist all through the day covering a large area, while

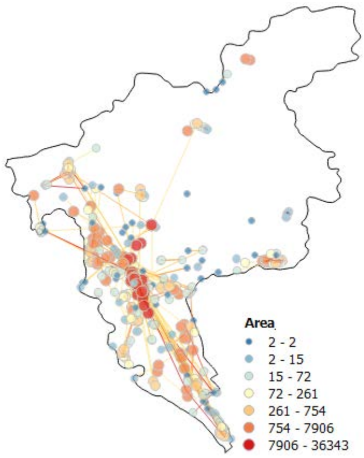

(a) Zone area in 07/31-08/06

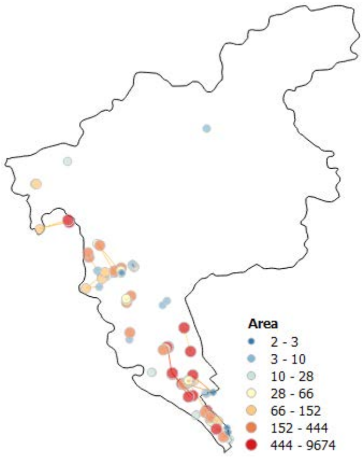

(b) Zone area in 07/31-08/06

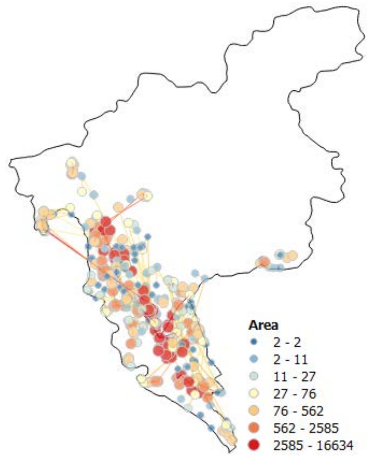

(c) Zone area in 09/25-10/01

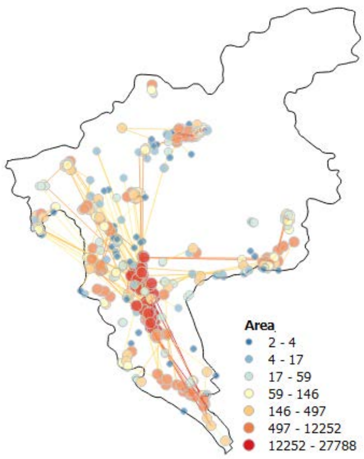

(d) Zone area in 10/23-10/29

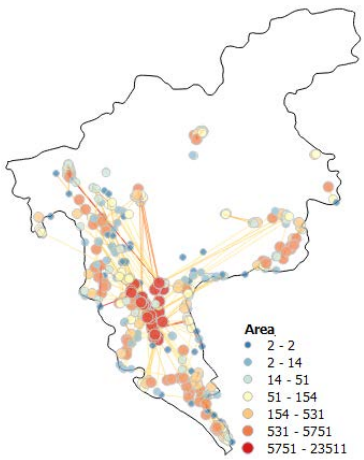

(e) Zone area in 11/20-11/26

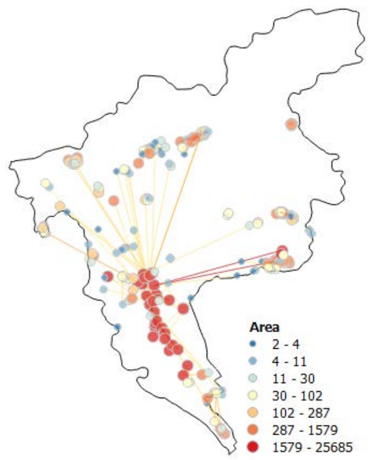

(f) Zone area in 12/18-12/24

Fig. 5.23 Zone of UHIs associated with their trajectories. Lager area of the zone has larger circle size.

UHIs with higher magnitude ($m = 5$) overwhelmingly occur in the night occupying much smaller area. All these findings suggest that UHIs having a low magnitude would associate in several urban areas while their occurrence time can decrease over seasons. In contrast, UHIs with a high magnitude would associate in a specific urban area while their occurrence time can only be in the night.

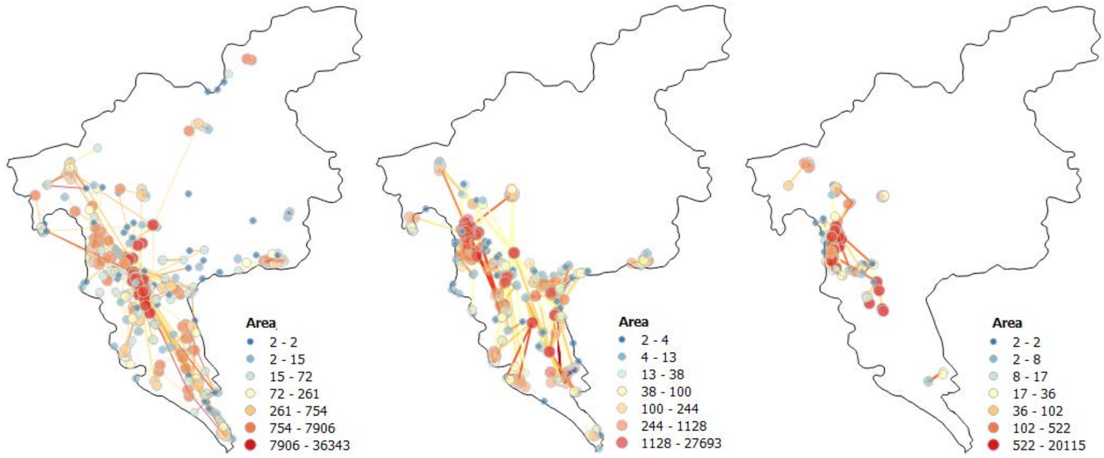

(a) Zone areas when $m = 3$ (b) Zone areas when $m = 4$ (c) Zone areas when $m = 5$

Fig. 5.24 Zone areas of UHIs in different magnitudes associate with their trajectories between July 31 and August 6.

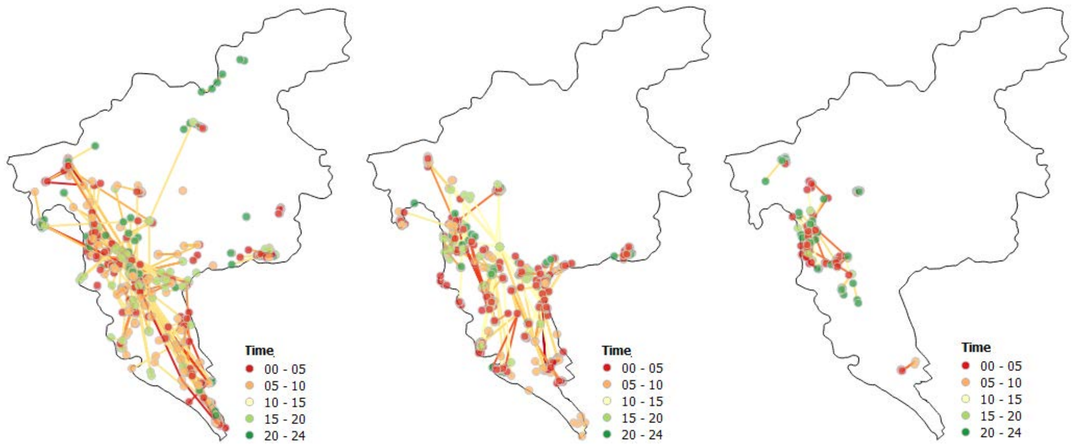

(a) Time of zones when $m = 3$ (b) Time of zones when $m = 4$ (c) Time of zones when $m = 5$

Fig. 5.25 Time-based location of zones associated with their trajectories between July 31 and August 6.

5.9 Discussion

Spatio-temporal resolution of the thermal images has profound influences on extracting zones of UHIs and consequentially determining the evolution of UHI behaviors. This study used 216 in-suit weather stations for spatial interpolation, in which 169 stations located in the urban areas and most of these stations were in the core urban areas. This suggests that a higher density of the stations corresponds to space where more spatial variability of UHIs is expected. Exploratory experiments found that Ordinary Kriging with the spherical semi-variogram model was able to highlight the hotspots much better, comparing with the Universal Kriging. Therefore, Ordinary Kriging was used to generate contiguous of the thermal images so that hotspots of UHIs could be fairly constructed. Thermal images were derived with spatial resolution as high as 100 m and standard deviation of (1 ± 0.4) °C. Even though spatial resolution is still coarse compared with the thermal band of Landsat ETM+ (i.e. 60 meters) and ASTER (i.e. 90 meters), it allows the proposed model to identify UHI object and track its spatial variability at block level, which means that its evolution still can be tracked as a monitoring of micro-climate in the urban area. Meanwhile, hourly thermal images provide a much higher temporal resolution compared with the conventional satellite images (e.g. revisit frequency is 16 days for Landsat 8), which enables the model to track the evolution instantly most of time. This could be the most favorable factor for using the in-situ weather station data. However, the hourly-based resolution still meets challenges to track all the spatial evolution unambiguously since UHIs can contract, split, and disappear dramatically in just several minutes in the early morning.

It is vital that the estimated thematic and spatial behaviors of UHIs have close relation to the physics of UHI process in the real world. Benefiting from appropriately constructed thermal images, zones of UHIs extracted from thermal images are thus promising in terms of the spatial extent and thematic intensity. Since computation of all the spatial behaviors relies on the significant overlapping analysis and rigorous topological calculation, the model can ensure that related zones for each two consecutive time instants correspond to the same UHI object, and therefore can depict evolutions of the UHI in physics reliably. In addition, the model allows UHIs to move as typical moving objects, while results found that UHIs in core urban area (with high magnitudes) were locational associated that did not move obviously from their origins, as other studies have suggested in Section 5.8.4. This uncovered pattern indicates that the proposed model can track evolution of UHIs in physics effectively. Thereby, thematic behaviors determined by comparing intensities of the related zones are convincing.

5.10 Summary

In this chapter, the study collected six weeks of the air temperatures to obtain contiguous thermal surfaces and proposed computational methods to determine behaviors of zones so that a spatial database system was developed to simulate the evolutionary process of UHIs continuously over time. Results suggested that spatial, thematic, and locational behaviors of UHIs with several periods can be tracked and their transitions can be detected simultaneously. Several findings are summarized as follows.

1. UHIs have periodic evolution in the daily basis, which can be caused by anthropogenic heat (i.e. heat produced by vehicles) and particular land covers (i.e. concrete seaports surrounded by vegetation).

2. UHIs have revolutionary trends over seasons. In summer, daily occurrence of UHIs extends, daily temperature variation enlarges, and areas of UHIs grow. However, the trends are contrary in winter. It is supposed that UHI evolution is also periodic in the seasonal basis.

3. UHI is normally significant in the nighttime in both summer and winter. As an abnormal, it can also obvious in the daytime if it is a raining day and the previous day was sunny.

4. UHIs defined in different magnitudes have different types of spatial behaviors, and sinks can affiliate to the UHIs in some particular time periods.

5. UHIs in the same magnitude would maintain their locational displacement but with the decrease of the total numbers over seasons. UHIs with a higher magnitude are smaller and more locational associated in the more density urban area, and their occurrence time decreases.

Chapter 6

Discussion and conclusion

6.1 Summary

This study conceptualizes each UHI as a two-dimensional field-object which has four properties (i.e. extent, location, temperature, and time). Then, an object-oriented data model is proposed to track the dynamic behaviors of UHIs instantly, which are expressed by three types of filiations (i.e., spatial, locational, and thematic filiations) between zones at each two consecutive time instants. For each time instant, spatial filiations are defined by areal changes and topological transformations. A zone at t_i associating with a single zone at t_{i-1} makes an areal change and a zone at t_i has association with several ones at t_{i-1} corresponds to a topological transformation. As a field-object, a UHI is also allowed to have active and inactive periods connecting with each other caused by status transitions, which finally construct a complete life-cycle. To track continuous evolution of UHIs observed by a series of discrete thermal images, six hierarchical graphs are proposed so that their evolutionary processes can be described in different description granularities.

Empirical evaluation based on a developed database system suggests that the proposed spatiotemporal data model is effective to record the changes of UHIs and is able to reveal evolutionary trends of UHIs. On a daily basis, UHIs normally appear after the sunset, mostly grow and merge together before the middle night, become stable and significant after the middle night, and finally split and disappear rapidly at dawn. On a seasonal basis, UHIs expand and their intensities increase, and the daily occurrences extend in the summer; while the trends are reverse in the winter. In addition, UHIs with higher magnitudes are more locationally associated while variability of their trajectories maintains in all the seasons. The results also suggest that the model is able to detect abnormal phenomena sensitively such as significant UHIs occurring at the noon in the raining days.

6.2 Discussion

In each set of the experiment, a specific magnitude was used to extract zones of UHIs, and temperatures within the zones are at least with a magnitude difference from the referenced rural temperatures. However, location of the rural temperatures used for extracting the extent of UHIs was selected empirically, which could not represent all the rural temperatures to precisely extract the boundaries of UHIs. An approach to determine the referenced rural temperatures more accurately is creating an outer-buffer of the investigated urban areas with a certain width so that the buffer shall cover certain rural areas. Hence, a threshold temperature can be determined by averaging all the rural temperatures within this buffer zone. The advantage of this approach is that all the rural temperatures are taken into account so that uncertainty of the reference rural temperatures caused by selection of the site can be avoided.

Initially, a UHI is conceptualized to have either areal change or topological transformation at each time instant. For example, a UHI may continue by splitting part from its own at t_i. In this case, this UHI has only transformation (i.e. *separation*) without any areal changes at t_i. Having more deliberate consideration, this study further refines the model that a UHI can have both areal changes and transformation at the same time in some particular scenarios. As long as a UHI continues, its zone will still continue without any interruption even when transformation occurs. In this consideration, when a UHI separates part from its origin (i.e. separation) or absorbs some into its own (i.e. annexation) at t_i, the UHI can still be determined as z_n^i so that the two areas of $(area(z_n^{i-1}), area(z_n^i))$ can be compared. That is to say, the UHI may simultaneously have transformation and areal change. This refinement allows a continuous tracking of the areal information during the whole active period.

This study still encounters two limitations. First, zones of UHIs are extracted from thermal images based on the reference rural temperatures. Because of the different magnitudes, the extracted zones sometimes cover rural areas which are not belonging to the urban areas. This causes an uncertainty that the discovered phenomenon can be influenced by rural areas. For example, two zones contain rural areas in two consecutive time instants and they are associated because of the significant overlapping. However, the two zones shall have no association if rural areas are excluded from the zones. Second, this study reveals some new patterns and suggests some causative factors based on the analysis between the zones, road networks, and land uses (Figure 5.13 and Figure 5.18). However, exploration of the causative mechanisms is still preliminary even though it is not the objective of this study.

6.3 Conclusion

From a unique view of the UHI research, this study proposes a complete spatiotemporal data model to track the evolutionary processes of UHIs. It suggests that the proposed model is effective for continuous tracking of UHIs and for uncovering evolutionary trends of UHIs over time. Based on the summary and discussion above, several conclusions can be made in the following.

- **This study establishes knowledge in the UHI phenomenon in Guangzhou.** First, UHIs are more significant in the summer and tend to occur in the nighttime. Second, UHIs have both daily periodicity and seasonal variation. Third, UHIs with higher magnitudes are more locationally associated in the core urban areas with shorter temporal occurrence.

- **This study provides more approaches for research of the field phenomena.**

First, the model accepts several types of the data sets, not only for discretized points (e.g. observed air temperatures) but also for remote sensing images given the condition that the spatiotemporal resolutions are fulfilled. This indicates a wide usage of the model. Second, compared with conventional object-oriented data models looking at discretized temporal snapshots, the proposed model is more flexibly since it provides an interactive interface that allows summative statistics (e.g. accumulation and aggregation) to uncover interesting patterns in forms of both textual and visualized information. Third, the model is helpful to determine potential causative factors and effects through continuous tracking of the interested phenomenon and correlation analysis.

- **This study develops the theory of spatiotemporal data modeling.** The proposed model allows a distributed geographical phenomenon to be conceptualized as a field-object such that its evolution can be modeled as continuous of the dynamic behaviors, acting as an object either develops independently or interacts with other objects with topological transformations. All the behaviors, transitions, and transformations can be tracked by the proposed six hierarchical graphs. Furthermore, this study for the first time proposes a complete life-cycle concept for each field-object that each one can have several periods connected by active or inactive transitions. This brings a remarkable benefit that tracking of the interested phenomenon can be extended into a longer time period.

6.4 Future work

The proposed model cannot be used and applied for tracking all the field phenomena. For example, urban heat sinks can be visually detected during the tests but cannot be tracked directly using the current established model. Yet, some results are still preliminary and more interesting patterns and causative factors shall be explored further with the systematic correlation analysis. Thus, future work is planned in the following five aspects.

1. **Discover long-term revolutionary trends.** Several seasonal trends of UHIs have yet been studied while this study only covers six months from August to December due to the data limitation. Future work will obtain long-term data so that patterns of yearly trends can be analyzed. Additionally, future work will propose an event-based behavior for UHIs by aggregating the sequences or periods according to the pre-defined.

2. **Extract UHI extent smartly.** The model can be used widely in different spatial scales for either an urban core area, several city clusters, or even continental regions. If the study area is a wide region, rural temperatures used as the threshold shall be selected simultaneously in multiple places since temperatures in different places that with different UHI. For example, urban areas of four Chinese cities (i.e. Shenzhen, Dongguan, Guangzhou, and Foshan) are spatial contiguous and they cover a large area so that intensities of the UHIs in the four cities shall be different. In a continental scale, Miami may not have a UHI when it is 31 degree because the whole Florida has temperature around 31. While, 29 degree in Buffalo may generate a UHI since its surrounding temperature is 26. Thereby, future work will further develop this model to smartly extract extents of UHIs. In this case, geostationary satellite images (e.g. MTAST with spatial resolution is 4 km and temporary resolution is 1 hour) or data from automatic weather stations with high spatial density may provide more comprehensive data source for the study.

3. Explore causative factors effectively. The current model can be used to investigate UHI at a finer scale of urban areas such that underlying mechanism of the UHIs phenomenon may be revealed by synchronously tracking other hypothetical influential factors. For instance, heat produced by vehicular flows can be a major contribution to the UHI in some specific places where the heat also has the peaks during the rushing hours in the morning and afternoon. In consideration of the urban morphology, different wind directions can either accumulate

or disperse the heat when the wind travels through different wind corridors in a city. Future work can track the UHI evolution using the developed model and simulate the urban dynamics (e.g. vehicles and winds) with multi-disciplinary knowledge, and analyze their spatio-temporal correlations systematically to explore and understand potential factors.

4. **Model urban sink islands.** Urban Sink Island (USI) is a very interesting phenomenon affiliated with the urban heat island that an enclosed urban area does not belong to the urban heat island but is surrounded by an urban heat island. Some but not many studies have discovered this phenomenon (Buyantuyev & Wu, 2010; Zhou *et al.*, 2013) and some investigated in its patterns and causative factors (Clinton & Gong, 2013; Nassar *et al.*, 2016). For instant, study in (Nassar *et al.*, 2016) found that the greatest effect of USI is during the daytime of summer in the desert, which mostly happens in zones of high-rising buildings since the cooling effect is promoted by the building shades and variations of airflow. However, previous work could not track this phenomenon over time with the exploration of other causative factors. In spatiotemporal data modeling, each USI can develop independently, affiliating with a UHI. Similarly, several USIs can depend on the same UHI and merge as a single one, which may also split into pieces. In this clue, USIs can be extracted from a series of thermal images, and their behaviors can be modeled. Obviously, the USI is parasitic on the UHI, and several USIs can be viewed as leaves growing from the same UHI root with certain associations. By reversely extracting the extents of UHIs, the proposed model can also be applied for tracking dynamic behaviors of USIs to investigate certain discovered phenomena.

5. **Spatial Big Data.** The model is implemented in an object-relational database management system (i.e. PostgreSQL) and estimation of all the filiations is through SQL queries. Thus, computation of the model can natively fall into the Spatial Big Data computing task. Computational cost of this study is low

because the data only covers a small region and for a short time period. However, the computing task can be significantly challenged if (i) the study area dramatically expand to a national or even continental scale; (ii) zones are extracted by multiple relative intensities so that behaviors of UHIs have to be determined simultaneously in different relative intensities; and/or (iii) the estimation is extended to much longer time periods (e.g. continuous of several months of even years). In this case, many strategies have to be used to fit the Spatial Big Data computing task such as cloud computing either centralized (e.g. Hadoop MapReduce (Hadoop, 2017)) or decentralized (e.g. HyperCGSF (Fei, 2017)), and SQL query optimization (e.g., `virtual table`, `index`, and `view`).

Appendix A

Curriculum Vitae

Contact

Website	http://911zrfelix.wixsite.com/giser
E-mail	r.zhu@
Mobile	+852-5308 / +86-147 1460
Telephone	+852-3400
Address	Room ZS602_9, Block Z Department of Land Surveying and Geo-Informatics The Hong Kong Polytechnic University, Hong Kong, China

Education

Time	Degree	University
2014 - 2017	Doctor of Philosophy	Dep. of Land Surveying and Geo-Informatics The Hong Kong Polytechnic University Hong Kong, China
2010 - 2013	Master of Science	Dep. of Urban Planning and Environment Royal Institute of Technology - KTH Stockholm, Sweden
2006 - 2010	Bachelor of Science	Dep. of Geographic Information Science Nanjing Normal University Nanjing, China
2015 - 2016	Exchange study	Dep. of Geomatics Laval University Québec, Canada

Experience

1. Founder and CEO of Shenzhen Vibour Co., Ltd. for augmented reality based navigation displayed by Vibour glasses (04/2015 -)
2. Internship for developing an intelligent transportation system (Eclipse) in Suzhou Industrial Parking Surveying, Mapping and Geoinformation Co., Ltd. (07/2013 – 12/2013)
3. Teaching assistant for course of Spatial Database (PostgreSQL, PostGIS, and pgRouting) at KTH (03/2013 – 05/2013)
4. Teaching assistant for course of web GIS (JSP, Servlet, JavaBeans, GeoServer, OpenLayers, WMS and WFS) and mobile GIS (OSM and Android) at KTH (08/2012 – 10/2012)
5. Research assistant for spatial data mining (Eclipse & Hadoop) at KTH (07/2011 – 09/2011)
6. Summer job for web GIS development (JavaScript, HTML, C#, and SQL) at Nanjing Normal University (07/2009 – 08/2009)
7. Summer job for database development (Oracle) in Nanjing Gimis System Integration Co., Ltd. (07/2007 – 08/2007)

Selected awards

1. Excellent research paper for the 7th national Geo-information forum for Ph.D students in China (5% Selection, 10/2016)
2. Award for the 2011 international-forum competition of young researchers in Russia (04/2011)
3. Outstanding graduate in School of Geographic Science, Nanjing Normal University (05/2010)

4. Second prize for the outstanding academic report "Spatio-temporal Distribution Pattern Prediction of Motor Stolen Cases in Urban Areas" (03/2009)

5. First prize for comprehensive ability scholarship (5% Selection, 12/2009)

6. Outstanding member of the student union, Nanjing Normal University (06/2006)

Computer Skills

1. **6 years experience**: PostgreSQL, PostGIS, pgRouting, and Java in Eclipse (J2EE)

2. **2 years experience**: Web GIS (JSP + Servlet + JavaBeans, GeoServer, OpenLayers, WMS and WFS), Mobile GIS (GPS + OpenStreetMap + Android), and ArcGIS solutions (ArcMap, ArcGIS Server)

3. **1 years experience**: Hadoop & MapReduce, HTML, JavaScript & CSS, Visual C#, Visual C++ (MFC), OpenGL, Oracle, Matlab

Referee

Assistant Prof. Man Sing Wong

Phone: +852 3400

E-mail: lswong@

Department of Land Surveying and Geo-Informatics

The Hong Kong Polytechnic University

Hong Kong, China

References

Alonso, M. S., Labajo, J. L., & Fidalgo, M. R. (2003). Characteristics of urban heat island in the city of Salamanca, Spain. *Atmósfera*, 137–148.

Aiazzi, B., Alparone, L., Baronti, S., Santurri, L., & Selva, M. (2005). Spatial Resolution Enhancement of ASTER Thermal Bands. *Proc. SPIE 5982, Image and Signal Processing for Remote Sensing XI*, 59821G.

Aplina, P., & Smith, G. M. (2011). Introduction to object-based landscape analysis. *International Journal of Geographical Information Science*, 25(6), 869–875.

Allen, L., Lindberg, F., & Grimmond, C. S. B. (2011). Global to city scale urban anthropogenic heat flux: model and variability. *International Journal of Climatology*, 31, 1990–2005.

Allegrini, J., Dorer, V., & Carmeliet, J. (2012). Influence of the urban microclimate in street canyons on the energy demand for space cooling and heating of buildings. *Energy and Buildings*, 55, 823–832.

Buyantuyev, A., & Wu, J. (2010). Urban heat islands and landscape heterogeneity: linking spatiotemporal variations in surface temperatures to land-cover and socioeconomic patterns. *Landscape Ecology*, 25, 17–33.

Bothwell, J., & Yuan, M. (2010). Apply concepts of fluid kinematics to represent continuous space–time fields in temporal GIS. *Annals of GIS*, 16(1), 27–41.

Buyantuyev, A., & Wu, J. (2010). Urban heat islands and landscape heterogeneity: linking spatiotemporal variations in surface temperatures to land-cover and socioeconomic patterns. *Landscape Ecology*, 25(1), 17–33.

Bothwell, J., & Yuan, M. (2011). A Kinematics-based GIS Methodology to Represent and Analyze Spatiotemporal Patterns of Precipitation Change in IPCC A2 Scenario. *ACM SIGSPATIAL GIS '11*, 152–161.

Bothwell, J., & Yuan, M. (2012). A Spatiotemporal GIS Framework Applied to the Analysis of Changes in Temperature Patterns. *Transactions in GIS*, 16(6), 901–919.

Bonamente, E., Rossi, F., Coccia, V., Pisello, A., L., Nicolini, A., Castellani, B., ... Santamouris, M. (2013). An energy-balanced analytic model for urban heat canyons: comparison with experimental data. *Advances in Building Energy Research*, 7, 222–234.

Bai, Y., Wong, M. S., Shi, W. Z., Wu, L. X., & Qin, K. (2015). Advancing of land surface temperature retrieval using extreme learning machine and spatio-temporal adaptive data fusion algorithm. *Remote Sensing*, 7(4), 4424–4441.

Claramunt C., & Thériault M. (1995). Managing Time in GIS: An Event-Oriented Approach. *Proceedings of the International Workshop on Temporal Databases: Recent Advances in Temporal Databases*, 23–42.

Cohn, E. G., & Rotton J. (2000). Weather, seasonal trends and property crimes in Minneapolis, 1987-1988. a moderator-variable time-series analysis of routine activities. *Journal of Environmental Psychology*, 20, 257–272.

Chai, H. X., Cheng, W. M., Zhou, C. Q., Chen, X., Ma, X. Y., & Zhao, S. M. (2011). Analysis and comparison of spatial interpolation methods for temperature data in Xinjiang Uygur Autonomous Region, China. *Natural Science*, 3(12), 999–1010.

Chen G., Hay, G. J., Carvalho, L. M. T., & Wulder, M. A. (2012). Object-based change detection. *International Journal of Remote Sensing*, 33(14), 4434–4457.

Clinton, N., & Gong, P. (2013). MODIS detected surface urban heat islands and sinks: Global locations and controls. *Remote Sensing of Environment*, 134, 294–304.

Chow, W. T. L., Salamanca, F., Georgescu, M., Mahalov, A., Milne, J. M., & Ruddell, B. L. (2014). A multi-method and multi-scale approach for estimating city-wide anthropogenic heat fluxes. *Atmospheric Environment*, 99, 64–76.

Chen, D., Wang, X., Thatcher, M., Barnett, G., Kachenko, A., & Prince, R. (2014). Urban vegetation for reducing heat related mortality. *Environmental Pollution*, 192, 275–284.

Dousset, B., & Gourmelon, F. (2003). Satellite multi-sensor data analysis of urban surface temperatures and landcover. *ISPRS Journal of Photogrammetry & Remote Sensing*, 58, 43–54.

Del Mondo, G., Rodríguez, M. A., Claramunt, C., Bravo, L., & Thibaud, R. (2013). Modelling Consistency of Spatio-temporal Graphs. *Data & Knowledge Engineering, Elsevier*, 84(1), 59–80.

Ding, Z., Guo, P., Xie, F., Chu, H., Li, K., Pu, J., ... Zhang, Q. (2015). Impact of diurnal temperature range on mortality in a high plateau area in southwest China: A time series analysis. *Science of the Total Environment*, 526, 358–365.

Field, S. (1992). The effect of temperature on crime. *British Journal of Criminology*, 32, 340–351.

Frihida, A., Marceau, D. J., & Thériault, M. (2002). Spatio-Temporal Object-Oriented Data Model for Disaggregate Travel Behavior. *Transactions in GIS*, 6(3), 277–294.

Fung, W. Y., Lam, K. S., Hung, W. T., Pang, S. W., & Lee, Y. L. (2006). Impact of urban temperature on energy consumption of Hong Kong. *Energy*, 31, 2623–2637.

Fei, X. (2017). *Sensor web and geospatial cloud computing modeling and its application in real-time collaborative earth observation data processing.* Retrieved from http://theses.lib.polyu.edu.hk/handle/200/8755

Goodchild, M. F., Yuan, M., & Cova, T. J. (2007). Towards a general theory of geographic representation in GIS. *International Journal of Geographical Information Science*, 21(3), 239–260.

Giridharan, R., Lau, S. S. Y., Ganesan, S., & Givoni, B. (2007). Urban design factors influencing urban heat island intensity in high rise high density environments of Hong Kong. *Building and Environment*, 42(10), 3669–3684.

Guilbert, É., & Lin, H. (2007). A New Model for Cloud Tracking and Analysis on Satellite Images. *Geoinformatica*, 11(3), 287–309.

Gerçeka, D., Toprakb, V., & Strobl, V. (2011). Object-based classification of landforms based on their local geometry and geomorphometric context. *International Journal of Geographical Information Science*, 25(6), 1011–1023.

Goggins, W. B., Chan, E. Y. Y., Ng, E., Ren, C., & Chen, L. (2012). Effect Modification of the Association between Short-term Meteorological Factors and Mortality by Urban Heat Islands in Hong Kong. *PLoS One*, 7(6), e38551.

Ghosh, A., & Joshi, P. K. (2014). Hyperspectral imagery for disaggregation of land surface temperature with selected regression algorithms over different land use land cover scenes. *ISPRS Journal of Photogrammetry and Remote Sensing*, 96, 76–93.

Grover, A., Singh, & R. B. (2015). Analysis of Urban Heat Island (UHI) in Relation to Normalized Difference Vegetation Index (NDVI): A Comparative Study of Delhi and Mumbai. *Environments*, 2, 125–138.

Guangzhou. (2017). *Guangzhou City.* Retrieved from https://en.wikipedia.org/wiki/Guangzhou#cite_note-12

Guilbert, G., & Moulin, B. (2017). Towards a Common Framework for the Identification of Landforms on Terrain Models. *ISPRS International Journal of Geo-Information*, 6(12), 1–21.

Hornsby, K., & Egenhofer, M. J. (2000). Identity-based change: a foundation for spatio-temporal knowledge representation. *International Journal of Geographical Information Science*, 14(3), 207–224.

Huang, G. B., Zhu, Q. Y., & Siew, C. K. (2004). In Extreme learning machine: A new learning scheme of feedforward neural networks. *Proceedings of International Joint Conference on Neural Networks*, 85–990.

Hornsby, K. S., & Cole, S. (2007). Modeling Moving Geospatial Objects from an Event-based Perspective. *Transactions in GIS*, 11(4), 555–573.

Hofstra, N., Haylock, M., New, M., Jones, P., & Frei, C. (2008). Comparison of six methods for the interpolation of daily, European climate data. *Journal of Geographical Research*, 113, D21110. doi:10.1029/2008JD010100

Hughes, C. G., & Ramsey, M. S. (2010). Super-resolution of THEMIS thermal infrared data: Compositional relationships of surface units below the 100 meter scale on Mars. *Icarus 208*, 704–720.

Huang, G. B., Zhou, H., Ding, X., & Zhang, R. (2012). Extreme learning machine for regression and multiclass classification. *IEEE Transactions on Systems, Man, and Cybernetics, Part B: Cybernetics*, 42(2), 513–529.

Hua, L., & Wang, M. (2012). Temporal and spatial characteristics of urban heat island of an estuary city, China. *Journal of Computers*, 7(12), 3082–3087.

Hughes, C. G., & Ramsey, M. S. (2013). A radiometrically-accurate super-resolution approach to thermal infrared image data. *International Journal of Image and Data Fusion*, 4(1), 52–74.

Holderness, T., Barr, S., Dawson, R., & Hall, J. (2013). An evaluation of thermal Earth observation for characterizing urban heatwave event dynamics using the urban heat island intensity metric. *International Journal of Remote Sensing*, 34(3), 864–884.

Hadoop. (2017). *Hadoop website.* Retrieved from https://hadoop.apache.org/docs/r1.2.1/mapred_tutorial.html

Irmak, A., Ranade, P. K., Marx, D., Irmak, S., Hubbard, K. G., Meyer, G. E., & Martin, D. L. (2010). Spatial Interpolation of climate variables in Nebraska. *Transactions of the ASABE*, 53(6), 1759–1771.

Jiang, J. X., & Worboys, M. (2009). Event-based topology for dynamic planar areal objects. *International Journal of Geographical Information Science*, 23(1), 33–60.

Jalan, S., & Sharma, K. (2014). Spatio-temporal asscessment of land use / land cover dynamics and urban heat island of Jaipur city using satellite data. *The International Archives of the Photogrammetry, Remote Sensing and Spatial Information Sciences*, XL-8, 767–772.

Khaddaj, S., Adamu, A., & Morad, M. (2005). Construction of an Integrated Object Oriented System for Temporal GIS. *American Journal of Applied Sciences*, 2(12), 1584–1594.

Kjenstad, K. (2006). On the integration of object-based models and field-based models in GIS. *International Journal of Geographical Information Science*, 20(5), 491–509.

Keramitsoglou, I., Kiranoudis, C. T., Ceriola, G., Weng, Q., & Rajasekar, U. (2011). Identification and analysis of urban surface temperature patterns in Greater Athens, Greece, using MODIS imagery. *Remote Sensing of Environment*, 115(12), 3080–3090.

Keramitsoglou, I., Kiranoudis, C. T., & Weng, Q. H. (2013). Downscaling Geostationary Land Surface Temperature Imagery for Urban Analysis. *IEEE Geoscience and Remote Sensing Letters*, 10(5), 1253–1257.

Kenney, W. L., Craighead, D. H., & Alexander, L. M. (2014). Heat Waves, Aging, and Human Cardiovascular Health. *Medicine & Science in Sports & Exercise*, 46, 1891–1899.

Kourtidis, K., Georgoulias, A. K., Rapsomanikis, S., Amiridis, V., Keramitsoglou, I., Hooyberghs, H., ... Melas, D. (2015). A study of the hourly variability of the urban heat island effect in the Greater Athens Area during summer. *Science of the Total Environment*, 517, 162–177.

Lo, C. P., Quattrochi, D. A., & Luvall, J. C. (1997). Application of high-resolution thermal infrared remote sensing and GIS to assess the urban heat island effect. *International Journal of Remote Sensing*, 18(2), 287–304.

Lindberg, F., Grimmond, C. S. B., Yogeswaran, N., Kotthaus, S., & Allen, L. (2013). Impact of city changes and weather on anthropogenic heat flux in Europe 1995–2015. *Urban Climate*, 1–15.

Li, J. W., Liang, Y. Y., & Wan, J. Z. (2013). Geo-Ontology-Based Object-Oriented Spatiotemporal Data Modeling. *Lecture Notes in Computer Science*, 7719, 302–317.

Long, Z. & Li, S. (2013). A complete classification of spatial relations using the Voronoi-based nine-intersection model. *International Journal of Geographical Information Science*, 27(10), 2006–2025.

Lee, S. H., McKeen, S. A., & Sailor, D. J. (2014). A regression approach for estimation of anthropogenic heat flux based on a bottom-up air pollutant emission database. *Atmospheric Environment*, 95, 629–633.

Liang, J., Gong, J., Li, W., & Abdoul, N. I. (2014). A visualization-oriented 3D method for efficient computation of urban solar radiation based on 3D–2D surface mapping. *International Journal of Geographical Information Science*, 28(4), 780–798.

Liang, J., Gong, J., Zhou, J., Abdoul, N. I., & Li, M. (2015). An open-source 3D solar radiation model integrated with a 3D Geographic Information System. *Environmental Modelling & Software*, 64, 94–101.

Mattos, M. M., Meyer-Wegener, K., & Mitschang, B. (1993). Grand tour of concepts for object-orientation from a database point of view. *Data and Knowledge Engineering*, 9, 321–352.

McKinney, D. C., & Cai, X. M. (2002). Linking GIS and water resources management models: an object-oriented method. *Environmental Modelling & Software*, 17, 413–425.

McIntosh, J., & Yuan, M. (2005). Assessing Similarity of Geographic Processes and Events. *Transactions in GIS*, 9(2), 223–245.

Merino, M.T., & Núñez, J. (2007). Super-Resolution of Remotely Sensed Images With Variable-Pixel Linear Reconstruction. *Transactions on geoscience and remote sensing*, 45(5), 1446–1457.

Miller, H. J., & Bridwell, S. A. (2009). A Field-Based Theory for Time Geography. *Annals of the Association of American Geographers*, 99(1), 49–75.

Moser, G., & Serpico, S. B. (2009). Automatic Parameter Optimization for Support Vector Regression for Land and Sea Surface Temperature Estimation From Remote Sensing Data. *IEEE Geoscience and Remote Sensing Letters*, 47(3), 909–921.

Morabito, M., Crisci, A., Moriondo, M., Profili, F., Francesconi, P., Trombi, G., ... Orlandini, S. (2012). Air temperature-related human health outcomes: Current impact and estimations of future risks in Central Italy. *Science of the Total Environment*, 441, 28–40.

Martin-Vide, J., Sarricolea, P., & Moreno-García1, M. C. (2015). On the definition of urban heat island intensity: the "rural" reference. *Frontiers in Earth Science*, 3, 24.

Mariani, L., Parisi, S. G., Cola, G., Lafortezza, R., Colangelo, G., & Sanesi, G. (2016). Climatological analysis of the mitigating effect of vegetation on the urban heat island of Milan, Italy. *Science of the Total Environment*, 569, 762–773.

Meijer, A. J., Gil-Garcia, J. R., & Bolívar, M. P. R. (2016). Smart City Research: Contextual Conditions, Governance Models, and Public Value Assessment. *Social Science Computer Review*, 34(6), 647–656.

Mills, C. M., Cassano, J. J., & Cassano, E. N. (2016). Midlatitude atmospheric responses to Arctic sensible heat flux anomalies in Community Climate Model, Version. *Geophysical Research Letters*, 43(23), 12270–12277.

Nichol, J. E. (2009). An emissivity modulation method for spatial enhancement of thermal satellite images in urban heat island analysis. *Photogrammetric Engineering & Remote Sensing*, 75(5), 547–556.

Nichol, J. E., Wing, Y. F., Lam, K., & Wong, M. S. (2009). Urban heat island diagnosis using ASTER satellite images and 'in situ' air temperature. *Atmospheric Research*, 94, 276–284.

Nixon, V., & Hornsby, K. S. (2010). Using geolifespans to model dynamic geographic domains. *International Journal of Geographical Information Science*, 24(9), 1289–1308.

Nassar, K. A., Blackburn, G. A., & Whyatt, J. D. (2016). Dynamics and controls of urban heat sink and island phenomena in a desert city: Development of a local climate zone scheme using remotely-sensed inputs. *International Journal of Applied Earth Observation and Geoinformation*, 51, 76–90.

Peuquet, D. J., & Duan, N. (1995). An event-based spatiotemporal data model (ESTDM) for temporal analysis of geographical data. *International Journal of Geographical Information Systems*, 9(1), 7–24.

Papakostas, K., Mavromatis, T., & Kyriakis, N. (2010). *Renewable Energy*, 35, 1376–1379.

Pultar, E., Cova, T. J., Yuan, M., & Goodchild, M. F. (2010). EDGIS: a dynamic GIS based on space time points. *International Journal of Geographical Information Science*, 24(3), 329–346.

Phelan, P. E., Kaloush, K., Miner, M., Golden, J., Phelan, B., Silva, H., & Taylor, R. A. (2015). Urban Heat Island: Mechanisms, Implications, and Possible Remedies. *Annual Review of Environment and Resources*, 40, 285–307.

Pal, S., Xueref-Remy, I., Ammoura, L., Chazette, P., Gibert, F., Royer, P., ... Ravetta, F. (2016). Spatio-temporal variability of the atmospheric boundary layer depth over the Paris agglomeration: An assessment of the impact of the urban heat island intensity. *Atmospheric Environment*, 63, 261–275.

Quah, A. K. L., & Roth, M. (2012). Diurnal and weekly variation of anthropogenic heat emissions in a tropical city, Singapore. *Atmospheric Environment*, 46, 92–103.

Renolen, A. (2000). Modelling the Real World: Conceptual Modelling in Spatiotemporal Information System Design. *Transactions in GIS*, 4(1), 23–42.

Rotton, J., & Cohn, E. G. (2004). Outdoor temperature, climate control, and criminal assault. *Environment and behaivor*, 36, 276–306.

Rajasekar, U., & Weng, Q. (2009a). Application of Association Rule Mining for Exploring the Relationship between Urban Land Surface Temperature and Biophysical / Social Parameters. *Photogrammetric Engineering & Remote Sensing*, 75(3), 385–396.

Rajasekar, U., & Weng, Q. (2009b). Urban heat island monitoring and analysis using a non-parametric model: A case study of Indianapolis. *ISPRS Journal of Photogrammetry and Remote Sensing*, 64, 86–96.

Radoux, J., Bogaert, P., Fasbender, D., & Defourny, P. (2011). Thematic accuracy assessment of geographic object-based image classification. *International Journal of Geographical Information Science*, 25(6), 895–911.

Rodriuez-Galiano, V. F., Pardo-Igiquiza, E., Chica-Olmo, M., & Rigol-Sichez, J. P. (2011). Increasing the spatial resolution of thermal infrared images using cokriging. *Procedia Environmental Sciences*, 3, 117–122.

Shi, W. Z., Yang, B. S., & Li, Q. Q. (2003). An object-oriented data model for complex objects in three-dimensional geographical information. *International Journal of Geographical Information Science*, 17(5), 411–430.

Stahl, K., Moore, R. D., Floyer, J. A., Asplin, M. G., & McKendry, I. G. (2006). Comparison of approaches for spatial interpolation of daily air temperature in a large region with complex topography and highly variable station density. *Agricultural and Forest Meteorology*, 139, 224–236.

Stathopoulou, M., & Cartalis, C. (2007). Daytime urban heat islands from Landsat ETM+ and Corine land cover data: An application to major cities in Greece. *Solar Energy*, 81, 358–368.

Stathopoulou, M., & Cartalis, C. (2007). Daytime urban heat islands from Landsat ETM+ and Corine land cover data: An application to major cities in Greece. *Solar Energy*, 81, 358–368.

Smith, C., Lindley, S., & Levermore, G. (2009). Estimating spatial and temporal patterns of urban anthropogenic heat fluxes for UK cities: the case of Manchester. *Theoretical and Applied Climatology*, 98, 19–35.

Susca, T., Gaffin, S. R., & Dell'Osso, G. R. (2011). Positive effects of vegetation: Urban heat island and green roofs. *Environmental Pollution*, 159, 2119–2126.

Srivanit, M., & Hokao, K. (2012). Effects of urban development and spatial characteristics on urban thermal environment in Chiang Mai metropolitan, Thailand. *Lowland Technology International*, 14(2), 9–22.

Sailor, D. J., Georgescu, M., Milne, J. M., & Hart, M. A. (2015). Development of a national anthropogenic heating database with an extrapolation for international cities. *Atmospheric Environment*, 118, 7–18.

Santos, A. R., Oliveira, F. S., Silva, A. G., Gleriani, J. M., Gonçalves, W., Moreira, G. L., ... Mota, P. H. S. (2017). Spatial and temporal distribution of urban heat islands. *Science of the Total Environment*, 605–606, 946–956.

Silva, B. N., Khan, M., & Han, K. (2017). Big Data Analytics Embedded Smart City Architecture for Performance Enhancement through Real-Time Data Processing and Decision-Making. *Wireless Communications and Mobile Computing*, 2017, 1–12.

Socioeconomic data and applications center. (2017). *Global Urban Heat Island Data Set*. Retrieved from http://sedac.ciesin.columbia.edu/data/set/sdei-global-uhi-2013

Tang, A. Y., Adams, T. M., & Usery, E. L. (1996). A spatial data model design for feature-based geographical information systems. *International Journal of Geographical Information Systems*, 10(5), 643–659.

Townshend, J. R. G., Huang, C., Kalluri, S. N. V., Defries, R. S., Liang, S., & Yang, K. (2000). Beware of per-pixel characterization of land cover. *International Journal of Remote Sensing*, 21, 839–843.

Tonooka, H. (2005). Resolution enhancement of ASTER shortwave and thermal infrared bands based on spectral similarity. *Proceedings of SPIE*, 5657, 9–19.

Unite States Environmental Protection Agency. (2017a). *Heat Island Effect*. Retrieved from https://www.epa.gov/heat-islands

United States Environmental Protection Agency. (2017b). *Learn About Heat Islands*. Retrieved from https://www.epa.gov/heat-islands/learn-about-heat-islands

Worboys, M. (1994). Object-oriented approaches to geo-referenced information. *International Journal of Geographical Information Systems*, 8(4), 385–399.

Worboys, M. (2005). Event-oriented approaches to geographic phenomena. *International Journal of Geographical Information Science*, 19(1), 1–28.

Wang, F. (2006). Modelling sheltering effects of trees on reducing space heating in office buildings in a windy city. *Energy and Building*, 38, 1443–1454.

Wu, F., Wang, X., Cai, Y., Yang, Z., & Li, C. (2012). Spatiotemporal analysis of temperature-variation patterns under climate change in the upper reach of Mekong River basin. *Science of the Total Environment*, 427-428, 208–218.

Wong, M. S., & Nichol, J. E. (2013). Spatial variability of frontal area index and its relationship with urban heat island intensity. *International Journal of Remote Sensing*, 34(3), 885–896.

Wang, J., & Ouyang, W. (2017). Attenuating the surface Urban Heat Island within the Local Thermal Zones through land surface modification. *Journal of Environmental Management*, 187, 239–252.

Wikipedia for latent heat. (2017). *Latent heat.* Retrieved from https://en.wikipedia.org/wiki/Latent_heat

Yuan, M., & Hornsby, K. (2008). *Computation and Visualization for Understanding Dynamics in Geographic Domains*. CRC Press.

Yuan, M. (2001). Representing Complex Geographic Phenomena in GIS. *Cartography and Geographic Information Science*, 28(2), 83–96.

Yao, W., & Han, M. (2010). Fusion of thermal infrared and multispectral remote sensing images via neural network regression. *Journal Image and Graphics*, 15, 1278–1284.

Yang, G. J., Pu, R. L., Zhao, C. J., Huang, W. J., & Wang, J. H. (2011). Estimation of subpixel land surface temperature using an endmember index based technique: A case examination on ASTER and MODIS temperature products over a heterogeneous area. *Remote Sensing of Environment*, 115, 1202–1219.

Zortea, M., Martino, M. D., Moser, G., & Serpico, S. B. (2006). Land surface temperature estimation from infrared satellite data using support vector machines. *2006 IEEE International Symposium on Geoscience and Remote Sensing*, 2109–2112.

Zaniolo, C. (2009). Event-Oriented Data Models and Temporal Queries in Transaction-Time Databases. *In: Proceeding of 16th International Symposium on Temporal Representation and Reasoning*, Bressanone-Brixen, Italy, 47–53.

Zhan, W. F., Chen, Y. H., Wang, J. F., Zhou, J., Quan, J., Liu, W., & Li, J. (2012). Downscaling land surface temperatures with multi-spectral and multi-resolution images. *International Journal of Applied Earth Observation and Geoinformation*, 18, 23–36.

Zhang, H. K., & Huang, B. (2013). Support Vector Regression-Based Downscaling for Intercalibration of Multiresolution Satellite Images. *IEEE Geoscience and Remote Sensing Letters*, 51(3), 1114–1123.

Zhou, J., Chen, Y., Zhang, X., & Zhan, W. (2013). Modelling the diurnal variations of urban heat islands with multi-source satellite data. *International Journal of Remote Sensing*, 34(21), 7568–7588.

Zhong, S., Qian, Y., Zhao, C., Leung, R., & Yang, X. Q. (2015). A case study of urbanization impact on summer precipitation in the Greater Beijing Metropolitan Area: Urban heat island versus aerosol effects. *Journal of Geophysical Research: Atmospheres*, 120, 10903–10914.

Zhu, R., Guilbert, E., & Wong, M. S. (2016). Object-oriented tracking of the dynamic behavior of urban heat islands. *International Journal of Geographical Information Science*, 31(2), 405–424.

Zhou, D., Zhang, L., Hao, L., Sun, G., Liu, Y., & Zhu, C. (2016). Spatiotemporal trends of urban heat island effect along the urban development intensity gradient in China. *Science of the Total Environment*, 544, 617–626.

Zhou, B., Kropp, J., & Rybski, D. (2016). Assessing Seasonality in the Surface Urban Heat Island of London. *Journal of Applied Meteorology and Climatology*, 55, 493–505.